ECONOMIC AND ENVIRONMENTAL IMPACTS OF OIL AND GAS DEVELOPMENT ON THE UINTA BASIN

by

Jonathan Eugene Wilkey

A dissertation submitted to the faculty of
The University of Utah
in partial fulfillment of the requirements for the degree of

Doctor of Philosophy

Department of Chemical Engineering

The University of Utah

May 2016

The University of Utah Graduate School

STATEMENT OF DISSERTATION APPROVAL

The dissertation of **Jonathan Eugene Wilkey**

has been approved by the following supervisory committee members:

Terry Arthur Ring	, Co-Chair	**02/05/2016** Date Approved
Jennifer P. Spinti	, Co-Chair	**02/03/2016** Date Approved
Donatella Pasqualini	, Member	**02/03/2016** Date Approved
Philip J. Smith	, Member	**02/15/2016** Date Approved
John David McLennan	, Member	**02/05/2016** Date Approved

and by **Milind Deo**, Chair of

the Department of **Chemical Engineering**

and by David B. Kieda, Dean of The Graduate School.

ABSTRACT

Conventional oil and gas (COG) development is a major source of employment and driver of economic development in Utah's Uinta Basin. However, it is also the primary cause of ground-level ozone pollution in the region and negatively impacts or consumes other limited public resources (e.g., water). All of these impacts will be amplified if oil shale resources in the Uinta Basin are ever developed. In order to optimize these trade-offs (i.e., minimizing the negative environmental impacts while maximizing the positive economic impacts), regulators, industry, policy makers, and the general public need to know when and how much development might occur in the Uinta Basin.

Therefore this research focuses on (1) forecasting the potential economic and environmental impacts of COG development on the Uinta Basin and (2) estimating the oil price necessary for oil shale processing to be economically viable. For COG, both impact estimates rely on a shared method of modeling drilling and production activity. In cross-validation tests, these methods have proven highly accurate, with energy price forecasts being the greatest source of uncertainty. Over the 2015 – 2019 period, median volatile organic compound emissions from the COG industry are expected to drop 45% compared to the 2010 – 2014 period due to decreases in drilling activity and tighter emission standards. The drop in drilling activity is expected to reduce employment by 23%. Royalty and tax revenue collected by the state of Utah is also expected to drop by

20% due to lower energy prices.

For oil shale, both in situ and ex situ processing methods could be economically viable if oil prices recover. Of the two options, ex situ processing faces fewer economic hurdles. The median oil price for ex situ processing is $94/bbl, vs. $272/bbl for in situ processing. Both processing methods have large upfront capital costs (on the order of billions of dollars) for drilling wells or building a mine and retorting complex. In situ scenarios are financially hindered compared to ex situ scenarios because most require multiple years of heating before reaching their maximum oil production rate.

TABLE OF CONTENTS

LIST OF TABLES

LIST OF FIGURES

ACKNOWLEDGEMENTS

I would not have been able to complete this dissertation without the help of my colleagues, friends, and family, to whom I am eternally grateful. Credit is especially due to my supervisory committee (Terry Ring, Jennifer Spinti, Donatella Pasqualini, Philip Smith, and John McLennan), Kerry Kelly, Isabel Cristina Jaramillo, Michael Hogue, Michal Hradisky, Whitney Oswald, Olga Baykova, Riccardo Boero, Bernardo Castro, Gibson Peters, Paul Oppegard, John Rogers, Sean Smith, Jean Sweet, David Tabet, Al Walker, Ian Walton, and Colin Young. Thank you.

CHAPTER 1

INTRODUCTION

Conventional oil and gas (COG) development is a major source of employment and driver of economic development in Utah's Uinta Basin. However, it is also the primary cause of ground-level ozone pollution in the region and negatively impacts or consumes other limited public resources (water, wildlife, transportation capacity, etc.). All of these impacts (positive and negative) will be amplified if oil shale resources in the Uinta Basin are ever developed. In order to optimize these trade-offs (i.e., minimizing the negative environmental impacts while maximizing the positive economic impacts), regulators, industry, policy makers, and the general public need to know when and how much development might occur in the Uinta Basin.

Therefore this research work focuses on (1) forecasting the potential economic and environmental impacts of COG development the Uinta Basin and (2) estimating the oil price necessary for oil shale processing to be economically viable. For COG, this work estimates (a) the emissions and (b) the employment and tax revenue from COG development over a five year period (2015 – 2019), both of which are based off of models of drilling and production activity from the COG industry in response to energy (oil and gas) prices. Similar estimates of the impacts of oil shale development cannot be made because to date no method of oil shale production has proven economically viable. Instead, the likely range of oil prices necessary for a prototypical (a) below ground (in

situ) and (b) above ground (ex situ) oil shale production facility to be economically viable are estimated as a function of a set of input parameters. All results (for both COG and oil shale) include uncertainty estimates and (when possible) are cross-validated to demonstrate model validity.

1.1 Article Synopses

Chapters 2 – 5 of this dissertation are composed of articles that have been submitted for publication. A brief synopsis of each chapter is presented below.

1.1.1 Chapter 2: Emissions from COG Development

This chapter discusses the emissions impact of the COG industry on the Uinta Basin. A full summary of the methodology for modeling drilling and production activity is presented, covering all steps required for the data analysis and Monte-Carlo (MC) simulation, including energy price forecasting, drilling activity modeling, estimating production through decline curve analysis, and calculating emission using emission factors. The results of a literature review of emission factors for CO_2, CH_4, and volatile organic compounds (VOCs) are presented for a variety of one-time and ongoing types of COG industry activities. Finally, the results of an MC simulation with 10^4 iterations are shared for a cross-validation time period (Jan. 2010 – Dec. 2014) and a prediction time period (Jan. 2015 – Dec. 2019). Given the projected downturn in the drilling activity and assuming that proposed emission regulations are implemented, the median VOC emissions rate will drop by 45% compared to the cross-validation period, even though oil production rates are expected to double and gas production will stay relatively constant. This result clearly shows that it is possible for oil and gas production to increase while

reducing overall emissions by raising emissions standards for new wells.

1.1.2 Chapter 3: Economic Impacts of COG Development

This chapter discusses the economic impacts of the COG industry on the Uinta Basin. A brief overview of the methodology for modeling drilling and production activity is given, followed by a detailed review of the methods used for estimating spending from the COG industry, the employment that results from that spending, and finally the methods used to calculate the various sources of revenue collected by the state of Utah from the COG industry (royalties, corporate income taxes, property taxes, and severance taxes). Like the preceding emissions chapter, the results of a MC simulation with 10^4 iterations are shared for a cross-validation time period (Jan. 2010 – Dec. 2014) and prediction time period (Jan. 2015 – Dec. 2019). However, the results shown are annual totals of (a) the number of jobs created by spending in the COG industry and (b) revenue from each source (royalties, corporate income taxes, etc.). Direct comparisons between the model's economic outputs and actual employment and revenue collections during the cross-validation period cannot be made in most cases due to differences in accounting and report methods. However, if energy price forecasts are accurate and the drilling and production modeling method continues to perform well in future time periods, then local leaders in the Uinta Basin can expect 23% lower employment in the oil and gas industry and the state of Utah will see 20% lower revenue from the COG industry over the next five years compared to the 2010 – 2014 period.

1.1.3 Chapter 4: Economic Analysis of In Situ Oil Shale Processing

In this chapter the oil supply price for in situ oil shale processing is determined as a function of six retort design and eight economic input parameters using a combination of discounted cash flow (DCF) analysis and design of experiments (DOE). The retort design parameters are used to generate 242 well geometries. Heat and mass balances for each geometry are determined as a function of time over a seven-year heating period using results obtained from computational fluid dynamics (CFD) simulations conducted by Hradisky and Smith (2016). The results for each CFD simulation are then combined with 2,000 unique combinations of the economic parameter set (all drawn from either a normal or log-normal distribution fitted to each economic input parameter), for a total of over 472,000 scenarios. The oil supply price for each of these scenarios is determined using the DCF analysis methodology. Regression analysis results show that the in situ retort parameters have a stronger impact on oil supply prices than any of the economic input parameters. Overall, few in situ oil shale processing scenarios are expected to be economically viable, assuming that oil prices recover to U.S. Energy Information Administration (EIA) forecasted levels. Only 5% of the scenarios analyzed have oil supply results $\leq$ \$90/bbl (the average Rocky Mountain region wellhead oil price over the 2015 – 2040 time period predicted by U.S. EIA (2015)), and the median oil supply price for all scenarios is \$272/bbl.

1.1.4 Chapter 5: Economic Analysis of Ex Situ Oil Shale Processing

Finally, this chapter determines the oil supply price for ex situ oil shale processing with a Paraho Direct retort as a function of six input parameters using the same DCF and

DOE methodologies applied in Chapter 4. A brief process description of the mining and retorting system is given, followed by a detailed discussion of the DCF and DOE methodologies. Oil supply price results are then shared for two different DOE procedures. In the first, the oil supply price is found for every unique combination of input parameters, assuming a uniform distribution sampled at every 10^{th} percentile between 0% and 100% for each input parameter (oil shale grade, production scale, relative capital and operating expense, oil royalty rates, and internal rate of return (IRR)), which results in 11^6 oil supply price results. In the second, the oil supply price for 11^6 unique combinations is again found, but a normal distribution for each input parameter is assumed instead, with sampling at every ninth percentile from 5% to 95%. Results from the first DOE analysis are used to perform a regression analysis, while results from the second analysis are used to show the probability distribution of possible supply price results. Regression analysis results show that oil shale grade and production have the strongest price-decreasing effect, while the IRR has the strongest price-increasing effect. Overall, ex situ oil shale production is more likely than in situ oil shale production to be economically viable. In the second DOE analysis, approximately 45% of the scenarios have oil supply prices $\leq$ \$90/bbl, and the median oil supply price for all scenarios is \$94/bbl.

1.2 References

Hradisky, M., & Smith, P. J. 2016. Simulations of In Situ Thermal Processing of Oil Shale. In J. Spinti (Ed.), *Utah Oil Shale - Science, Technology, and Policy Perspectives*. CRC Press.

U.S. EIA. 2015. *Annual Energy Outlook 2015*. Washington, DC. Retrieved from http://www.eia.gov/forecasts/aeo/pdf/0383(2015).pdf

CHAPTER 2

EMISSIONS FROM CONVENTIONAL OIL AND GAS DEVELOPMENT

In preparation for Journal of the Air and Waste Management Association. Predicting Emissions from Oil and Gas Operations in the Uinta Basin. J.E. Wilkey, K.E. Kelly, J.C. Spinti, T.A. Ring, M.T. Hogue, D. Pasqualini ©

2.1 Introduction

Oil and gas exploration and production (E&P) in Utah's Uinta Basin is both a key part of the region's economy and the primary source of ozone precursor emissions that lead to winter-time, ground-level ozone formation events. Measured ozone concentrations in the Uinta Basin have repeatedly exceeded national ambient air quality standards (NAAQS) (Environ, 2015), and the region will likely be found in nonattainment for ground-level ozone. Developing a state implementation plan to meet NAAQS for ground-level ozone will require accurate estimates of the emissions inventory from the oil and gas industry so that state regulators can make informed decisions about potential reduction and control strategies. However, unlike traditional emission sources, oil and gas wells have unsteady emission rates, which makes developing an emissions inventory for the industry particularly difficult. Oswald et al. (2014) developed a model projecting future-year emission inventories from oil wells, accounting for both growth within the sector as well as production decline due to the natural lifecycle of production wells. This study seeks to improve upon the previous method for estimating emissions from the oil and gas industry in the Uinta Basin by tracking one-time (well drilling, completion, and reworks) and ongoing (production, processing, transport) emission events from both oil and gas wells on a well-by-well basis with uncertainty estimates. If similar input data is available in other oil- and gas-producing regions, then the method developed here could be applied to those regions as well.

2.2 Methodology

The overall structure of the model is summarized in Figure 2.1. Each step in the data analysis and Monte-Carlo (MC) simulation are discussed in detail in subsequent sections. In summary, source data primarily from the U.S. Energy Information Administration (EIA) and Utah Division of Oil, Gas and Mining (UDOGM) are collected and analyzed to find either (a) a cumulative distribution function (CDF) or (b) a least-squares regression fit to the following model input parameters:

1. Forecast error (CDF): The range of relative error between actual energy prices and EIA energy price forecasts.
2. Drilling model (regression): A fitted model that predicts the number of new wells drilled in response to current and/or past energy prices.
3. Reworks (CDF): The probability that existing wells will be reperforated or recompleted as a function time.
4. Decline curve analysis (CDF and regression): Production from all wells tends to decrease over time. Individual decline curves are fitted using nonlinear least-squares regression to the unique production histories of every well in the Uinta Basin. Then, the range of values of the fitted decline curve coefficients are described using CDFs.
5. Emissions factors (CDF): The range of emission factors for various oil and gas drilling and production activities are modeled as a normal distribution based on the mean and standard deviation of reported emission factors we collected in a literature review.

After analyzing the source data, a MC simulation is then run to determine the

distribution of possible emission inventory outcomes. The following algorithm is executed for each iteration (i.e., run) of the MC simulation:

1. Generate a simulated oil and gas price forecast. EIA forecasts are used as a basis and are adjusted up or down based on the CDF of forecasting error. Price forecasts are interpolated from an annual to a monthly basis (the time step used in the rest of the MC simulation).
2. Calculate the number of new wells drilled in response to simulated energy prices by using the fitted drilling model. Additionally, randomly draw from the rework CDF to determine if and when a rework event will occur for each new and existing well.
3. For every well (new and existing):
    a. Pick/collect well attributes (well depth, decline curve coefficients, emission factors, etc.). Attributes for new wells are randomly picked by selecting from CDFs created in the data analysis step. Existing wells use their actual (or fitted) attributes.
    b. Calculate production rates of oil and gas for each well. Production from existing wells is found by extrapolating from each well's individually fitted decline curves. Production from new wells is calculated using the randomly picked decline curve coefficients generated in the previous step.
    c. Calculate emissions from one-time (drilling, completions, reworks) and ongoing (production, processing, etc.) events. Emissions are calculated by multiplying each randomly selected emission factor (for each well and for each emission activity type) by that factor's quantity of interest (i.e., the

date for one-time events such as completion, or the amount of oil or gas produced).

4. Sum together results for all wells to find the total emissions inventory for a given run of the MC simulation.

By repeating the above algorithm many times ($\geq 10^4$ iterations) and randomly drawing from the CDFs for each input parameter (where applicable), a representative sample of all possible emissions inventory outcomes is generated. The range of MC simulation results can then be analyzed to determine the probability of possible outcomes, clearly quantifying the uncertainty in the model's results.

All data analysis and MC simulation steps are written in R (R Core Team, 2015), which allows for the entire model to be run automatically in either a "cross-validation" or "predictive" mode. In the cross-validation mode the available data is separated into two time intervals. Data in the first interval, referred to as the "training" period, is used to generate all of the input parameter CDFs and regression fits. The MC simulation is then run over the second time interval. Data points in the second "testing" time interval can then be used to gauge the accuracy and validity of the MC simulation results. In predictive mode the model is trained using all available data, and the MC simulation estimates emissions for a future time period.

The details of each step in the data analysis and MC simulation process are discussed further below.

2.2.1 Energy Price Forecast

The first step of the MC simulation is generating a set of simulated energy price forecasts for the first purchase price (FPP) oil and gas prices. We use the U.S. EIA's Annual Energy Outlook (AEO) forecasts (U.S. EIA, 2015b) for wellhead oil and gas prices in the Rocky Mountain region as the basis for our forecasting work. While EIA's AEO forecasts are frequently used as a standard estimate for future energy prices, they are also frequently wrong, with prices being off by as much as ± 100% of their actual value after just five years (U.S. EIA, 2015a). The range of possible error in EIA forecasts must be included in the simulated energy price forecast to propagate that uncertainty into emissions inventory estimates. We calculated the relative error between actual FPPs of oil and gas in Utah and EIA's forecasted prices over the 1999-2014 time period (the full time period for which Rocky Mountain wellhead price forecasts were included in AEO reports) using Eqs. (2.1) and (2.2):

$$RE = \frac{FP}{AP} \tag{2.1}$$

$$RE = \frac{AP}{FP} \tag{2.2}$$

where RE is the relative error between the forecasted price FP and the actual price AP. Equation (2.1) is used to find RE if $FP > AP$, otherwise Eq. (2.2) is used. Defining RE this way is useful because

1. The value of RE is always bounded between 0 and 1 and can be described using a beta probability distribution.
2. It captures the absolute magnitude of the relative error. While EIA under-predicted actual FPPs for oil over the 1999-2007 time period, forecasts from

2009 onwards have overpredicted actual FPPs for oil (gas prices have followed a similar pattern). There is no evidence that EIA's forecasts are systemically under- or over-predicting energy prices.

3. Equations (2.1) and (2.2) avoid a mathematical pitfall that occurs with a simple absolute value calculation of *RE*. Suppose that *RE* was defined as

$$RE = \frac{|FP - AP|}{FP} \tag{2.3}$$

Substituting the simulated price (*SP*) for *AP* and rearranging gives

$$SP = FP(1 \pm RE) \tag{2.4}$$

If a negative value of *RE* is selected during the MC simulation process, *SP* may be negative, which is not a realistic result. By comparison, solving Eqs. (2.1) and (2.2) always returns a result bounded between [0,+∞]

$$SP = \frac{FP}{RE} \tag{2.5}$$

$$SP = RE \cdot FP \tag{2.6}$$

Figure 2.2 shows a boxplot of the distribution of values for *RE* for oil and gas by future-year (i.e., how far into the future the forecast is) calculated according to Eqs. (2.1) and (2.2).

A beta distribution with shape parameters α and β was fitted to the empirical distributions of *RE* values in Figure 2.2, resulting in the parameter values given in Table 2.1. The beta distribution was selected to model values of *RE* because it is a continuous probability distribution bounded between 0 and 1 (the same range of values possible for *RE* using Eqs. (2.1) and (2.2)). These shape parameters are used to create two theoretical CDFs for *RE* by future year, one for oil and one for gas. During the MC simulation,

percentiles of these two CDFs are randomly selected, and then the percentiles are traced through the two CDFs by future-year. For example, if the 50th (median) percentile were selected for gas, the values of *RE* would be 0.81, 0.75, 0.66, 0.62, and 0.58 for future-years 1 through 5. The value for *SP* is then calculated using either Eq. (2.5) or (2.6) with an *FP* value obtained from the EIA AEO forecast. Which form of the equation to use is also selected randomly (with equal probability). Lastly, both the EIA AEO forecasts and the *RE* CDFs are converted from an annual basis to a monthly basis using linear interpolation since all other components in the modeling process are calculated on a monthly basis.

2.2.2 Drilling Forecast

Forecasting drilling activity is a key part of estimating overall emissions in the Uinta Basin because new wells are (a) responsible for the overall growth rate of oil and gas production in the region and (b) are major sources of one-time emissions. Drilling activity can occur either in the form of drilling new wells or "reworking" existing and/or abandoned wells to stimulate new production. The methods used for forecasting each type of drilling activity are discussed below.

2.2.2.1 New Wells

The number of wells drilled each month in the Uinta Basin can be modeled as a function of energy prices using a variety of distributed lag models. We tested four different distributed lag price models:

$$W_t = aOP_t + bGP_t + cW_{t-1} + d \tag{2.7}$$

$$W_t = aOP_{t-1} + bGP_{t-1} + c \tag{2.8}$$

$$W_t = aOP_{t-1} + b \quad (2.9)$$

$$W_t = aGP_{t-1} + b \quad (2.10)$$

where W is the number of new wells drilled at time t, OP is the FPP of oil in dollars per barrel ($ / bbl), GP is the FPP of gas in dollars per thousand cubic feet ($ / MCF), and all other terms (a, b, c, and d) are coefficients fitted using linear regression. Data on the number of wells drilled (Utah DOGM, 2015) and the values of OP and GP in the Uinta Basin (U.S. EIA, 2015g; U.S. EIA, 2015e) were used to find the best fit for each model over the time period of January 1995 – December 2009 (the training period) and were cross-validated against data from the January 2010 – December 2014 time period (the test period). Results for the training fit and cross-validation test are summarized in Table 2.2 and plotted in Figures 2.3 and 2.4.

In general, all of the distributed lag models fit the drilling record from 1995 – 2009 reasonably well. The correlation between energy prices and drilling activity in the Uinta Basin is particularly strong after 2000. Equation (2.7) gives the best fit during the training period because (a) the prior well term dampens the effect of monthly energy price fluctuations on drilling activity and (b) Eq. (2.7) contains more fitted terms. Equations (2.8) – (2.10) all underpredict drilling rates from 2006 – 2007, particularly Eq. (2.10) (which also fails to follow the spike in drilling in 2008 due to higher oil prices). While Eq. (2.7) would appear to be the best model, the cross-validation results shown in Figure (2.4) and Table (2.2) both reveal that Eq. (2.7) fails to respond to the energy price changes in the 2010 – 2014 time period, indicating that the model is most likely over-fitted to the training period's drilling and energy price history. Equation (2.8) performs slightly better than Eq. (2.7), and Eq. (2.10) fails completely. Overall, drilling activity in

the Uinta Basin over the last twenty years (and especially the last 15 years) has been closely correlated with oil prices, and the fit and cross-validation of Eq. (2.9) demonstrates that a simple distributed lag model based on oil prices is sufficient for estimating future drilling activity in the Uinta Basin. As a result, Eq. (2.9) was selected for use in estimating the number of new wells drilled in the MC simulation.

In addition to determining how many new wells are drilled, the geographical location and type of well (oil or gas) must also be selected. We assume that the geographical distribution of new wells (i.e., what oil or gas field a new well will be located in) and the ratio of oil wells to gas wells (which is location specific) can both be described by empirical CDFs based on historical data (Utah DOGM, 2015), and that the well type ratio in a given location is constant. It should be noted that well type merely indicates what type of product (oil or gas) is predominantly produced by a well. In reality (and in the simulation) all wells produce both oil and gas.

2.2.2.2 Reworked Wells

Reworks are drilling events where an existing well is either recompleted or re-perforated to stimulate oil and gas production rates. Reworks have a large impact on emissions both because (a) reworking a well is a large one-time source of fugitive emissions and (b) production rates usually rise dramatically after reworks. The timings of rework events are estimated using an empirical CDF based on well history data from Utah DOGM (2015) (1,137 rework events) to describe the probability that a well is reworked based on (a) well type (oil or gas) and (b) how long the well has been in operation, as shown in Figure 2.5. For each MC simulation run, every well (new and

existing) randomly draws a rework date from the CDFs in Figure 2.5. Note that rework dates can be selected which are outside of the simulation timeframe. For example, if a well that is 50 months old at the start of a 60-month (five-year) simulation draws a rework time that is earlier than 50 months or later than 110 months, the rework event for that particular well is effectively ignored.

2.2.3 Production Forecast

In general, production rates of oil and gas from any well decline over time. Arps (1945) proposed a set of empirically based "decline curve" equations to estimate a well's future production rates based on its rate of decline. Subsequently, the theoretical basis for decline curves has been established by other authors (Doublet et al., 1994; Fetkovich, Fetkovich, and Fetkovich, 1996; Shirman, 1998; Ling and He, 2012; Okouma Mangha et al., 2012). Numerous decline curve equations have been developed for specific oil and gas reservoir conditions. The two forms of decline curve equations used here are the hyperbolic decline curve equation (Eq. (2.11), (Arps, 1945)), and the cumulative production equation (Eq. (2.12), (Walton, 2014)):

$$q(t) = q_o(1 + bD_i t)^{-\frac{1}{b}} \tag{2.11}$$

$$Q(t) = C_p\sqrt{t} + c_1 \tag{2.12}$$

In Eq. (2.11), q is the oil or gas production rate at time t, q_o is the initial production rate, b is the decline exponent, and D_i is the initial decline rate. In Eq. (2.12) Q is the cumulative production at time t, and C_p and c_1 are fitted coefficients. Equations (2.11) and (2.12) are fitted to the oil and gas production records of every unique well in the Uinta Basin (Utah DOGM, 2015) using nonlinear least-squares regression. The fits found for Eq. (2.11) are

then extrapolated to estimate the future production for all existing wells, while the fits for Eq. (2.12) are used to generate CDFs for use in simulating the production rates of new wells. Production from new wells is estimated using Eq. (2.12) because monthly production rates (calculated by difference from the value of Q) are a function of only a single fitted coefficient, C_p, as opposed to three coefficients (q_o, D_i, and b) in Eq. (2.11). Random and independent draws from the CDFs for the coefficients in Eq. (2.11) almost always return unrealistic results (e.g., thousands of wells with no production, then a single well with higher production rates than the entire Uinta Basin combined). However the fits for Eq. (2.11) are frequently more accurate at longer time periods than Eq. (2.12). Therefore Eq. (2.11) is preferred for estimating the production rates for existing wells.

Unfortunately many wells have complicated production histories (shut-ins, workovers, water-flooding, etc.) that prevent easy fitting. To overcome this problem, we developed an algorithm that automatically identifies the start and stop points of distinct decline curves in each well's production records and then fits Eqs. (2.11) and (2.12) to each curve separately. An example of this approach is shown in Figure 2.6. Only the fits of the "first" and "last" curve segments are saved. If only a single curve is found, then that curve is counted as both the "first" and "last" curve. The production rates of existing wells are calculated directly from the "last" fits of Eq. (2.11) for each existing well (for both oil and gas). Production of oil and gas from new wells can be simulated by either

1. Randomly picking coefficients for Eq. (2.12) from the empirical CDFs of fitted coefficients from the "first" curves. This method works well if new wells are expected to have the same production rates as existing wells.
2. Utilizing log-normal distribution fitting to account for changing trends in the

production rates of new wells. Specifically:

a. Fit log-normal distributions to values of C_p and c_1 by year
b. Use linear regression to fit the log-normal distribution shape parameters, log-mean and log-standard deviation (SD).
c. Extrapolate from fitted log-mean and log-SD trendlines to estimate the distribution of C_p and c_1.

Given recent production trends, we have found that gas production from new wells is best simulated using the empirical CDF method, while oil production from new wells is most successfully handled by using the log-normal distribution method.

There are several other important caveats to the production forecast, as detailed below.

2.2.3.1 Existing Wells without Decline Curve Fits

In total, applying the curve-fitting algorithm to the 12,071 unique wells in the Uinta Basin results in approximately 48,000 unique curve-fitting attempts (both oil and gas production records for each well using both Eq. (2.11) and (2.12)). The algorithm is fairly robust; only 4% of the attempted fits fail to find a fit. However, 22% of the wells are skipped because they contain too few (< 12 months) nonzero production records. Existing wells without fits are treated using the same methodology applied to new wells.

2.2.3.2 Production Impact of Well Reworks

As discussed previously, reworking a well usually results in substantially increased production rates. To model the effect of reworks, any well that is randomly selected for rework is treated as a new well from the time step that the rework occurs. For

example, if an existing well that was 40 months old at the beginning of the simulation is scheduled for a rework in month 10 of a 60-month-long simulation period, production for months 40-49 would occur according to the original decline curve (Eq. (2.11)), while production for months 50–99 would be computed using Eq. (2.12) with a randomly selected set of coefficients.

2.2.3.3 Well Abandonment

Eventually, the decline in a well's production rates will become so low that it becomes uneconomical to continue to operate. To correct for wells that are producing at uneconomical rates, the last step in the production forecasting process is to estimate each well's operating cost ratio *CR* as a function of time:

$$CR(t) = \frac{LOC(t)}{GR(t)} \tag{2.13}$$

where *LOC* is the lease operating costs (pumping, labor, maintenance, etc.) for the well and *GR* is the gross revenue from oil and gas sales. *LOC* is estimated from EIA (2010b) data based on well type, depth, energy prices, and production rates, giving the following linear regression fits:

$$LOC_{oil}(t) = 25.9 \cdot OP(t) + 0.189 \cdot D \tag{2.14}$$

$$LOC_{gas}(t) = 0.586 \cdot q_{gas}(t) + 268 \cdot GP(t) + 0.225 \cdot D \tag{2.15}$$

where q_{gas} is the monthly production rate of gas (MCF / month), *D* is well depth (in ft), and "oil" and "gas" subscripts denote well type. The fit given in Eq. (2.14) is based on 64 data points ($R^2 = 0.982$) and Eq. (2.15) on 160 data points ($R^2 = 0.927$), which represent all of the available *LOC* data for both well types from EIA (2010b). Any well which is found to have a $CR(t) \geq 0.8$ is assumed to be shut-in and permanently abandoned (since

approximately 15% of *GR* is paid in royalties and severance taxes).

2.2.4 Emissions

Given the uncertainty in reported emission factors for the oil and gas industry, we elected to use the same approach applied to other input parameters in our model to compute emissions from oil and gas development – namely, we described emission factor ranges using CDFs, and from the CDFs (for each well) randomly selected the emission factor values to apply to the drilling and production forecast. The details of implementing this approach to calculate total emissions are described below.

2.2.4.1 Emission Factor Sources

This study groups emission factors for greenhouse gases (GHG), methane (CH_4), and volatile organic compounds (VOCs) into the categories that correspond to the process steps: site preparation; material transport; well drilling; fracturing and completion (including flowback); production; product processing; and product transport. Emission factors were estimated from a review of published studies aimed at emissions from oil and gas operations with an emphasis on the Uinta Basin and tight-gas/tight-sand formations. Methane emissions were converted to CO_2 equivalents (CO_2e) on a 100-year time frame (using a global warming potential of 21), and nitrous oxide (N_2O) emissions were converted to CO_2e using a global warming potential of 310. VOC emissions were estimated using the ratio of VOCs to CH_4 at the wellhead in the Uinta Basin from Zhang et al. (2009) (CH_4 75%, VOCs 12%) and from EPA's smoke model (55 % methane and 33 % VOC) (University of North Carolina at Chapel Hill, 2014). The composition difference between Zhang et al. and EPA's smoke model was considered as part of the

emission-factor uncertainty.

For the same process steps, emission factors can vary by orders of magnitude (Figure 2.7). These differences are most likely due to different conditions at the study sites and different study methods. For example, formation properties and well productivity affect emissions. In addition, the emission factors come from different types of studies: surveys, emission measurements made on individual operations or pieces of equipment, and regional (top-down) measurements. The survey-based studies tend to report lower emissions than the other two types. Furthermore, the measurements at individual locations may not be representative of the operations from the entire region. For example, Karion et al. (2013) performed a top-down study and estimated that between 6.2 – 11.7% of natural gas produced is emitted in the Uinta Basin, while Pétron et al. (2012) estimated losses of 1.7 - 7.7% from the Piceance Basin. These top-down estimates are significantly higher than emissions estimated from survey-based emission factors (Western Regional Air Partnership, 2008) or other inventories (U.S. EPA, 2013; Utah State University, 2013). Recent modeling studies by Ahmadov et al. (2015) suggest that the Karion estimate may be in the correct range. However, because many of the oil- and gas-producing regions also have natural gas seeps, it can be difficult to resolve natural gas production activities from naturally occurring sources of CH_4 and VOCs.

2.2.4.2 Emission Factor Values

Table 2.3 provides the average and standard deviation of emission factors by process. Assuming that all of the emission factors follow a normal distribution, the mean and SD values in Table 2.3 can be used to generate CDFs for each factor. Emission

factors are assumed to follow a normal distribution because of the limited number of data points available. Table 2.4 presents the emission factors for CO_2, CH_4, and VOC emissions from the production and transport of oil. This study assumes that the emissions from site preparation, drilling, fracturing, and completion for oil wells are the same as those reported for gas wells.

2.2.4.3 Emissions Calculation

The emissions categories from Tables 2.3 and 2.4 are simplified into one-time events (drilling, reworking, and completing a well) and ongoing emissions (from production and transportation of produced oil and gas). The largest one-time emission source is completion, which is assumed to occur every time a well is drilled or reworked. Emissions from completion are tracked separately from the rest of the drilling and reworking activity. Noncompletion-related emissions for drilling are assumed to be the sum of the emission factors for site preparation and transportation of materials for drilling, completion, and production. Noncompletion rework emissions are assumed to be the sum of emission factors for transportation of materials for completion and reworking. The drilling schedule then determines the quantity and timing of all one-time emissions events. All of the ongoing emissions are calculated directly from the production schedule by multiplying production volumes by the per unit volume emissions factors specified in Tables 2.3 and 2.4.

2.2.4.4 Effect of New Regulations

The EPA recently finalized New Source Performance Standards (NSPS) for the oil and natural gas sector (U.S. EPA, 2012). Table 2.5 summarizes the effect of the NSPS

on emission factors and their implementation schedule. Additionally, beginning in 2015 new state rules require the replacement of existing high-bleed pneumatic control devices with low-bleed devices. These rules apply to oil and gas operations on state and federal lands but not to operations on tribal lands. The pneumatic controller regulations will result in a 1.2% reduction of all VOC and CH_4 emissions for Uinta County and an 11% reduction for Duchesne County (Oswald, 2015).

All of these reductions are implemented in the model by reducing the base emissions calculated from Tables 2.3 and 2.4 by the percentages specified in Table 2.5 and in the state pneumatic controller rules. The November 2012 NSPS in Table 2.5 is applied only to new gas wells. The January 2015 NSPS impact on construction is applied to all wells and very slightly increases the emissions related to the transportation of materials for drilling and the drilling activity itself. The January 2015 NSPS applies to all completions and reworks. The pneumatic controller regulations are implemented by reducing all VOC and CH_4 emissions by the overall reductions for each county.

2.3 Results and Discussion

Two sets of results are shown below for running the model in (a) cross-validation mode and (b) predictive mode. The cross-validation run presents the results of training the model with data from 1984 – 2009 and then testing the model against data from the 2010 – 2014 time period. The predictive run uses all of the available data (1984 – 2014) to predict emissions over the 2015 – 2019 time period. The range of results shown for both runs was obtained by performing a MC simulation with 10^4 iterations.

2.3.1 Energy Price Forecasts

Simulated energy price forecasts for oil and gas FPPs are shown in Figure 2.8 and Figure 2.9 for the cross-validation and prediction cases, respectively. Dotted lines represent various percentiles of simulation results (10^{th} percentile, 20^{th} percentile, etc.), while the solid black lines show the actual oil and gas price paths. Additionally, the reference and outlier (highest price/lowest price) forecasts from EIA's AEO reports are shown as shaded grey lines. The cross-validation case uses EIA's AEO 2010 report (U.S. EIA, 2010a) as a basis, while the prediction case uses AEO 2015 (U.S. EIA, 2015b).

In general, the simulated energy price paths (a) cover the range of observed prices, (b) meet or exceed the range of variability in EIA's extreme price forecasts, and (c) have a median (50^{th} percentile) result that closely follows the reference forecast. There are some exceptions. Actual gas prices in Figure 2.8b drop below even the 10^{th} percentile of the simulated forecast during 2012. Additionally, the median simulated price forecasts for gas in Figure 2.8b and 2.9b are lower than the EIA reference gas forecast. Whether a forecast under- or over-predicts is determined by randomly drawing from a binomial distribution, with each outcome having equal probability. With the specified random number generation seed, the binomial draws result in a nearly even split of under- and over-predictions for oil prices but a skew towards under-predictions for gas prices. Since the cross-validation and prediction cases use the same probability draw sequence, the same result appears in both Figures 2.8b and 2.9b. Repeated tests with different random number seeds and varying numbers of MC simulation iterations have shown that while the directionality of the error for the median case can change, all of the other percentiles are relatively stable (e.g., there is almost no change in the distribution of

the forecast results between 10^4 and 10^5 MC simulation iterations; see Figure 2.10).

2.3.2 Drilling Forecasts

Applying Eq. (2.9) to the simulated price forecasts in Figures 2.8 and 2.9 produces the drilling forecasts presented in Figure 2.11 for the (a) cross-validation and (b) prediction cases. In cross-validation mode, the median drilling forecast over the 60-month period shown in Figure 2.11a (total of 4,486 wells) is a reasonable match for the actual drilling schedule (total of 4,272 wells). In prediction mode, lower energy prices result in reduced drilling activity (median case has a total of 3,121 wells).

2.3.3 Production Forecasts

Several production forecasts for different cases and assumptions are shown in Figures 2.12 – 2.15. Figure 2.12 shows monthly oil production rates from (a) new wells and (b) existing wells, as well as the monthly gas production rates from (c) new wells and (d) existing wells for the cross-validation case. The median result for oil production from new wells is an excellent match for the actual oil production from wells drilled during the 2010 – 2014 time period (73.1E+06 bbl simulated versus 71.9E+06 bbl actual). Simulated gas production from new wells is a good match to the actual production rate until 2013, at which point the median simulated gas production rate continues to increase while the actual gas production rate decreases. However, the actual gas production rate from new wells is still fully covered within the 10% - 90% interval. Oil and gas production from existing wells is also a reasonably close match (simulated production of 46.2E+06 bbl oil and 941E+06 MCF gas versus actual production of 47.3E+06 bbl oil and 956E+06 MCF gas), although there is a small but clear trend to underpredict

production at the beginning and overpredict production at the end of the simulation period. The under/over trend is due to well reworks; as more time passes, it becomes increasingly likely that a larger portion of the existing well population will be reworked (boosting production rates from reworked wells). However, neglecting reworks (by setting the rework probability to zero) leads to a substantial underprediction of production rates from existing wells (especially oil wells); see Figure 2.13.

Almost all of the variability in the production forecasts stems from the uncertainty in the drilling forecast (and its antecedent, the energy price forecast). Figure 2.14 shows the production rates of oil and gas from new wells if the actual drilling rates during the simulation period are taken as a given (i.e., the total number of wells drilled in each month is used for W instead of simulating W using Eq. (2.9)). Effectively, Figure 2.14 shows just the variability in production rates that stems from the random selection of (a) well location, (b) well type (oil or gas wells), and (c) decline curve coefficients from Eq. (2.12). Production rates in Figure 2.14 are nearly an exact match to actual production rates except for gas production after 2013. Given the close match between simulated versus actual gas production from 2010 – 2013, the discrepancy from 2013 – 2015 is due to (a) the well rework probability and (b) a drop in the actual number of gas wells being drilled. Assuming zero rework activity only partially reduces the discrepancy (median simulated gas production rates assuming no reworks is approximately 20E+06 MCF/month vs. the actual rate of 17.3E+06 MCF/month). As for the second cause, well location and type have certainly changed in the Uinta Basin over time, so there is likely some error introduced by the assumption that the location and type of new wells will follow the same pattern as past wells. Over the time period of 1984 – 2009, 53% of new

wells in the Uinta Basin were gas wells, however, during the time period of 2010 – 2014, that fraction dropped to 36%.

The total oil and gas production from all wells (new and existing) is shown in Figure 2.15 for the prediction case. Interestingly, even though fewer oil wells are drilled in the prediction case (as a consequence of the reduced energy price forecast) than in the cross-validation case, oil production rates nearly double. The higher oil production rate is a consequence of extrapolating the increased production rates that the industry has demonstrated over the last decade via the log-normal trendline fitting method discussed in the production forecast methodology section. Gas production rates, which are modeled using the empirical CDF method (and therefore assume that new gas wells will show the same production histories as previously drilled wells), increase more slowly over most of the simulation period.

Lastly, it is interesting to note how much production occurs from new wells versus existing wells. Figure 2.16 shows the fraction of production that is attributable to new wells for both oil and gas production in the cross-validation case for the simulated production forecast (median results) versus the actual production history. Presumably, new wells could be required to adhere to higher emissions standards than existing wells, which over time would drop out of production. The point at which new wells become responsible for more than 50% of the overall production is about two years for oil and three years for gas.

2.3.4 Emissions

VOC emissions calculated by applying the emission factors to the drilling and production forecasts are shown in Figures 2.17 and 2.18 on a monthly and annual basis, respectively. Both figures indicate the baseline and reduced emissions (as a result of implementing NSPS and state rules) for the cross-validation and prediction modes. As shown in Figure 2.17a and 2.18a, there is very little reduction in VOC emissions as a result of implementing the November 2012 NSPS rules in Table 2.5, since these emissions are only applied to newly drilled wells and the emissions reductions are not applied to the largest emissions categories (completions and gas transmission). The reductions that occur starting January 2015 have a much larger impact, as illustrated in Figure 2.17b. With these control reductions, emission rates remain flat at around 2,000 metric tons/month for the entire prediction period (nearly 50% lower than the base level emissions). Figure 2.18 gives a breakdown of emissions by source on an annual basis, and shows that the majority of the emissions are due to completion events, followed by gas transmission and gas production. As with Figure 2.17b, Figure 2.18b illustrates the impact of the emissions reductions and in particular of the EPA green completion rule, which dramatically decreases emissions from the completion category.

Comparing final emission results at the end of the cross-validation case (2014) in Figure 2.18a to the start of the prediction case (2015) in Figure 2.18b, we can see that there is an almost 25% reduction in median baseline emissions. The disparity is due to the differences in drilling and production rates at the end of the cross-validation case period (December 2014) versus the beginning of the prediction case period (January 2015). The step change indicates both the sensitivity of emissions rates (in the model and in reality)

to the oil and gas industry's business cycle and the importance of the uncertainty quantification. The starting point of the prediction period's median VOC emissions is equivalent to the 15th percentile of the cross-validation cases VOC emissions in December 2014.

2.4 Conclusions

In this study, we demonstrated a method for estimating (with uncertainty) the drilling, production, and emissions inventory of the oil and gas industry in Utah's Uinta Basin. In cross-validation tests, the median simulation results have proven to be highly accurate at matching the test history data. Assuming that the emission factors found in our literature review are representative, the VOC emissions rate for the oil and gas industry during the 2010 – 2015 time period would be 43.7E+06 (mean) ± 9.86E+06 (SD) kg VOCs per year. Given the downturn in the oil and gas industry and assuming that proposed regulations are implemented, the VOC emissions rate for the oil and gas industry during the 2015 – 2019 time period will drop by 45% to 24.1E+06 ± 2.67E+06 kg VOCs per year. This emissions reduction occurs despite the fact that oil production rates are expected to roughly double over the course of the prediction period (and gas production rates are expected to slightly increase). Higher production rates do not increase VOC emission rates in the prediction case because (a) emissions from well completions are reduced by both lower drilling rates and EPA green completion rules, (b) emission factors from oil production are small compared to gas production and gas processing, and (c) production from new wells with stricter emissions standards rapidly replace production from older wells without emission controls (within two to three years

in the cross-validation case).

Energy prices are the largest source of uncertainty and volatility in drilling and production forecasting. Other sources of error exist such as the distributed drilling lag models, the well rework probability CDFs, and the changing patterns in the location, production, and types of wells. However, the demonstrated unpredictability of energy markets makes any forecast of future oil and gas development difficult to gauge with certainty.

2.5 References

Ahmadov, R., S. McKeen, M. Trainer, R. Banta, A. Brewer, S. Brown, P.M. Edwards, et al. 2015. "Understanding High Wintertime Ozone Pollution Events in an Oil- and Natural Gas-Producing Region of the Western US." *Atmospheric Chemistry and Physics* 15 (1): 411–29. doi:10.5194/acp-15-411-2015.

Allen, D.T., V.M. Torres, J. Thomas, D.W. Sullivan, M. Harrison, A. Hendler, S.C. Herndon, et al. 2013. "Measurements of Methane Emissions at Natural Gas Production Sites in the United States." *Proceedings of the National Academy of Sciences of the United States of America*, October, 1–6. doi:10.1073/pnas.1304880110.

American Petroleum Institute, and America's Natural Gas Alliance. 2012. "Characterizing Pivotal Sources of Methane Emissions from Natural Gas Production." http://www.api.org/~/media/Files/News/2012/12-October/API-ANGA-Survey-Report.pdf.

Argonne National Laboratory. 2014. "Greenhouse Gases, Regulated Emissions, and Energy Use in Transportation Model." https://greet.es.anl.gov/.

Arps, J.J. 1945. "Analysis of Decline Curves." *Transactions of the American Institute of Mining, ...* 160 (160): 228. http://www.pe.tamu.edu/blasingame/data/z_zCourse_Archive/P689_reference_02C/z_P689_02C_ARP_Tech_Papers_(Ref)_(pdf)/SPE_00000_Arps_Decline_Curve_Analysis.pdf.

Bar-Ilan, A., J. Grant, R. Parikh, R. Morris, and A.B. Ilan. 2011. "Oil and Gas Mobile Sources Pilot Study." Novato, CA. http://www.wrapair2.org/pdf/2011-07_P3 Study Report (Final July-2011).pdf.

Canadian Association of Petroleum Producers. 1999. "Fugitive Emissions from Oil and Natural Gas Activities." http://www.ipcc-nggip.iges.or.jp/public/gp/bgp/2_6_Fugitive_Emissions_from_Oil_and_Natural_Gas.pdf.

Clark, C., J. Han, A. Burnham, J. Dunn, and M. Wang. 2011. "Life-Cycle Analysis of Shale Gas and Natural Gas." Argonne, IL. http://www.transportation.anl.gov/pdfs/EE/813.PDF.

Doublet, L., P. Pande, T. McCollum, T. Blasingame, and T. McColum. 1994. "Decline Curve Analysis Using Type Curves--Analysis of Oil Well Production Data Using Material Balance Time: Application to Field Cases." In *International Petroleum Conference and Exhibition of Mexico*. Veracruz, Mexico: Society of Petroleum Engineers. https://www.onepetro.org/conference-paper/SPE-28688-MS.

Environ. 2015. "Final Report 2014 Uinta Basin Winter Ozone Study." Salt Lake City, UT. http://www.deq.utah.gov/locations/U/uintahbasin/ozone/docs/2015/02Feb/UBWOS_2014_Final.pdf.

Fetkovich, M., E. Fetkovich, and M. Fetkovich. 1996. "Useful Concepts for Decline Curve Forecasting, Reserve Estimation, and Analysis." *SPE Reservoir Engineering* 11 (1): 13–22. http://www.onepetro.org/mslib/servlet/onepetropreview?id=00028628.

HDR Engineering. 2013. "Final Report : Uinta Basin Energy and Transportation Study." Salt Lake City, UT. http://www.utssd.utah.gov/documents/ubetsreport.pdf.

Howarth, R.W., R. Santoro, and A. Ingraffea. 2011. "Methane and the Greenhouse-Gas Footprint of Natural Gas from Shale Formations." *Climatic Change* 106 (4): 679–90. doi:10.1007/s10584-011-0061-5.

IPCC. 2007. "Fourth Assessment Report: Climate Change 2007 IPCC, Section 2.10.2 Direct Global Warming Potentials." https://www.ipcc.ch/publications_and_data/ar4/wg1/en/ch2s2-10-2.html.

Jiang, M., W. Michael Griffin, C. Hendrickson, P. Jaramillo, J. VanBriesen, and A. Venkatesh. 2011. "Life Cycle Greenhouse Gas Emissions of Marcellus Shale Gas." *Environmental Research Letters* 6 (3): 034014. doi:10.1088/1748-9326/6/3/034014.

Karion, A., C. Sweeney, G. Pétron, G. Frost, R. Michael Hardesty, J. Kofler, B.R. Miller, et al. 2013. "Methane Emissions Estimate from Airborne Measurements over a Western United States Natural Gas Field." *Geophysical Research Letters* 40 (16): 4393–97. doi:10.1002/grl.50811.

Ling, K., and J. He. 2012. "Theoretical Bases of Arps Empirical Decline Curves." In *Abu Dhabi International Petroleum Conference and ...*. Abu Dhabi, UAE: Society of Petroleum Engineers. http://www.onepetro.org/mslib/servlet/onepetropreview?id=SPE-161767-MS.

O'Sullivan, F., and S. Paltsev. 2012. "Shale Gas Production: Potential versus Actual Greenhouse Gas Emissions." *Environmental Research Letters* 7 (4): 044030. doi:10.1088/1748-9326/7/4/044030.

Okouma Mangha, V., D. Ilk, T.A. Blasingame, D. Symmons, and N. Hosseinpour-zonoozi. 2012. "Practical Considerations for Decline Curve Analysis in Unconventional Reservoirs - Application of Recently Developed Rate-Time Relations." In *SPE Hydrocarbon Economics and Evaluation Symposium*. Calgary, Alberta, Canada: Society of Petroleum Engineers. doi:10.2118/162910-MS.

Oswald, W. 2015. Personal Communication. Utah Division of Air Quality.

Oswald, W., K. Harper, P. Barickman, and C. Delaney. 2014. "Using Growth and Decline Factors to Project VOC Emissions from Oil and Gas Production." *Journal of the Air & Waste Management Association* 65 (1): 64–73. doi:10.1080/10962247.2014.960104.

Pétron, G., G. Frost, B.R. Miller, A.I. Hirsch, S. a. Montzka, A. Karion, M. Trainer, et al. 2012. "Hydrocarbon Emissions Characterization in the Colorado Front Range: A Pilot Study." *Journal of Geophysical Research* 117 (D4): D04304. doi:10.1029/2011JD016360.

R Core Team. 2015. "R: A Language and Environment for Statistical Computing." Vienna, Austria. http://www.r-project.org/.

Santoro, R.L., R.H. Howarth, and A.R. Ingraffea. 2011. "Indirect Emissions of Carbon Dioxide from Marcellus Shale Gas Development." Ithaca, NY. http://www.eeb.cornell.edu/howarth/publications/IndirectEmissionsofCarbonDioxidefromMarcellusShaleGasDevelopment_June302011.pdf.

Shirman, E. 1998. "Universal Approach to the Decline Curve Analysis." In *Proceedings of 49th Annual Technical Meeting*. Calgary, Alberta, Canada: Society of Petroleum Engineers. doi:10.2118/98-50.

Skone, T.J., J. Littlefield, J. Marriott, G. Cooney, M. Jamieson, J. Hakian, and G. Schivley. 2014. "Life Cycle Analysis of Natural Gas Extraction and Power Generation." http://www.netl.doe.gov/File Library/Research/Energy Analysis/Life Cycle Analysis/NETL-NG-Power-LCA-29May2014.pdf.

U.S. EIA. 2010a. "Annual Energy Outlook 2010." Washington, DC. http://www.eia.gov/oiaf/archive/aeo10/index.html.

———. 2010b. "Oil and Gas Lease Equipment and Operating Costs 1994 Through 2009." Washington, DC. http://www.eia.gov/pub/oil_gas/natural_gas/data_publications/cost_indices_equipment_production/current/coststudy.html.

———. 2015a. "Annual Energy Outlook 2014 Retrospective Review." Washington, DC. http://www.eia.gov/forecasts/aeo/retrospective/.

———. 2015b. "Annual Energy Outlook 2015." Washington, DC. http://www.eia.gov/forecasts/aeo/pdf/0383(2015).pdf.

———. 2015c. "Utah Crude Oil First Purchase Price." *Domestic Crude Oil First Purchase Prices by Area*. http://www.eia.gov/dnav/pet/hist/LeafHandler.ashx?n=pet&s=f004049__3&f=m.

———. 2015d. "Utah Natural Gas Wellhead Price." *Natural Gas Wellhead Price*. http://www.eia.gov/dnav/ng/hist/na1140_sut_3a.htm.

U.S. EPA. 2012. *Oil and Natural Gas Sector: New Source Performance Standards and National Emission Standards for Hazardous Air Pollutants Reviews; Final Rule*. *Federal Registrar*. Vol. 77. United States: Federal Register. http://www.gpo.gov/fdsys/pkg/FR-2012-08-16/pdf/2012-16806.pdf.

———. 2013. "Inventory for the Oil and Gas Sector for the Uintah Basin." http://ftp.epa.gov/EmisInventory/2011v6/flat_files.

University of North Carolina at Chapel Hill. 2014. "SMOKE v3.6 User's Manual." University of North Carolina-Chapel Hill. https://www.cmascenter.org/smoke/documentation/3.6/html/.

Utah DOGM. 2015. "Data Research Center." *Division of Oil, Gas & Mining - Oil and Gas Program*. http://oilgas.ogm.utah.gov/Data_Center/DataCenter.cfm.

Utah State University. 2013. "2012 Uinta Basin Winter Ozone & Air Quality Study Final Report." Logan, UT. http://rd.usu.edu/files/uploads/ubos_2011-12_final_report.pdf.

Walton, I. 2014. "Shale Gas Production Analysis - Phase 1." Salt Lake City, UT.

Western Regional Air Partnership. 2008. "Oil/Gas Emissions Workgroup: Phase III Inventory." http://www.wrapair.org/forums/ogwg/PhaseIII_Inventory.html.

Zhang, Y., C.W. Gable, G. a. Zyvoloski, and L.M. Walter. 2009. "Hydrogeochemistry and Gas Compositions of the Uinta Basin: A Regional-Scale Overview." *AAPG Bulletin* 93 (8): 1087–1118. doi:10.1306/05140909004.

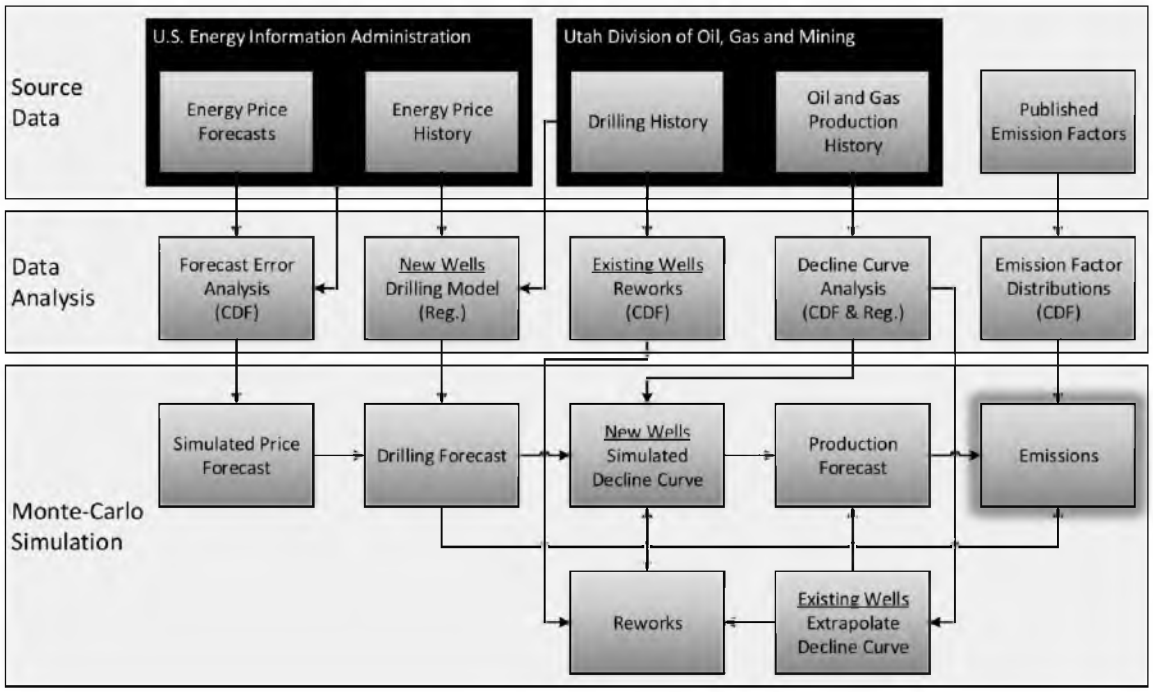

Figure 2.1: Diagram of emissions model.

(a)

(b)

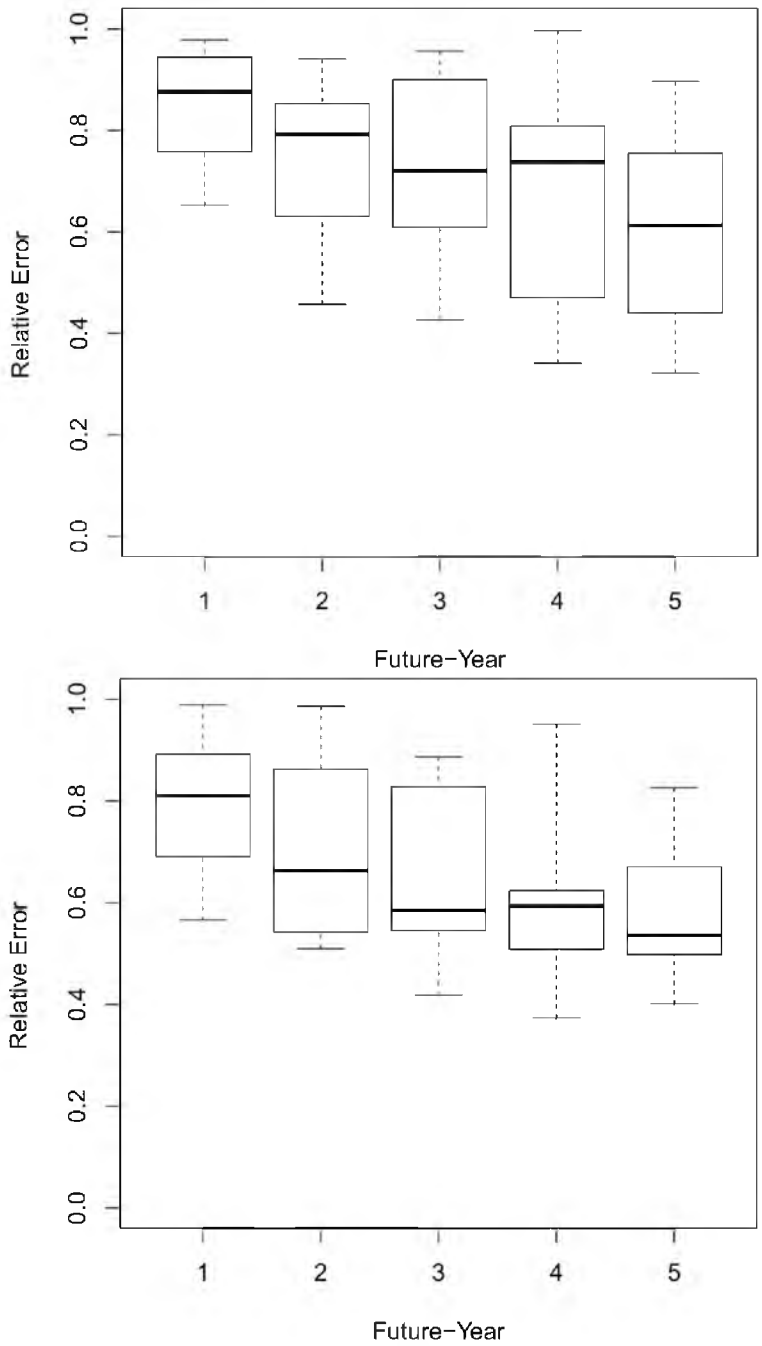

Figure 2.2: Boxplot of relative error between actual FPPs of (a) oil and (b) gas vs. EIA AEO wellhead oil and gas prices in the Rocky Mountain region as calculated by Eq. (1). Negative values indicate that EIAs forecasted underpredicted actual prices, while positive values indicate that they overpredicted.

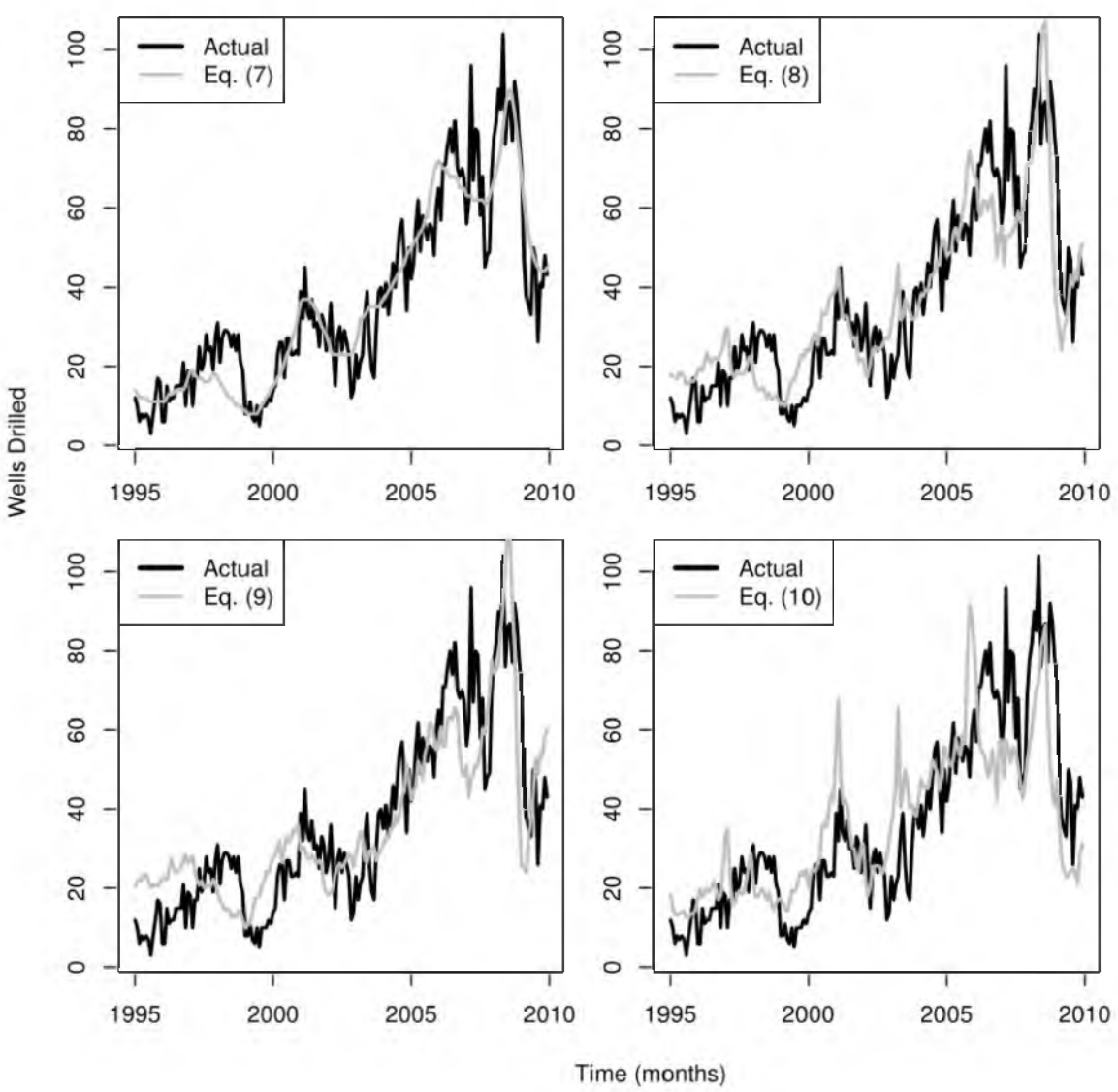

Figure 2.3: Training fit of distributed lag drilling models Eqs. (2.7) – (2.10). Actual drilling (Utah DOGM 2015) and energy price (U.S. EIA 2015d; U.S. EIA 2015c) histories from Jan. 1995 – Dec. 2009 were used to find the best fit for each model using least-squares regression.

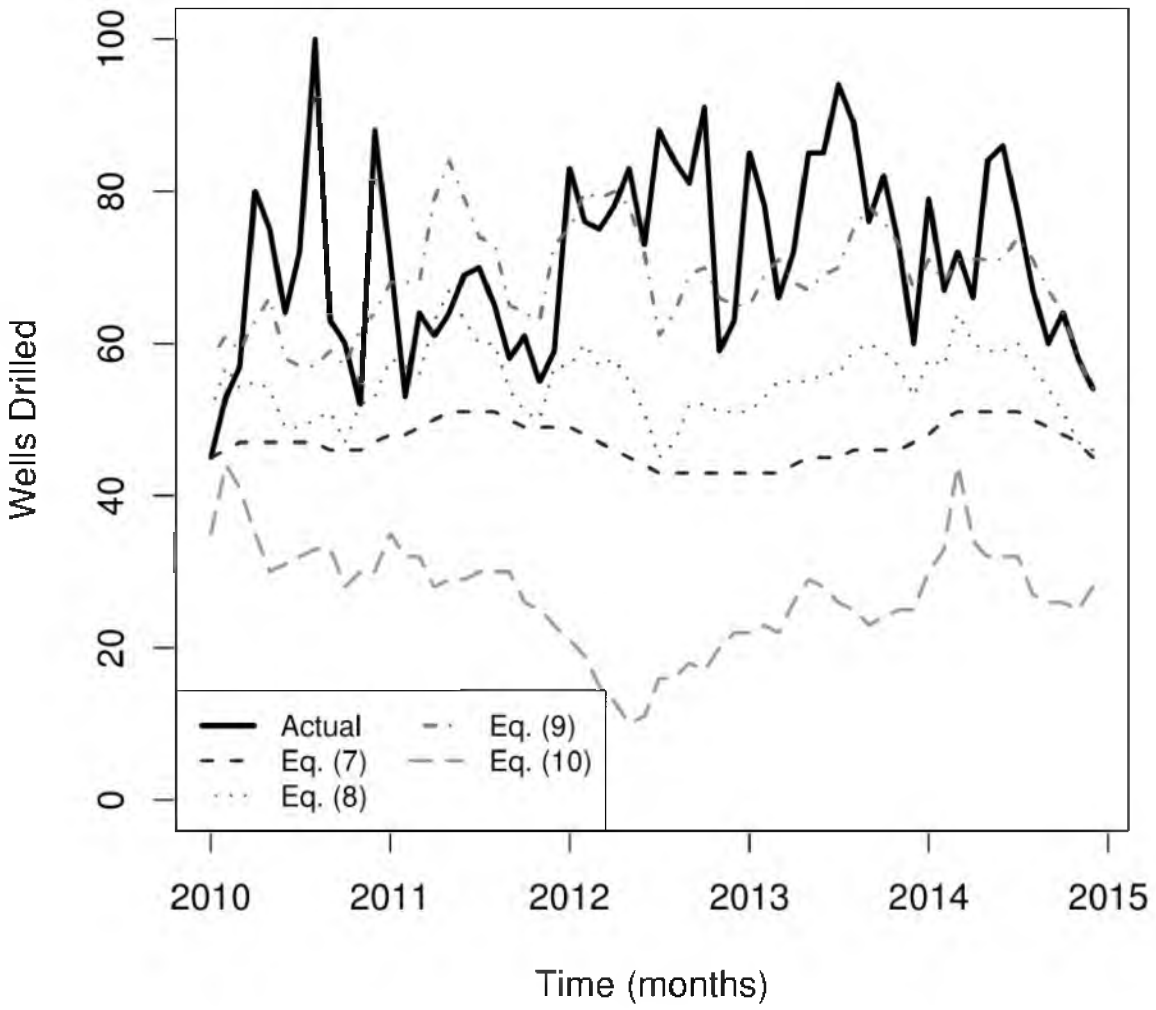

Figure 2.4: Cross-validation test of distributed lag drilling models Eqs. (2.7) – (2.10). Each model was tested against actual drilling (Utah DOGM 2015) and energy price (U.S. EIA 2015d; U.S. EIA 2015c) histories from Jan. 2010 – Dec. 2014.

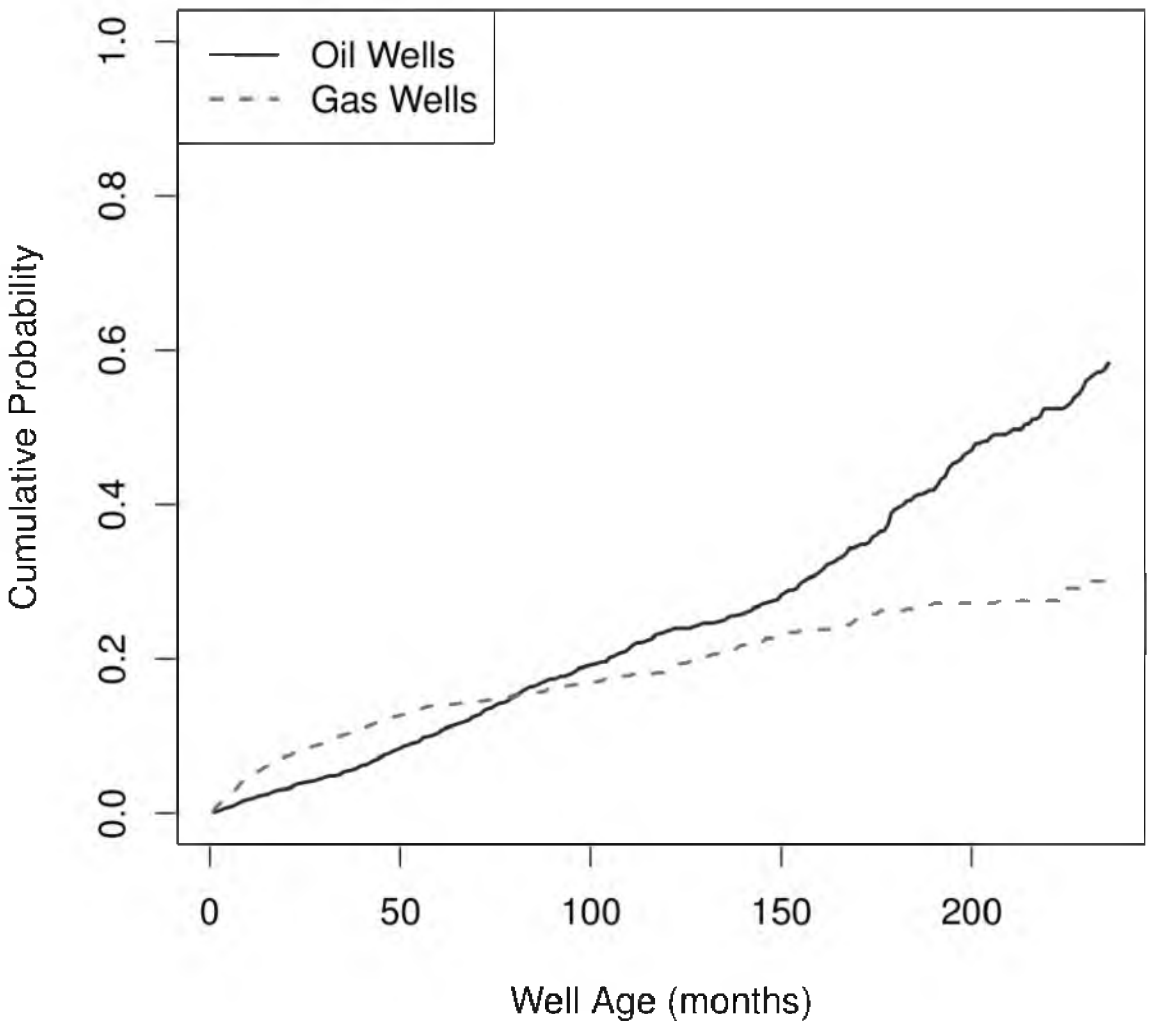

Figure 2.5: Well rework CDF describing probability of a well having at least one rework event based on (a) well age and (b) well type (oil or gas).

(a)

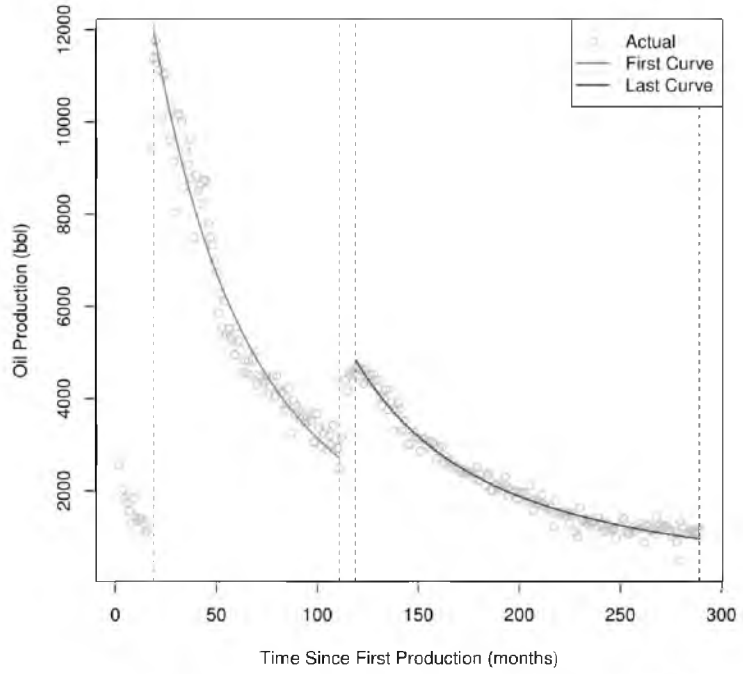

(b)

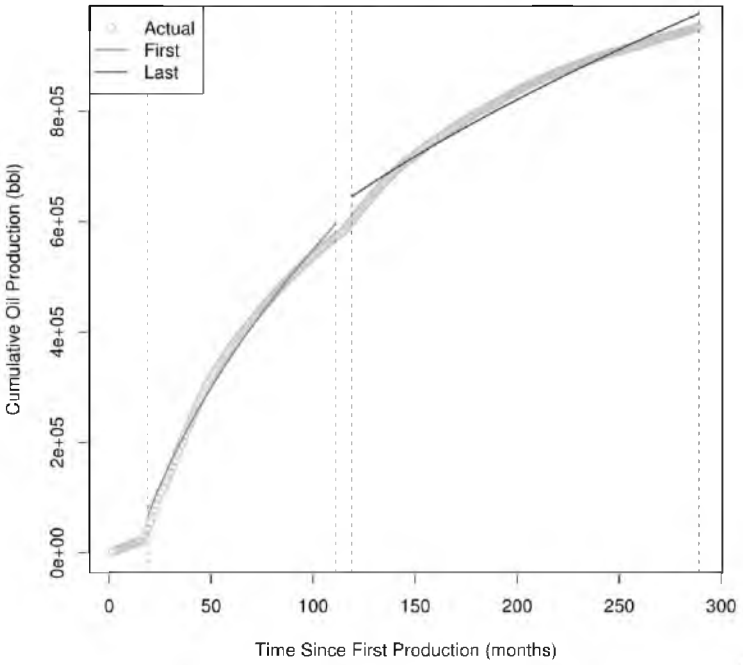

Figure 2.6: Decline curve analysis fitting (a) Eq. (11) to monthly oil rates and (b) Eq. (12) to cumulative oil production from an oil well in the Uinta Basin (API # 43-013-31123). Dashed lines indicate the time index identified as a start/stop point by the algorithm responsible for finding distinct decline curve segments. Both the hyperbolic and cumulative curve fits use the same start/stop points. If only a single curve is found then that curve counts as both the "first" and "last" curve. The production segment at the very beginning ($t < 24$ months) is ignored by the algorithm because some wells have short and sporadic decline curves during their first few years of operation.

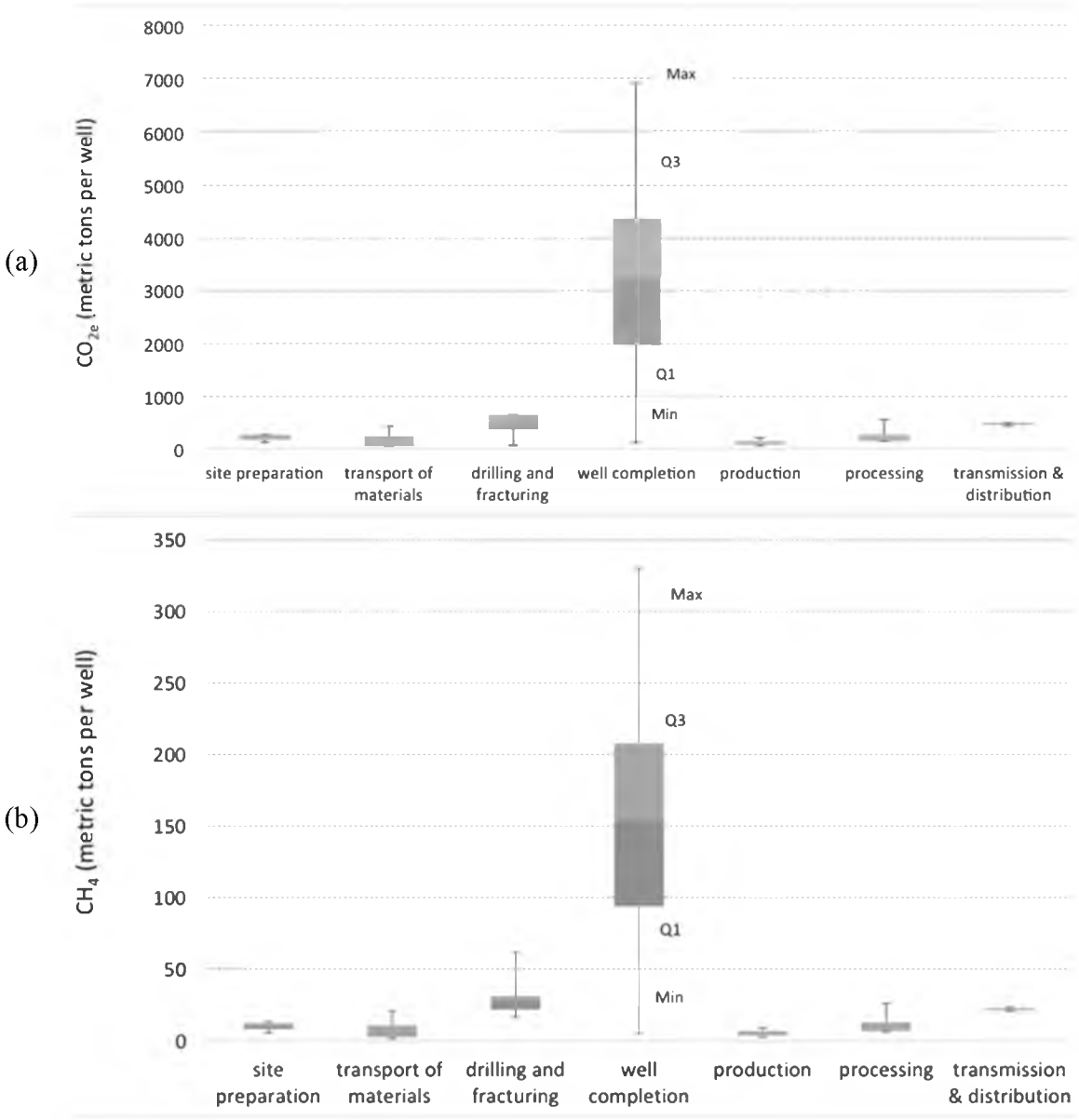

Figure 2.7: Boxplot of (a) CO2e and (b) CH4 emissions per gas well. This includes all emissions identified in the literature, both controlled and uncontrolled.

(a)

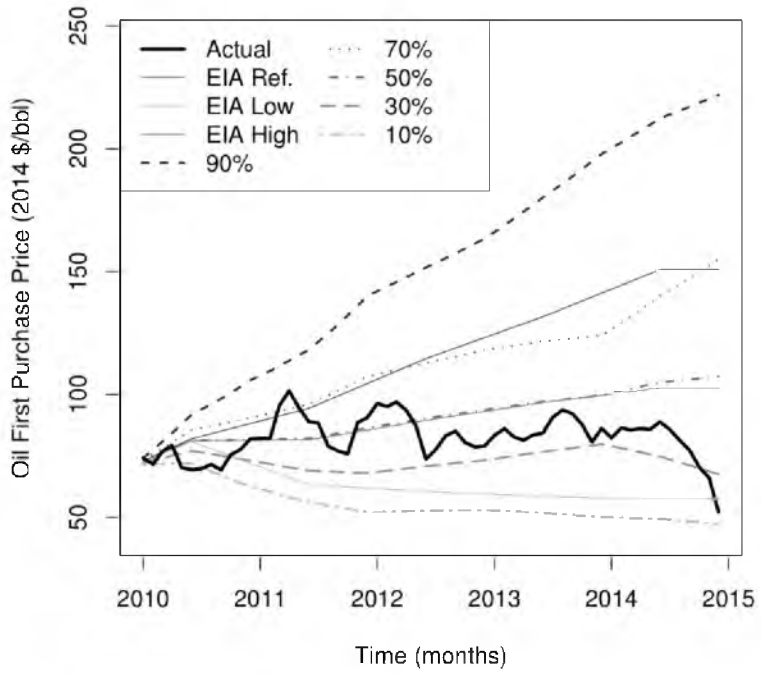

(b)

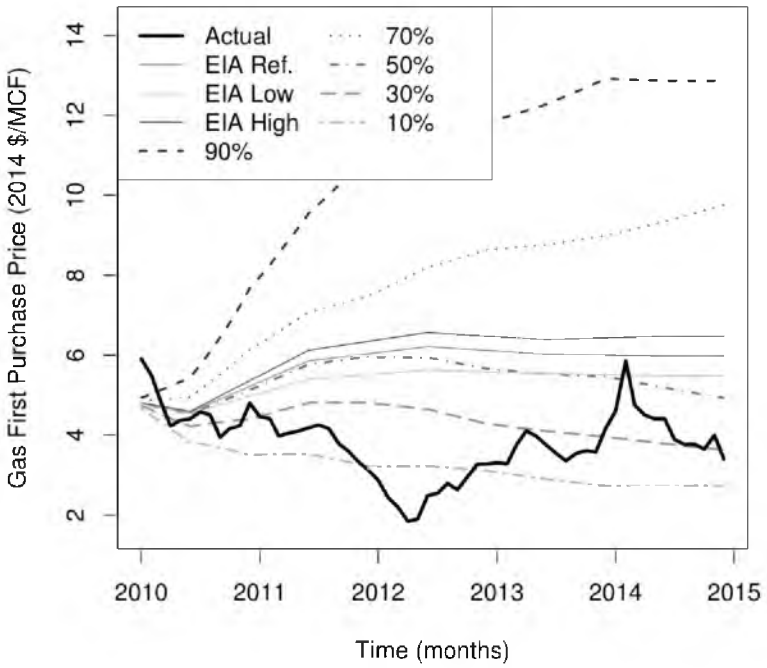

Figure 2.8: Simulated energy price forecast for the cross-validation case for (a) oil and (b) gas FPPs. Various percentiles of results are shown as dotted lines, actual prices as solid black lines, and EIA AEO 2010 (U.S. EIA 2010a) price forecasts as grey scale lines.

(a)

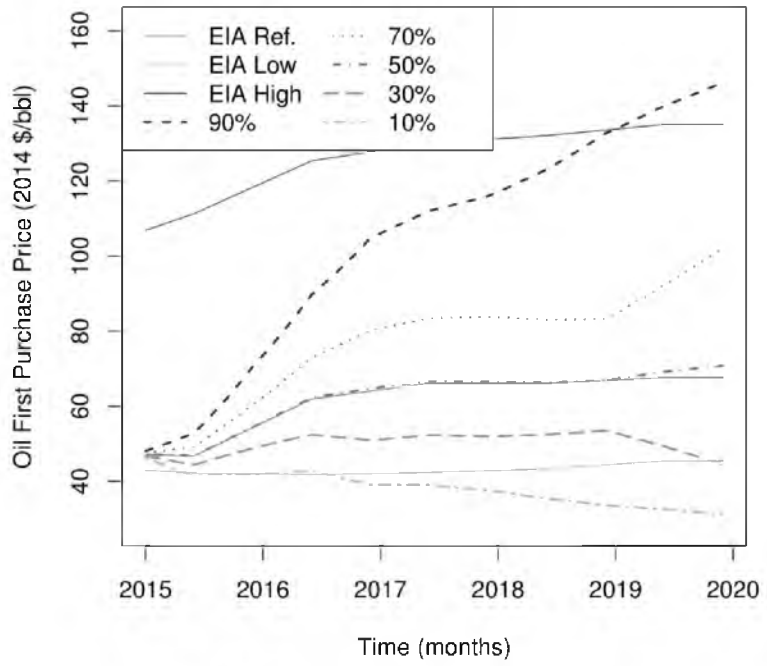

(b)

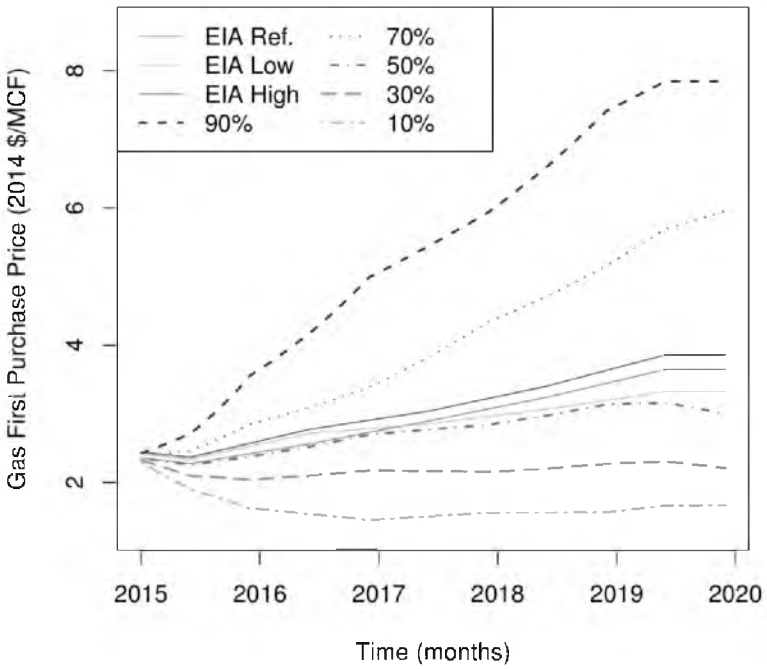

Figure 2.9: Simulated energy price forecast for the prediction case for (a) oil and (b) gas FPPs. Various percentiles of results are shown as dotted lines, actual prices as solid black lines, and EIA AEO 2015 (U.S. EIA 2015b) price forecasts as grey scale lines.

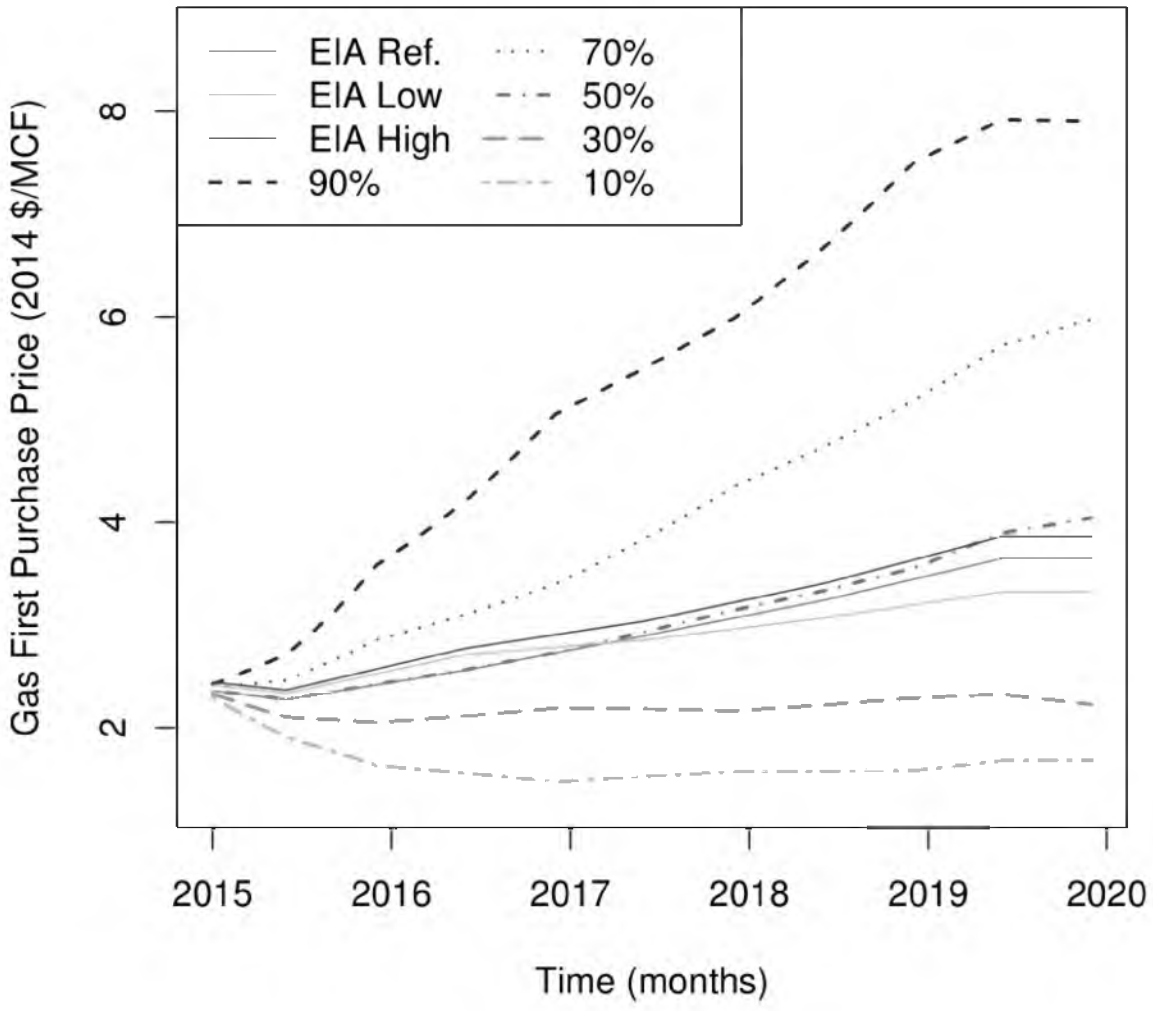

Figure 2.10: Simulated energy price forecast for the prediction case for gas FPPs using the same random number generation seed as Figures (8b) and (9b), but with 105 MC simulation iterations instead of 104 iterations. Since the number of random draws changes, the directionality of the under/over-prediction changes for the median case, but the other percentile results are nearly identical between the two sample sizes.

(a)

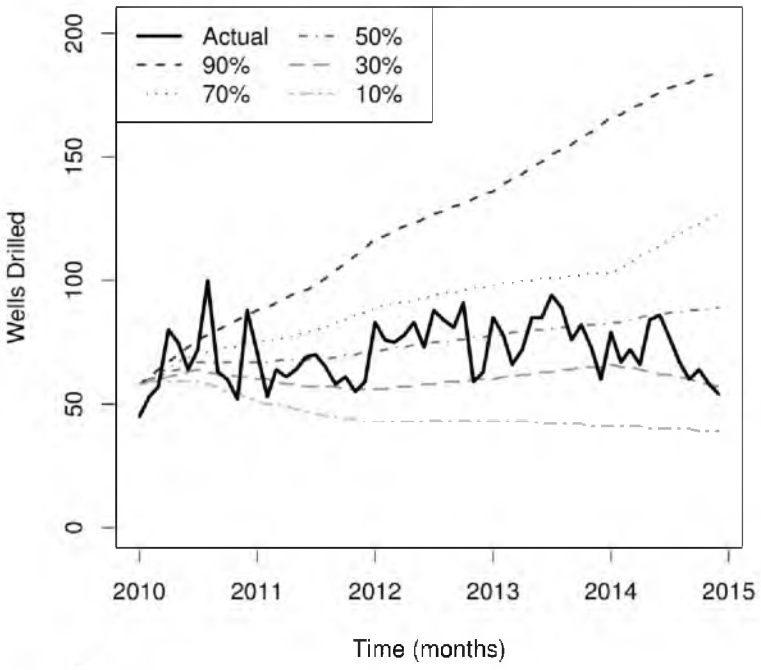

(b)

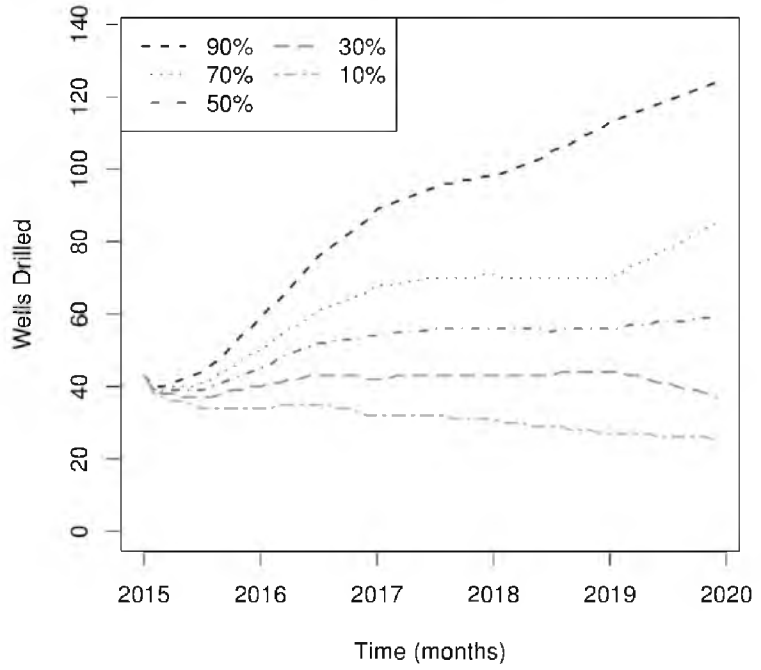

Figure 2.11: Drilling forecast for the (a) cross-validation and (b) prediction cases.

(a)

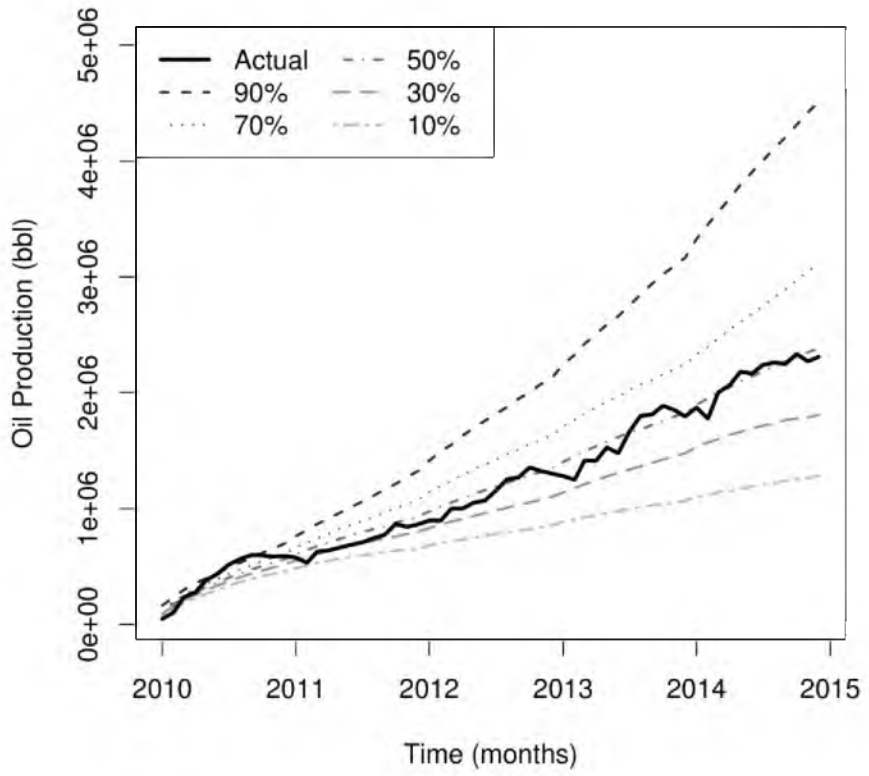

(b)

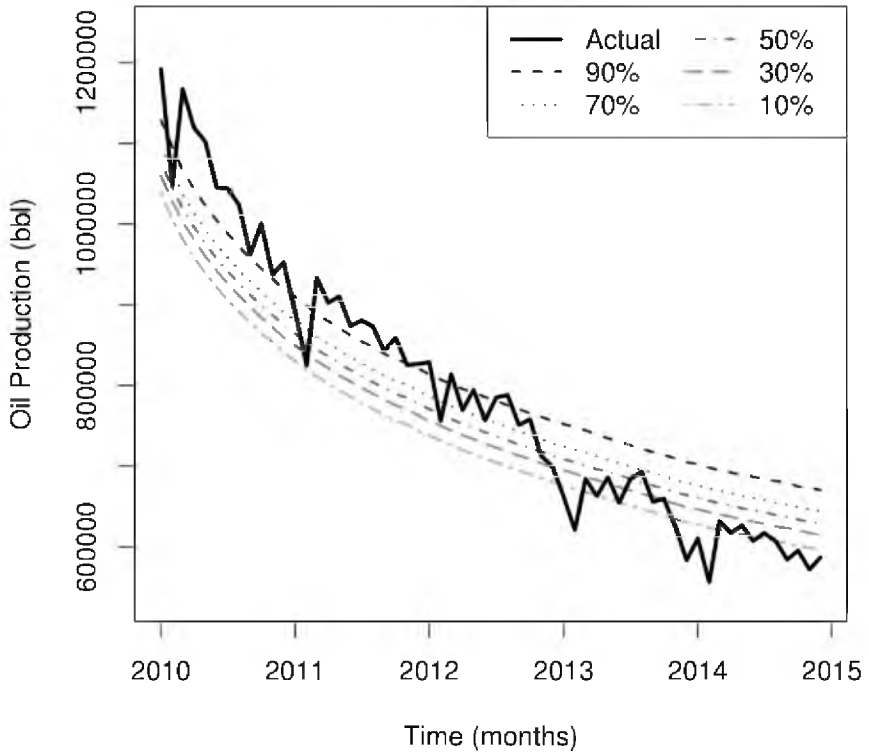

Figure 2.12: Production forecast for the cross-validation case for (a) oil production from new wells, (b) oil production from existing wells, (c) gas production from new wells, and (d) gas production from existing wells.

(c)

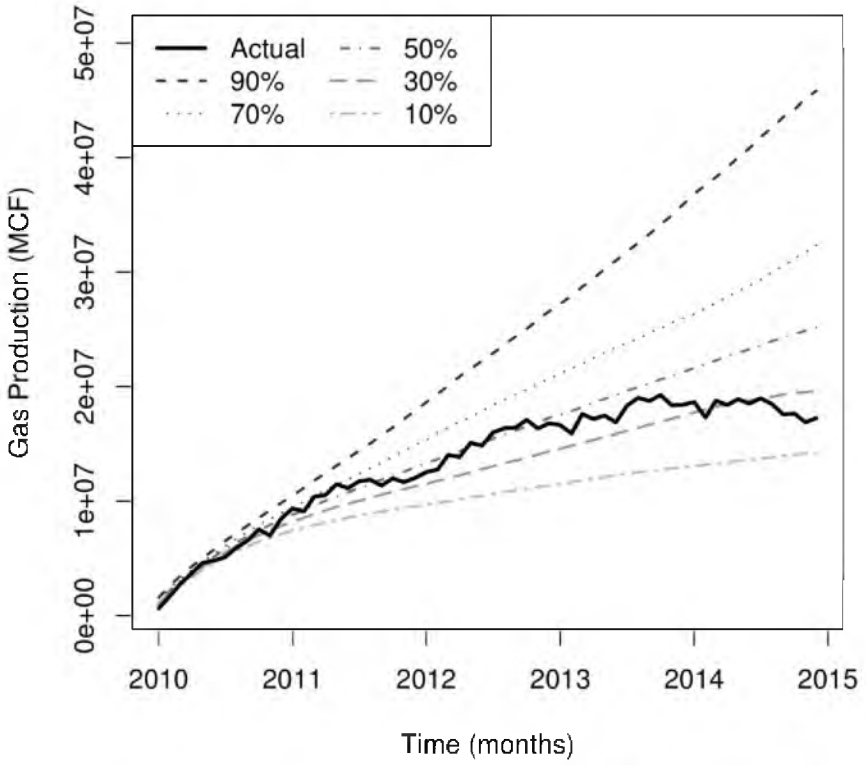

(d)

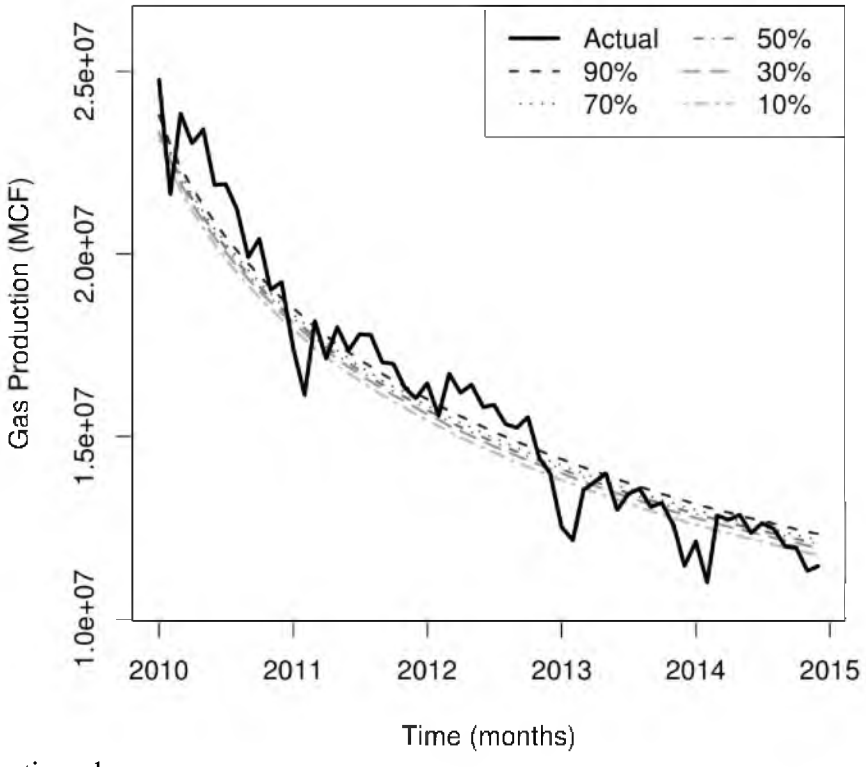

Figure 2.12: Continued.

(a)

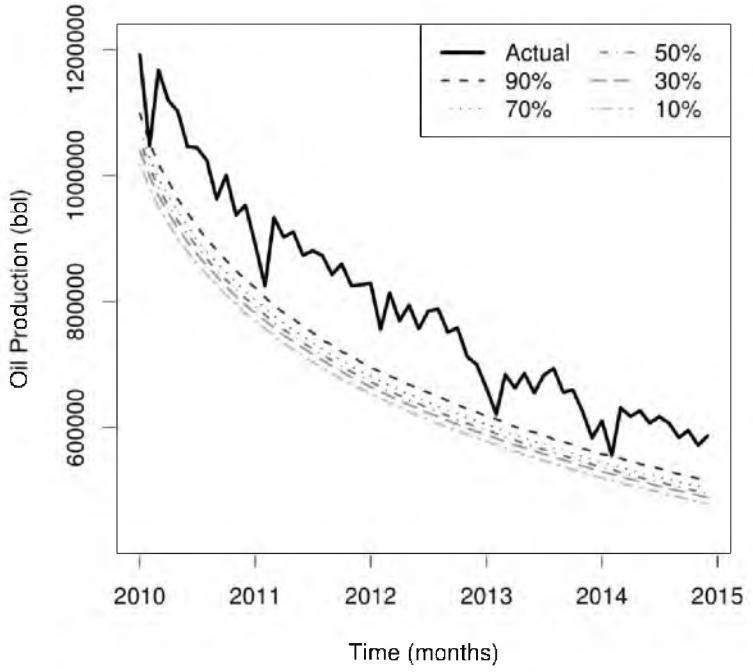

(b)

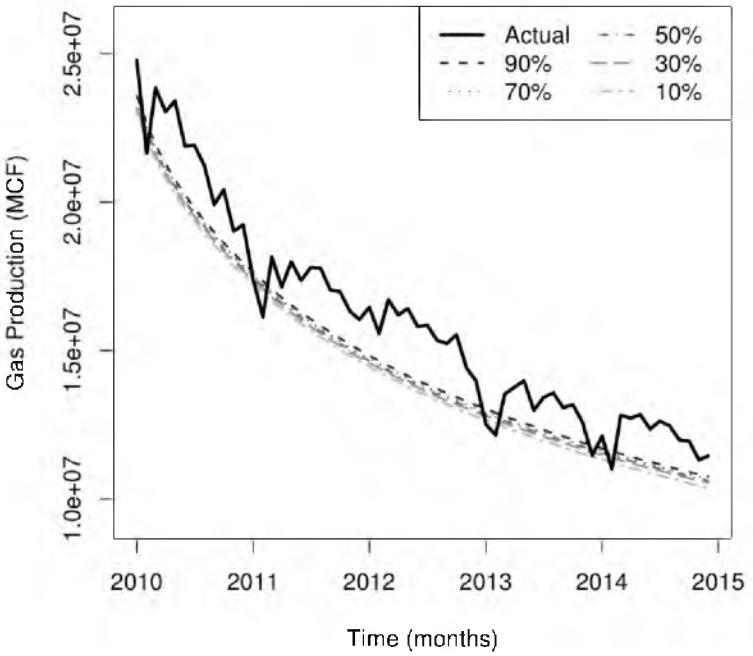

Figure 2.13: Production forecast for the cross-validation case for production of (a) oil and (b) gas from existing wells, assuming no well reworks occur.

(a)

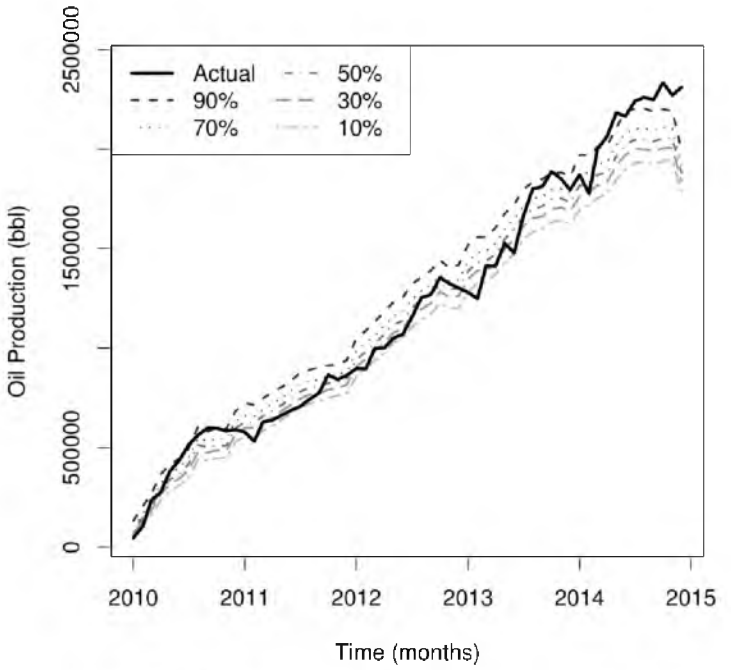

(b)

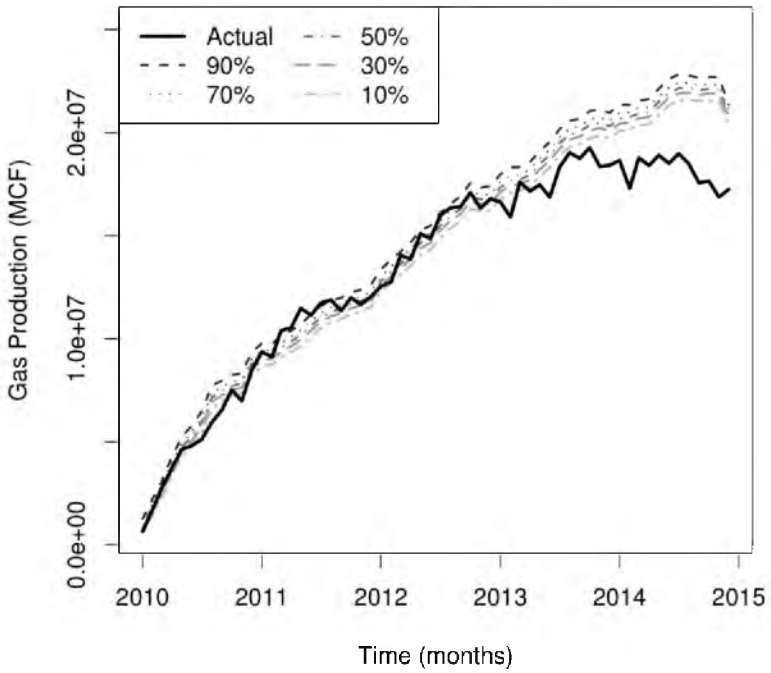

Figure 2.14: Production forecast for the cross-validation case for (a) oil and (b) gas production from new wells, taking the actual drilling schedule as a given.

(a)

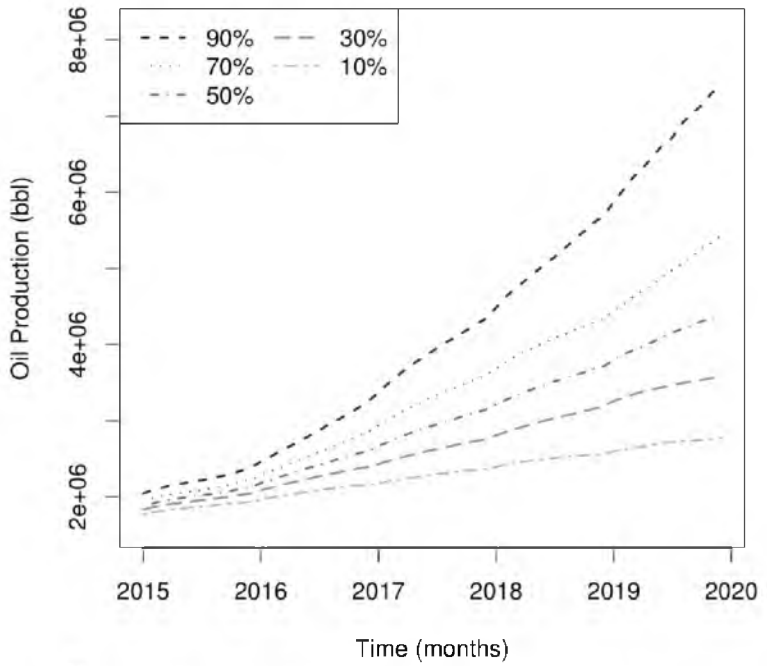

(b)

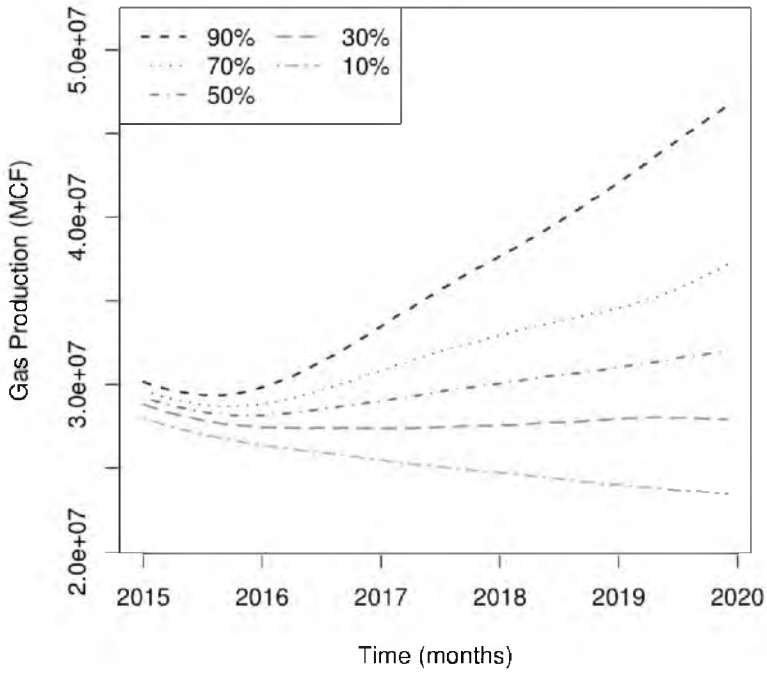

Figure 2.15: Production forecast for the prediction case for (a) oil and (b) gas production from all (new and existing) wells.

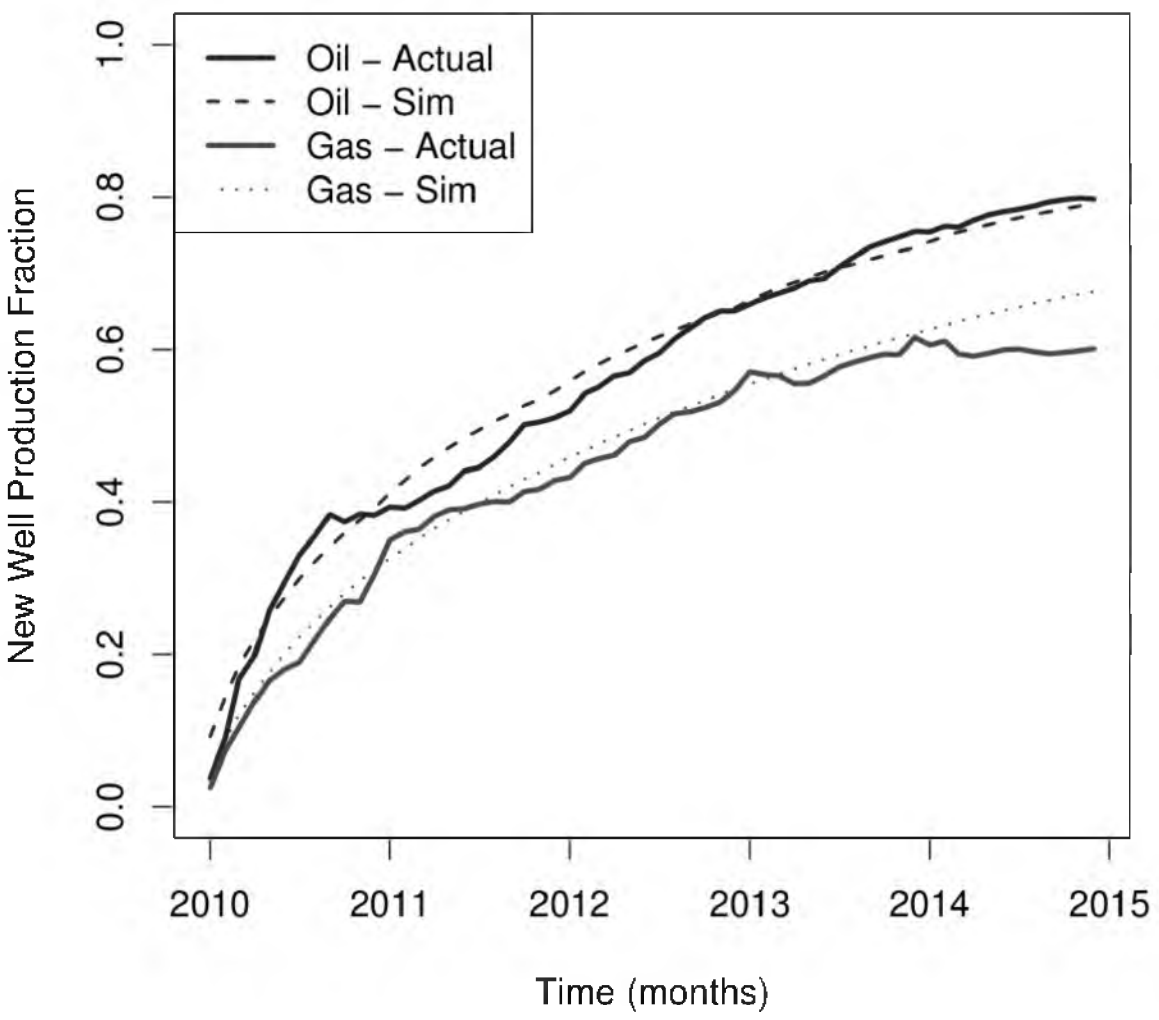

Figure 2.16: Fraction of total production that is generated from new wells as a function of time for the cross-validation case. Simulated results are shown as dotted lines and the actual production history as solid lines.

(a)

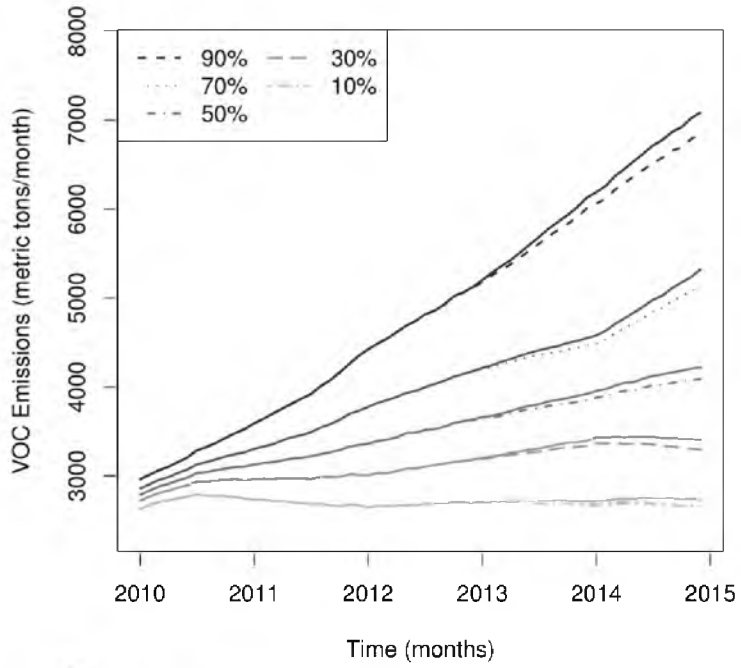

(b)

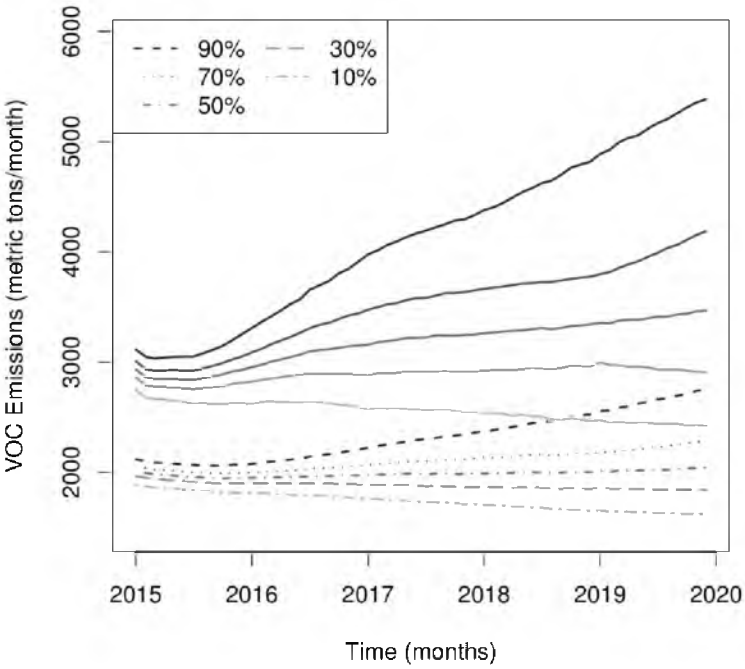

Figure 2.17: VOC emissions percentile results for the (a) cross-validation and (b) prediction cases. Base emissions are shown as solid grey-scale lines and reduced emissions from NSPS and state rules are shown as dotted lines.

(a)

(b)

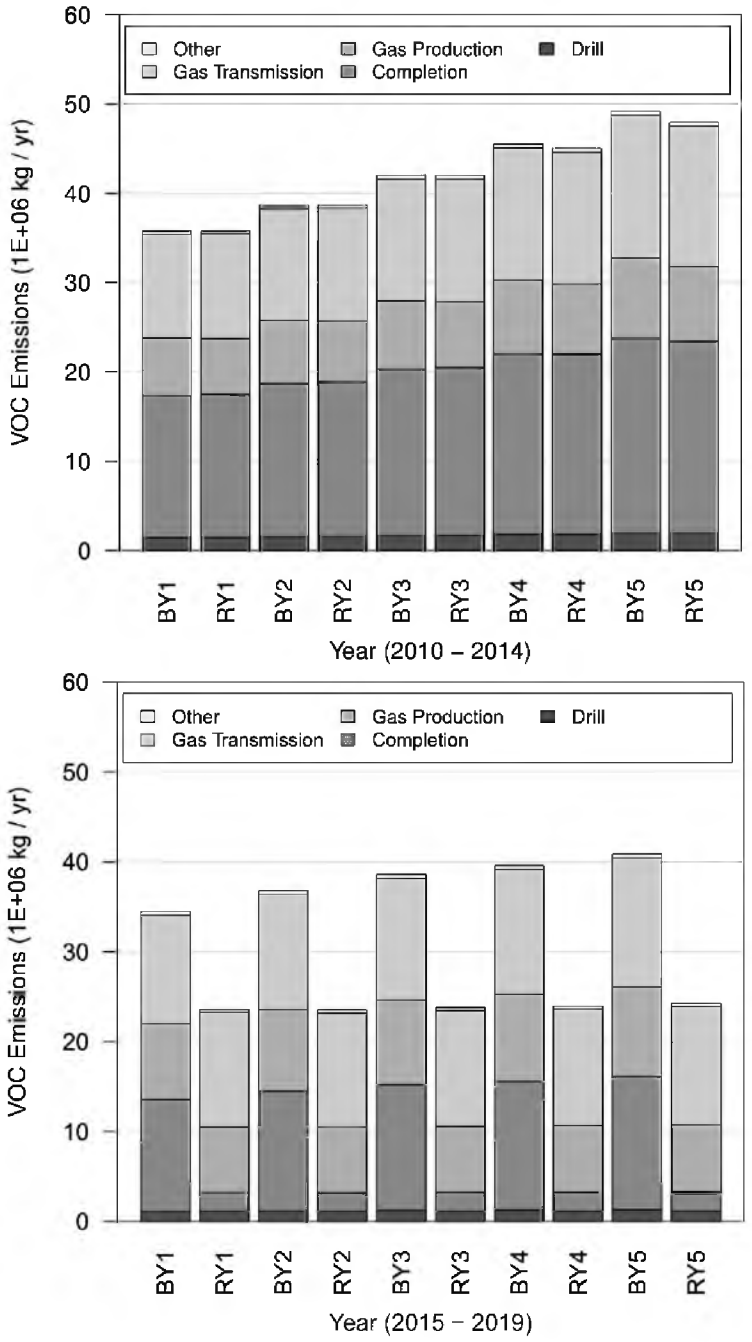

Figure 2.18: Total median (50th percentile) VOC emissions for the (a) cross-validation and (b) prediction cases. Results are shown by year (Y1, Y2, etc.) and source for baseline emissions (B) and reduced emissions (R). Activities in the "Other" category include reworking, gas processing, oil production, and oil transportation.

Table 2.1: Relative error beta distribution shape parameters α and β for oil and gas by future-year.

Forecast Type	Future-Year	α parameter	β parameter	R^2	Data points
Gas	1	6.214	1.666	0.988	16
Gas	2	3.034	1.212	0.875	15
Gas	3	5.330	2.859	0.897	14
Gas	4	4.575	2.937	0.887	13
Gas	5	8.047	5.995	0.908	12
Oil	1	8.650	1.507	0.976	16
Oil	2	5.549	1.975	0.974	15
Oil	3	4.185	1.642	0.949	14
Oil	4	2.345	0.998	0.957	13
Oil	5	4.736	3.058	0.976	12

Table 2.2: Distributed lag drilling model fit (training period 1995 – 2009) and cross-validation (test period 2010 – 2014) results. "Test period RSS" refers to the residual sum of squares during the cross-validation test period.

Distributed Lag Model	Coefficient a	b	c	d	Training Period R^2	Test Period RSS
Eq. (7)	0.072	0.742	0.867	-1.987	0.865	4.50E+04
Eq. (8)	0.590	3.382	-6.889		0.736	2.53E+04
Eq. (9)	0.844	-1.451			0.699	9.31E+03
Eq. (10)	8.293	-4.923			0.609	1.33E+05

Table 2.3: Best estimates of emission factors for the Uinta Basin prior to implementation of EPA's New Source Performance Standards (NSPS) and new state rules on pneumatic controllers. The acronym "TM" stands for transportation of materials.

Activity	CO_2e	CH_4	VOCs	Units
Site-preparation (excluding rig transportation) [1]	208±79	9.9±3.37	1.58±0.60	10^3 kg/well
TM Drilling[2]	0.40±0.56	8.6E-06±1.22E-05	1.38E-06±1.95E-06	10^3 kg/well
TM Completions[2]	0.21±0.29	4.36E-06±6.16E-06	6.97E-07±9.86E-07	10^3 kg/well
TM Rework[2]	3.05±4.31	7.71E-05±1.01E-04	1.15E-05±1.62E-05	10^3 kg/well
TM Production[2]	1.36±1.93	3.29E-05±4.65E-05	5.26E-06±7.43E-06	10^3 kg/well
Well completion[3]	1940±967	92.4±46	14.8±7.37	10^3 kg/well completion
Gas production[4]	43±40	2.07±1.90	0.78±0.73	10^3 kg/year well
Gas processing[5]	901±46	5.58±3.91	0.89±0.62	10^3 kg / 10^9 ft^3 of total natural gas production
Gas transmission & distribution[6]	4177±3423	199±163	31.8±26	10^3 kg / 10^9 ft^3 of total natural gas production

Table 2.3: Continued.

Activity	CO_2e	CH_4	VOCs	Units
Gas transmission & distribution[6]		1.04±0.85	0.17±0.14	% of CH_4 produced over well's lifecycle

1. Corresponds to the average of the emission factors by Jiang et al. (2011) and Santoro et al. (2011).
2. Based on a study of transportation emissions in the Piceance Basin of Northwestern Colorado (Bar-Ilan et al., 2011). Uncertainty estimates for VOCs not available.
3. This value corresponds to the average of the emission factors reported by O'Sullivan and Paletsev (2012) for tight oil wells, Skone et al. (2014) for tight gas wells, API (2012) for the Rocky Mountain region, Allen et al. (2013) for the Rocky Mountain region. Skone et al. assumes that tight gas well completion emission factor is 40% of the emission factor for shale gas wells completion. This value includes both controlled and uncontrolled emissions.
4. Rocky Mountain region (Allen et al., 2013). This value includes both controlled and uncontrolled emissions.
5. Average of the emission factors reported by Burnham (2011), Jiang et al. (2011), Skone et al. (2014)and Canadian Association of Petroleum Producers (1999). This value includes both controlled and uncontrolled emissions. The contribution of CH_4 to the CO_2e emissions from processing activities before NSPS implementation was estimated to be around 13% (Skone et al., 2014). This same percentage was applied to estimate the CH_4 contribution from processing activities.
6. Corresponds to the average of emission factor values reported by Howarth et al. (2011) for several studies. These values include both controlled and uncontrolled emissions.

Table 2.4: CO_2 and CH_4 emission factors for oil extraction activities.

Activity	CO_2e emission factors	CH_4 emission factors	VOC emission factors	Units
Production	1.69E-5 - 8.13E-5[1]	8.05E-07- 3.87E-06[1]	3.06E-07- 1.47E-06[1]	10^3 kg/ bbl
Transport	1.15 E-3 [2]	2.82E-07[2]	3.84E-07[2]	10^3 kg / bbl transported tanker truck

1. Ranging from conventional to heavy oil. VOCs are estimated from Zhang et al. (2009) (CH_4 75 %, VOCs 12%) and from the EPA-smoke speciate composition (55 % CH_4 and 33 % VOC). The standard deviation includes the two different compositions.
2. CO_2, CH_4, N_2O and VOC emissions for Heavy-Heavy Duty Truck from GREET 2014 (Argonne National Laboratory, 2014). CO_2e estimated for global warming potential of 1 for CO_2, 21 for CH_4 and 310 for N_2O. Average distance from the oil reservoirs to Daniel's Summit Lodge (Heber, UT) is 121 miles. Crude oil is assumed to be carried by trucks with an average capacity of 200 barrels (HDR Engineering, 2013).

Table 2.5: Change in emission factors for CO_2e, CH_4 and VOCs after the NSPS implementation for new wells (NETL 2014). The beginning dates are the effective dates of NSPS.[1]

	CO_{2e} (%)	CH_4 (%)	VOCs (%)	Beginning
Construction	+2	-	-	January, 2015
Completion	-96	-96	-96	January, 2015
Production	-66	-66	-66	November, 2012
Processing	-20	-40[2]	-40[2]	November, 2012
Transport[3]	-0.5	-0.5	-0.5	November, 2012

1. Some of the categories, such as production, encompass several activities, such as pneumatic controllers and workovers. In this case the beginning date is the date of the largest contributor to the category.
2. Based on the Skone et al. (2014) data. Value assumes that emissions from other point sources and valve fugitives are mainly due to methane.
3. Based on the Skone et al. (2014) data. Methane emitted due to pipeline construction was not included.

CHAPTER 3

ECONOMIC IMPACTS OF CONVENTIONAL OIL AND GAS DEVELOPMENT

In preparation for The Energy Journal. Economic Impacts of the Oil and Gas Industry on the Uinta Basin and State of Utah. J.E. Wilkey, M.T. Hogue, T.A. Ring, J.C. Spinti, D. Pasqualini ©

3.1 Introduction

The oil and gas industry plays a major economic role in the state of Utah. In particular, in the northeastern region of Utah known as the Uinta Basin (comprised of Uintah and Duchesne counties) approximately 20% of the workforce (and 34% of earned income) is directly related to the oil and gas industry (Utah DWFS, 2015). Recent oil and gas price drops have substantially impacted the region, resulting in a loss of 9% and 13% of the total employment base in Uintah and Duchesne counties, respectively, between June 2014 and June 2015 (Utah DWFS, 2015). Given the size of the downturn, both local and state government officials have a clear interest in accurate forecasts of the employment and fiscal impacts of the oil and gas industry. In this study, we demonstrate a method for forecasting (with uncertainty estimates) energy prices, drilling activity, oil and gas production, and ultimately the employment as well as fiscal impacts, including royalties, severance taxes, property taxes, and corporate income taxes from the oil and gas industry in the Uinta Basin.

3.2 Methodology

The overall structure of the model is summarized in Figure 3.1. Source data, primarily from the U.S. Energy Information Administration (EIA) and Utah Division of Oil, Gas and Mining (UDOGM), are collected and analyzed to describe important input parameters in the model as either (a) cumulative distribution functions (CDF) or (b) least-squares, regression-fitted functions of other parameters. A Monte-Carlo (MC) simulation can then be used to find the range of economic impacts by randomly and repeatedly drawing values of all parameters described as CDFs and calculating the resulting values

of all fitted functions. Specifically, for each iteration (i.e., run) of the MC simulation, the model executes the following algorithm:

1. Generate a simulated oil and gas price forecast.
2. Calculate the number of new wells drilled in response to simulated energy prices.
3. For every well (new and existing):
    a. Pick/collect well attributes (well depth, decline curve coefficients, tax conversion factors, etc.).
    b. Calculate production rates of oil and gas using decline curve analysis techniques.
    c. Calculate royalties and severance taxes by directly applying tax laws to the energy price and production forecasts.
    d. Calculate property and corporate income taxes (at the state and federal level) by finding gross income and applying a tax conversion factor.
4. Find total job creation as a result of oil and gas industry activity by summing together capital and operating spending for all wells and applying U.S. Bureau of Economic Analysis (BEA) Regional Input-Output Modeling System (RIMS II) job creation multipliers.
5. Find total royalty and tax payments by summing together the results for all wells for each royalty and tax category.

The MC simulation results can then be analyzed to determine the probability distribution of possible employment, royalty, and tax outcomes, which quantifies the uncertainty in the model's results. All data analysis and MC simulation steps are written in R (R Core Team, 2015), which allows for the data analysis and modeling work to be

run automatically in either a "cross-validation" or "predictive" mode. In cross-validation mode, observations are split into two data sets for training and testing the model, while in predictive mode the model uses all available data for training the model and then makes projections about future time periods. The technical details of the data analysis and MC simulation process steps for energy price, drilling, and production forecasting are available in Chapter 2. However, a general overview of these steps is presented below, followed by a thorough discussion of the methodology for performing the data analysis and simulation steps for determining the economic impacts.

3.2.1 Energy Price Forecast

The first step in the MC simulation is to generate a set of simulated energy price forecasts for the oil and gas first purchase price (FPP). We use the Annual Energy Outlook (AEO) reference forecasts (U.S. EIA, 2015b) for wellhead oil and gas prices in the Rocky Mountain region as the basis for our forecasting work. While EIA's AEO forecasts are frequently used as a standard estimate for future energy prices, they are also frequently wrong, with prices being off by as much as ± 100% of their actual value after just five years (U.S. EIA, 2015a). We incorporate the range of observed error in EIA forecasts by (a) calculating the relative error rates between forecasted and actual wellhead prices, (b) fitting a beta distribution to the range of relative error values at each future year, and (c) randomly drawing from those distributions to adjust the EIA reference forecasts at each future year up or down (with equal probability) by the selected relative error rate. Results of this relative error method are given in the Results and Discussion section.

3.2.2 Drilling Forecast

Drilling activity can occur either in the form of drilling new wells or "reworking" existing and/or abandoned wells to stimulate new production. We modeled the number of new wells drilled each month in the Uinta Basin as a function of oil and gas FPPs using a variety of distributed-lag models based on similar work by Moroney (1997). Data on the number of wells drilled (Utah DOGM 2015) and the FPPs for oil and gas in the Uinta Basin (U.S. EIA 2015c; U.S. EIA 2015b) were used to find the best fit for a variety of distributed-lag models over the time period of Jan. 1995 – Dec. 2009 (the training period). The fitted models were then cross-validated against data from the Jan. 2010 – Dec. 2014 time period (the test period). We found that the best model was the one based solely on lagged oil prices, as shown in Eq. (3.1):

$$W_t = 0.844 \cdot OP_{t-1} - 1.451 \qquad (3.1)$$

where W is the number of new wells drilled at time t and OP is the FPP of oil in 2014 dollars per barrel ($ / bbl). While Eq. (3.1) has a relatively low R^2 value ($R^2 = 0.70$), the residual sum of squares was an order of magnitude smaller than other distributed-lag models during cross-validation tests.

Reworks are drilling events where an existing well is either recompleted or re-perforated to stimulate oil and gas production rates. The timing of rework events is estimated using an empirical CDF to describe the probability that a well is reworked based on (a) well type (oil or gas) and (b) how long the well has been in operation. An analysis of the available historical data indicates that about 15% - 20% of oil and gas wells are reworked within 10 years of operation. During each MC simulation run, every well (new and existing) randomly draws a rework date from the empirical CDF. If the

date falls within the simulation period, the cost of recompleting the well is charged and production is restarted for that well.

In addition to determining how many new wells are drilled, the model also simulates (a) where the wells are located geographically and (b) the well type (oil or gas). Well type indicates which product type (oil or gas) is predominantly produced by each well, but all wells produce both oil and gas (in the model and in reality). Location and well type are both determined from empirical CDFs, assuming that the distribution of new well locations and types will follow the same pattern as prior drilling activity.

3.2.3 Production Forecast

In general, production rates of oil and gas from any well decline over time. Many decline curve equations have been developed; the two forms used in this study are the hyperbolic decline curve equation (Eq. (3.2), (Arps 1945)), and the cumulative production equation (Eq. (3.3), (Walton 2014)):

$$q(t) = q_o \cdot (1 + b \cdot D_i \cdot t)^{\left(-\frac{1}{b}\right)} \tag{3.2}$$

$$Q(t) = C_p \cdot \sqrt{t} + c_1 \tag{3.3}$$

In Eq. (3.2), q is the oil or gas production rate at time t, q_o is the initial production rate, b is the decline exponent, and D_i is the initial decline rate. In Eq. (3.3) Q is the cumulative production at time t, and C_p and c_1 are fitted coefficients. Equation (3.2) is used to estimate the production rates for existing wells by extrapolating from well-by-well fits of oil and gas production records, as it tends to be more accurate than Eq. (3.3) at making long-term projections. However, Eq. (3.2) cannot be used to simulate the production from new wells using a MC simulation approach because random and independent picks from

CDFs for each coefficient (q_o, D_i, and b) are highly likely to return unrealistic results. Instead, Eq. (3.3) is used to estimate production from new wells, since monthly production rates, calculated by the difference in Q values, are only a function of a single fitted coefficient (C_p).

Since gas production rates from new wells have not changed much in the Uinta Basin over the last decade, production rates of gas from new wells are randomly drawn from an empirical CDF of past decline curve fits of Eq. (3.3). Production rates from new oil wells have changed over time, so a slightly different approach is taken. The CDFs are determined by fitting a log-normal distribution to values of C_p and c_1 by year and then extrapolating from trends in the log-mean and log-standard deviation to estimate the distribution of C_p and c_1 in Eq. (3.3) for each future time period.

In total, production records from 12,071 unique wells in the Uinta Basin are individually fitted, resulting in approximately 48,000 unique curve fitting attempts (both oil and gas production records for each well using both Eq. (3.2) and (3.3)). The algorithm used is fairly robust: only 4% of the attempted fits fail to converge. However, many wells (22%) are skipped because they contain too few (< 12 months) production records (and are therefore prone to overfitting). Existing wells without fits are treated using the same methodology applied to new wells.

Eventually the production rate for a well will decline to the point where it is no longer profitable to operate. To correct for wells that should be shut in due to unfavorable economics, the last step in the production forecasting process is to estimate each well's operating cost ratio CR as a function of time:

$$CR(t) = \frac{LOC(t)}{GR(t)} \tag{3.4}$$

where LOC is the lease operating cost (pumping, labor, maintenance, etc.) for the well and GR is the gross revenue from oil and gas sales. Since approximately 15% of GR is paid in royalty and severance taxes, any well with a $CR \geq 0.8$ is assumed to be shut-in and permanently abandoned. The methodology used for estimating LOC, as well as other well capital and operating expenses, is discussed below.

3.2.4 Capital and Operating Expenses of Oil and Gas Extraction

3.2.4.1 Capital Costs

Capital costs for wells include the cost of drilling and completing the wells and of purchasing production, separation, and storage (PSS) equipment. Well costs (drilling and completion) are estimated by fitting the well capital costs as an exponential function of well depth:

$$\ln(C_{DC}) = a \cdot D + b \tag{3.5}$$

where C_{DC} is the cost of drilling and completion and D is the total measured well depth (i.e., the total length of the well). Capital cost data are collected by randomly selecting a set of 100 wells drilled in the Uinta Basin over the last decade and then searching publically reported well documents for expenditures (Utah DOGM, 2015). Of the original 100-well dataset, 65 wells report capital costs. The best fit ($R^2 = 0.77$) of Eq. (3.5) to the available information is achieved with a = 2.723E-04 and b = 11.71, as shown in Figure 3.2.

The drilling and completion costs are utilized in two ways. First, whenever a new well is drilled, the full cost of C_{DC} is charged as calculated from Eq. (3.5) using the well's

randomly selected well depth (drawn from empirical CDFs for both oil and gas wells). Secondly, whenever a well is reworked, only the capital cost of completion (C_{compl}) is charged. The completion costs can be back calculated using the completion cost ratio R_C:

$$R_C = \frac{C_{Compl}}{C_{Drill}} \tag{3.6}$$

where C_{Drill} is the capital cost of drilling. The mean and standard deviation (SD) of R_C are calculated for the well dataset (mean = 0.675, SD = 0.345), and R_C is assumed to follow a normal distribution (see Figure 3.3). The value of R_C is randomly drawn from the CDF of this normal distribution for each well in each iteration of the MC simulation. During the simulation, all wells that randomly draw an R_C value < 0 from the normal CDF draw again until all values of R_C are ≥ 0.

The capital costs of PSS equipment are estimated from EIA's oil and gas lease equipment cost (LEC) index (U.S. EIA, 2010b). EIA's index reports costs based on well type (oil or gas), geographical location, depth, energy prices, and (for gas wells) production rate. The best fit of EIA Rocky Mountain region LEC data (excluding well tubing, which is included in drilling costs) is given below in Eq. (3.7) for oil wells (R^2 = 0.96) and Eq. (3.8) for gas wells (R^2 = 0.94):

$$LEC_{oil} = 1777 \cdot OP + 7.726 \cdot D \tag{3.7}$$

$$LEC_{gas} = 5400 \cdot GP + 4.134 \cdot D + 15.49 \cdot P_{gas} \tag{3.8}$$

where OP is the FPP of oil ($ / bbl), D is well depth (ft), GP is the FPPs of gas in dollars per thousand standard cubic feet ($ / MCF), and P_{gas} is the daily production rate of gas in MCF per day (MCFD). All dollar value terms in Eq. (3.7) and (3.8) are in 2014 dollars. LECs for each new well are determined using simulated energy prices during the time

step in which the well is drilled, the randomly selected well depth, and for gas wells, the maximum simulated gas production rate.

3.2.4.2 Operating Costs

Well operating costs are estimated from EIA's oil and gas lease operating cost (LOC) index (U.S. EIA, 2010b). LOCs are reported with the exact same factors as LECs (well type, location, depth, and production rate for gas wells). The best fit of EIA Rocky Mountain region LOC data is given below in Eq. (3.9) for oil wells ($R^2 = 0.98$) and Eq. (3.10) for gas wells ($R^2 = 0.93$) in 2014 dollars:

$$LOC_{oil} = 25.92 \cdot OP + 0.1887 \cdot D \quad (3.9)$$

$$LOC_{gas} = 268.2 \cdot GP + 0.2247 \cdot D + 0.5862 \cdot P_{gas} \quad (3.10)$$

3.2.5 Job Creation

The number of jobs created as a result of spending by the oil and gas industry is estimated using the U.S. Bureau of Economic Analysis (BEA) Regional Input-Output Modeling System (RIMS II). RIMS II is a regional economic model that estimates the multiplying effect that spending in one industry has on all other industries in the local area. In this study, we use the RIMS II final-demand job creation multipliers for the oil and gas industry in the Uinta Basin in 2004 (U.S. BEA, 2004). In particular, we use the multiplier for employment in the mining industry as a result of spending in the oil and gas industry (2.2370 jobs / 2004 million $) to estimate how many mining jobs are directly created by the oil and gas industry. We use the total employment multiplier (4.4526 jobs / 2004 million $) to estimate the total jobs impact of the oil and gas industry on the Uinta Basin.

3.2.6 Taxes and Royalties

A number of taxes and royalties are collected on oil and gas extraction by state, federal, Indian, and private land owners. The approaches taken for calculating each of these fees are laid out below.

3.2.6.1 Royalties

Mineral-rights owners may collect royalty payments (R) on oil and gas production based on the gross revenue (GR) of the product, although the royalty rate (r) differs by owner:

$$R = r \cdot GR \tag{3.11}$$

On both state and federal lands, the royalty rate for conventional oil and gas production is set at 12.5% (Code of Federal Regulations, 2011; Utah Administrative Code, 2015). Indian lands charge a higher rate of 16.67% (Code of Federal Regulations, 2015). We assume that private mineral-rights owners receive the same 12.5% royalty rate charged on federal lands. During the MC simulation, the mineral-rights owner for each well is randomly selected based on the distribution of mineral-rights (state, federal, Indian, private) in the region where the well is located. Royalty payments are then directly calculated from the energy price and production forecasts using Eq. (3.11) and the appropriate value of r.

3.2.6.2 Severance Taxes

The state of Utah collects severance taxes on all oil and gas production (regardless of mineral-rights ownership) using a split rate system based on the market price of each product at the wellhead as specified in Utah Code 59-5-102 (2015). The

first $13/bbl for oil and $1.50/MCF for gas are taxed at a rate of 3%; any additional value above these thresholds is taxed at a rate of 5%. An additional 0.2% of the total value (TV) is taxed as a conservation fee (r_{cf}). This set of tax rules is implemented using Eq. (3.12):

$$ST = TV\{r_{cf} + [0.03(1 - f_{st}) + 0.05f_{st}]\} \tag{3.12}$$

where ST is the severance tax due to the state on a dollar-per-barrel basis and f_{ST} is the fraction of TV above the threshold value. The results of Equation (3.12) are then multiplied by the volume of oil or gas produced to find the total severance tax due for each product. Finally, there are two important exemptions on severance taxes (both included in the model). If a well (a) is in its first six months of production, or (b) can be classified as a "stripper" well (oil wells with oil production < 20 bbl/day or gas wells with gas production < 60 MCFD), then none of the produced oil or gas is subject to severance taxes.

3.2.6.3 Property Taxes

Property taxes on oil and gas companies are centrally assessed by the Utah State Tax Commission (USTC). Given the complexity of estimating property taxes, in this study we approximate property taxes (PT) as a fraction of GR using a property tax conversion factor f_{PT}:

$$f_{PT} = \frac{PT}{GR} \tag{3.13}$$

Based on property taxes collected on the oil and gas industry in the Uinta Basin from 2000 – 2014 (Utah State Tax Commission, 2015a), the fraction of GR paid in property

taxes ranges from 0.63% to 1.44% as shown in Table 3.1. Assuming that f_{PT} can be approximated as a normal distribution, we use the mean (0.98%) and SD (0.25%) of f_{PT} to randomly select f_{PT} values for every well in the MC simulation and then calculate PT based on GR. Any randomly selected values for f_{PT} that are < 0 are set equal to zero.

3.2.6.4 Corporate Income Taxes

Corporate income taxes are estimated using a two-step process. First, the net taxable income (NTI) for oil and gas companies is approximated using the same methodology as property taxes with a conversion factor f_{NTI}:

$$f_{NTI} = \frac{NTI}{GR} \tag{3.13}$$

Unfortunately, data on the aggregate NTI of the oil and gas industry in the state of Utah is scarce. Only three years of data are available, see Table 3.2. Again, assuming that f_{NTI} can be approximated as a normal distribution, we use the mean (4.65%) and SD (1.92%) of f_{NTI} to randomly select f_{NTI} values for every well in the MC simulation. Any randomly selected values for f_{NTI} that are < 0 are replaced with $f_{NTI} = 0$.

Once the NTI is selected, the second step of the corporate income tax calculation process is to apply the appropriate tax rate. State corporate income taxes ($SCIT$) can be estimated from NTI using Eq. (3.14), and federal corporate income taxes ($FCIT$) from Eq. (3.15), assuming that oil and gas companies (a) pay a 5% state and 35% federal corporate income tax rate, and (b) have the same NTI at the federal and state level.

$$SCIT = 0.05 \cdot NTI \tag{3.14}$$

$$FCIT = 0.35 \cdot NTI - SCIT \tag{3.15}$$

3.3 Results and Discussion

Two sets of results are shown below for running the model in (a) cross-validation mode and (b) predictive mode. The cross-validation run presents the results of training the model with data from 1984 – 2009 and then testing the model against data from the 2010 – 2014 time period. The predictive run uses all of the available data (1984 – 2014) to predict economic impacts over the 2015 – 2019 time period. Results shown below for both types of runs were obtained by performing a MC simulation with 10^4 iterations.

Results for the cross-validation and prediction runs for the energy price, drilling, and production forecasts are briefly summarized below, followed by a detailed discussion of the employment and fiscal impacts.

3.3.1 Energy Price Forecasts

Selected percentiles of the simulated energy price paths for (a) oil and (b) gas were shown previously in Figure 2.8 and 2.9 for the cross-validation and prediction cases, respectively. EIA forecasts were shown as grey lines in both Figure 2.8 and 2.9; actual energy price paths were overlaid as solid black lines in Figure 2.8. EIA's AEO 2010 (U.S. EIA, 2010a) forecast was used as the basis for the cross-validation case, and AEO 2015 (U.S. EIA, 2015b) was used as the basis for the predictive case. In general, results from the cross-validation case show that the median simulated energy prices closely follow EIA's reference forecast and cover the entire range of observed energy prices.

3.3.2 Drilling Forecasts

The drilling forecasts are calculated by applying Eq. (3.1) to the simulated price forecasts in Figures 2.8 and 2.9. For the cross-validation case (Figure 2.11a), the median

drilling forecast (total of 4,486 wells) is a reasonable match for the actual drilling schedule (total of 4,272 wells). In the predictive case (Figure 2.11b), drilling activity is reduced due to the lower energy prices (the median drilling forecast has a total of 3,121 wells).

3.3.3 Production Forecasts

Total oil and gas production for the cross-validation case are shown in Figure 3.4. The median result for oil production from new wells is an excellent match for the actual oil production during the 2010 – 2014 time period (119.3 million bbl simulated versus 119.2 million bbl actual). The median result for simulated gas production from new wells is also a good match to the actual production rate until 2013, at which point the median simulated gas production begins to pull away from the actual gas production rate, which flattens out at a rate of approximately 30E+06 MCF/month. The disparity is most likely due to changes in the rate of drilling oil wells vs. gas wells, which has fluctuated over time (and most recently has favored drilling oil wells) but is treated as a constant in our model.

Oil and gas production for the prediction case are shown in Figure 2.15. Oil production doubles due to expected increases in the production rates from new wells, which more than offsets the reduced drilling rates during the prediction period. Gas production slows initially but is expected to recover and slowly increase as prices (and thus drilling activity) recover.

3.3.4 Employment

The total number of jobs created according to the RIMS II calculation method for the cross-validation and prediction cases are shown in Figure 3.5 and Figure 3.6, respectively. Technically, the jobs estimates in Figure 3.5 from the RIMS II method cannot be compared to employment data from U.S. BEA (2015) or Utah's Department of Workforce Services (DWFS) (Utah DWFS, 2015) for several reasons. First, there is no time dimension to job creation estimates in the RIMS II model. That is, when a job is created, how long it lasts, and whether it represents full or partial employment are all unknown. Secondly, each data source uses slightly different job and industry categories. U.S. BEA jobs data report total employment in the mining industry in the Uinta Basin (the same category as the RIMS II estimates), while Utah DWFS jobs data (a) cover the oil and gas and mining support industries, and (b) only include direct employees (i.e., sole proprietors and independent contractors are excluded). Lastly, the 2004 RIMS II multipliers available to us are clearly outdated. However, the available jobs data are still provided for context and to illustrate how employment estimates from the RIMS II method compare to other employment statistics.

In total, 14,903 jobs are created in the mining industry in the median cross-validation case from 2010 – 2014, versus 11,436 jobs in the prediction case from 2015 – 2019. In addition to providing the mining industry employment estimate, Figure 3.6 also includes the direct and indirect employment estimates for the entire Uinta Basin using the total jobs creation multiplier, which results in 22,762 total jobs from 2015 – 2019. Given the age (2004) of the available RIMS II multiplier data, the exact values of these numbers are probably inaccurate, but the overall trend should remain the same. Employment in the

Uinta Basin is not likely to recover to the same levels as the 2010 – 2014 time period in the next five years.

3.3.5 Fiscal Impacts

Figures 3.7 – 3.11 show the annual fiscal impacts of oil and gas production for the cross-validation case versus their actual values for the entire state of Utah. An important note about all of these figures is that simulated values are shown as totals by calendar year, while all the data points for actual values are given by fiscal year (which can vary by agency); no adjustment has been made for this discrepancy in any of the plots. However, source data points are adjusted for inflation; all values are given in 2014 dollars.

Royalties on oil and gas production are shown in Figure 3.7 for wells located on state land. These results are compared with two "actual" royalty payments; those for the Utah School and Institutional Trust Lands Administration's (SITLA) oil and gas program statewide, and those for the Uinta Basin (UB), which are calculated by scaling down the statewide royalty payment values by the average of the fraction of oil and gas produced in the Uinta Basin versus the rest of the state in each year. Overall, the Uinta Basin accounts for 70% - 80% of total oil and gas production in the state of Utah. The variance between the actual values and the median predicted result in most years is small and is likely due to the fact that (a) SITLA reports both royalty payments and mineral-rights leasing auction proceeds as a single line item, and (b) the previously mentioned fiscal year versus calendar year discrepancy. However for most years the median result is a close match to the Uinta Basin royalty payment approximation.

Figure 3.8 compares severance taxes during the cross-validation period with two "actual" datasets; the first is the total oil and gas severance taxes collected statewide by USTC, and the second is the production-adjusted Uinta Basin (UB) value. Discrepancies between the MC simulation results and the actual reported revenues for the USTC are significant. While the severance tax calculations performed by the model include many of the same provisions included in Utah Code (2015), several provisions are ignored (all of which reduce severance tax liability), including:

- The 4% severance tax rate on natural gas liquids (NGL)
- If oil and gas is stockpiled, the severance taxes are not imposed until the time of sale (up to a maximum of two years)
- Wildcat wells are allowed a 12-month severance tax exemption (versus the 6-month exemption for development wells)
- Part of the expense of performing well reworks can be taken as a deduction on severance taxes (20% of the cost up to a maximum of $30,000 per well)
- Any production from an enhanced recovery project (e.g., waterflooding) is taxed 50% less

Interestingly, the difference between the simulated and actual values is not especially large in the first two years of the cross-validation period. Comparing the actual energy prices in Figure 2.8, actual oil and gas production rates in Figure 2.12, and the actual severance tax revenue in Figure 3.8, it is clear that the per unit volume (bbl oil or MCF gas) severance tax payments decreased from 2010 through 2013 and then began increasing again in 2014.

Property taxes for the cross-validation period are shown in Figure 3.9. Of all the

fiscal results, the actual and simulated property tax values show the most agreement during the cross-validation period.

Figure 3.10 shows the simulated SCIT payments versus actual corporate income tax payments for the oil and gas industry statewide (Utah State Tax Commission, 2011). Data were only available for the payments made in 2009 – 2011, so only years 2010 and 2011 show the actual values. For all other years, the average fraction of state corporate income taxes paid by the oil and gas industry (4%) was applied to total corporate income data. Without additional USTC data, it is difficult to draw conclusions about the accuracy of corporate tax payment estimates from the simulations.

Finally, Figure 3.11 shows the MC simulation results for all revenue for the state of Utah from oil and gas production during the prediction period by revenue source. Comparing median case results, the prediction case ($826 million 2014 dollars) generates 20% less revenue than the cross-validation case ($1,032 million 2014 dollars). Initially severance taxes are the largest source of revenue as they are applied to all wells; royalties are only paid to the state of Utah on the approximately 17% of wells in the Uinta Basin that are located on SITLA lands. However, as the forecasted energy prices expand upwards, the higher rate on royalty payments meets and exceeds the magnitude of severance tax payments. Property tax payments are roughly half the size of severance taxes, and SCIT payments are negligible.

3.4 Conclusions

In this study we have demonstrated a method for estimating the economic impacts of the oil and gas industry on state and local governments. Cross-validation tests have

shown that the model is highly accurate at estimating overall oil and gas production rates. Gauging the accuracy of the economic impact forecasts is more difficult because of limited data availability and differences in the accounting practices between various agencies. However, there is still value in comparing the overall trends in employment and fiscal impacts. If EIA's AEO (2015b) reference oil and gas forecasts are accurate and the drilling and production forecasting method continues to perform well in future time periods, local leaders in the Uinta Basin can expect 23% lower employment in the oil and gas industry and the state of Utah will see 20% lower revenue over the next five years compared to the 2010 – 2014 period.

3.5 References

Code of Federal Regulations. 2011. "Mineral Leasing Act of 1920 30 CFR § 223." http://www.gpo.gov/fdsys/pkg/USCODE-2011-title30/html/USCODE-2011-title30-chap3A-subchapIV-sec223.htm.

———. 2015. "25 CFR § 211.41(c)." http://www.gpo.gov/fdsys/pkg/CFR-2015-title25-vol1/xml/CFR-2015-title25-vol1-sec211-41.xml.

Moroney, John R. 1997. *Exploration, Development, and Production: Texas Oil and Gas, 1970-1995*. Greenwich, CT. Jai Press.

R Core Team. 2015. "R: A Language and Environment for Statistical Computing." Vienna, Austria. http://www.r-project.org/.

U.S. BEA. 2004. "RIMS II." Washington, DC. https://www.bea.gov/regional/rims/rimsii/.

———. 2015. "Table CA25N Total Full-Time and Part-Time Employment by NAICS Industry - Private Nonfarm Employment: Mining." *Interactive Data Application*. http://www.bea.gov/iTable/iTableHtml.cfm?reqid=70&step=30&isuri=1&7022=11&7023=7&7024=naics&7033=-1&7025=4&7026=49013,49047&7027=2013,2012,2011,2010&7001=711&7028=200&7031=49000&7040=-1&7083=levels&7029=33&7090=70.

U.S. EIA. 2010a. "Annual Energy Outlook 2010." Washington, DC.

http://www.eia.gov/oiaf/archive/aeo10/index.html.

———. 2010b. "Oil and Gas Lease Equipment and Operating Costs 1994 Through 2009." Washington, DC. http://www.eia.gov/pub/oil_gas/natural_gas/data_publications/cost_indices_equipment_production/current/coststudy.html.

———. 2015a. "Annual Energy Outlook 2014 Retrospective Review." Washington, DC. http://www.eia.gov/forecasts/aeo/retrospective/.

———. 2015b. "Annual Energy Outlook 2015." Washington, DC. http://www.eia.gov/forecasts/aeo/pdf/0383(2015).pdf.

———. 2015c. "Utah Crude Oil First Purchase Price." *Domestic Crude Oil First Purchase Prices by Area*. http://www.eia.gov/dnav/pet/hist/LeafHandler.ashx?n=pet&s=f004049__3&f=m.

———. 2015d. "Utah Natural Gas Wellhead Price." *Natural Gas Wellhead Price*. http://www.eia.gov/dnav/ng/hist/na1140_sut_3a.htm.

Utah Administrative Code. 2015. "R652-20-1000." http://www.rules.utah.gov/publicat/code/r652/r652-020.htm#T9.

Utah Code. 2015. "59-5-102." http://www.le.utah.gov/xcode/Title59/Chapter5/59-5-S102.html?v=C59-5-S102_1800010118000101.

Utah DOGM. 2015. "Data Research Center." *Division of Oil, Gas & Mining - Oil and Gas Program*. http://oilgas.ogm.utah.gov/Data_Center/DataCenter.cfm.

Utah DWFS. 2015. "Industry Employment and Wages." *Utah Economic Data Viewer*. https://jobs.utah.gov/jsp/wi/utalmis/default.do.

Utah SITLA. 2015. "FY2010 - FY2015 Annual Report." Salt Lake City, UT. http://trustlands.utah.gov/our-agency/financial-reports-statistics/.

Utah State Tax Commission. 2011. "2009-2011 Corporate Statistics of Income for Oil and Gas Extraction Industries and Support Activities." Salt Lake City, UT: Utah State Tax Commission.

———. 2015a. "2000-2014 Property Tax Annual Statistical Reports." Salt Lake City, UT. http://propertytax.utah.gov/index.php/information/reports-and-statistics/annual-statistical-report.

———. 2015b. "2010-2014 Tax Commission Annual Reports." Salt Lake City, UT. http://tax.utah.gov/commission-office/reports.

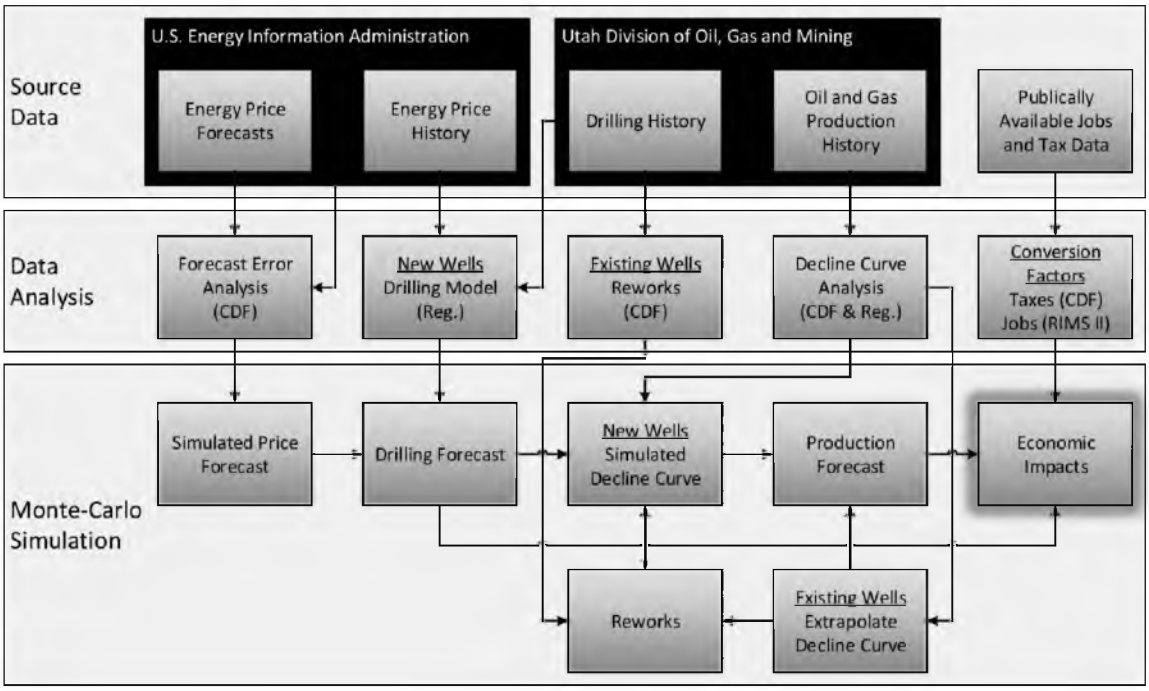

Figure 3.1: Model diagram indicating major steps in the modeling process.

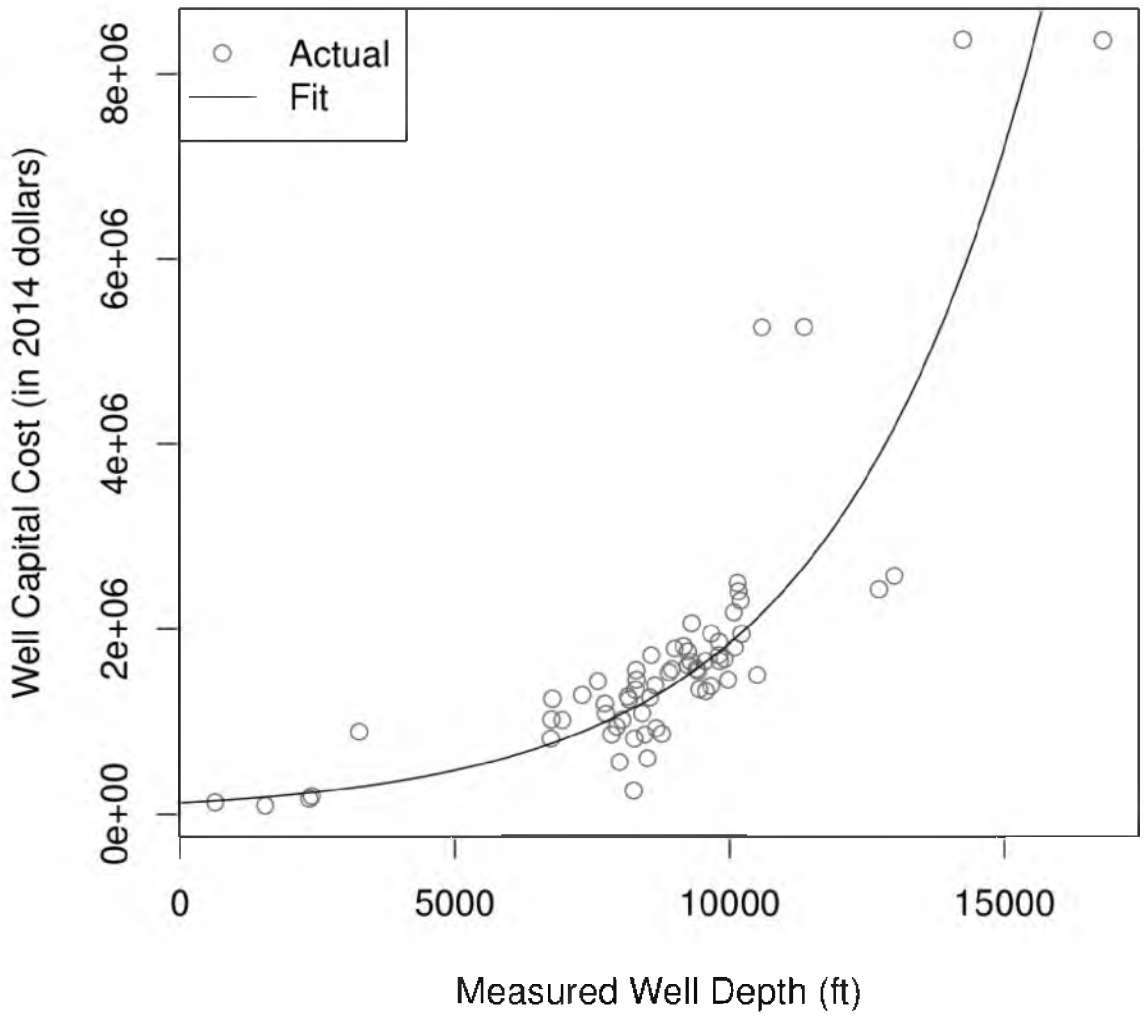

Figure 3.2: Well drilling and completion capital cost (C_{DC}) fitted as a function of total measured well depth (ft) according to Eq. (4.5) for a randomly selected set of wells in Utah's Uinta Basin (Utah DOGM, 2015).

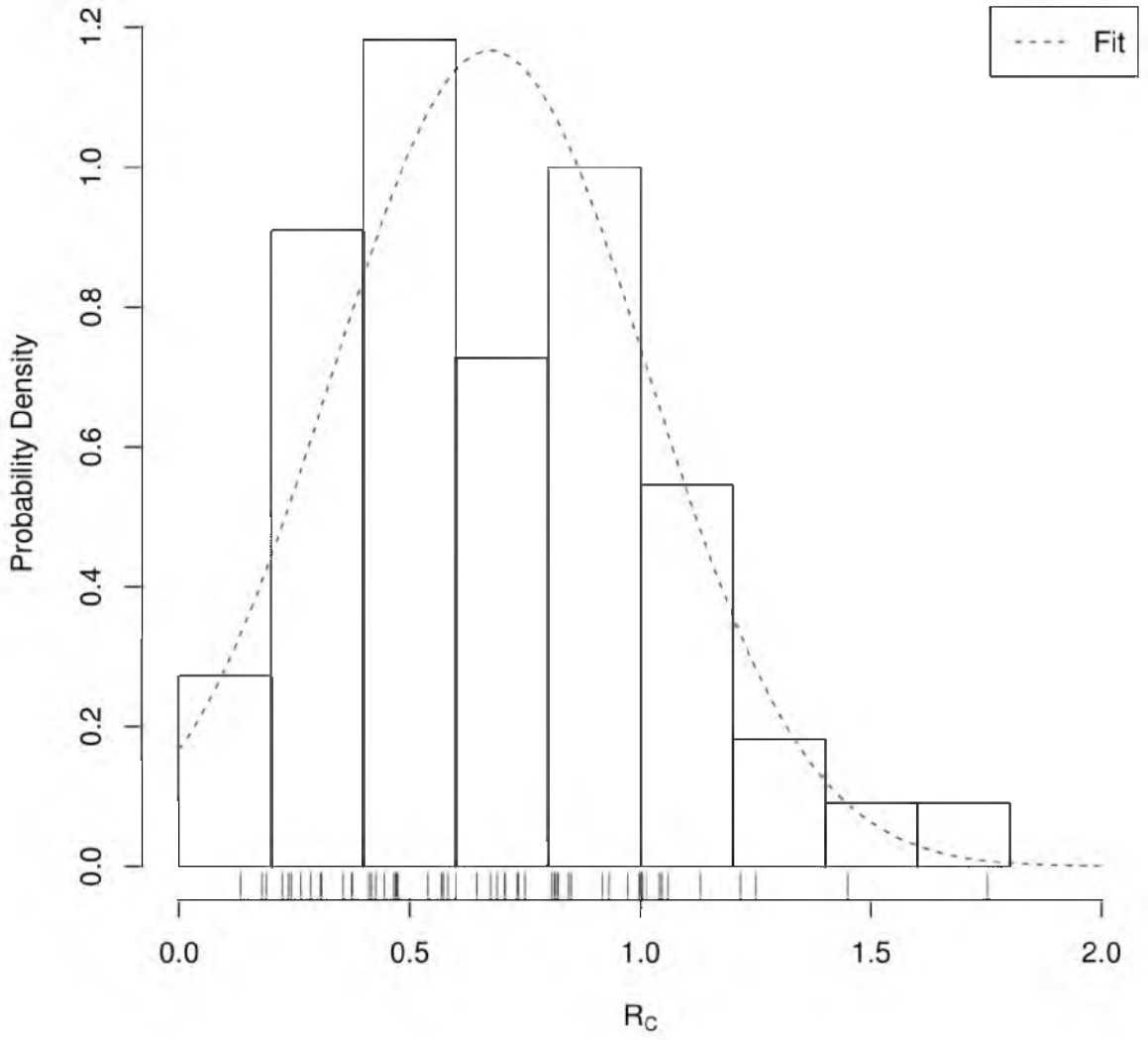

Figure 3.3: Histogram of R_C values for the same set of randomly selected wells shown in Figure 3.2. The dotted line shows the resulting normal distribution (mean = 0.675, SD = 0.345) for the sample set, and individual observations of R_C are shown as tick marks on the x-axis.

(a)

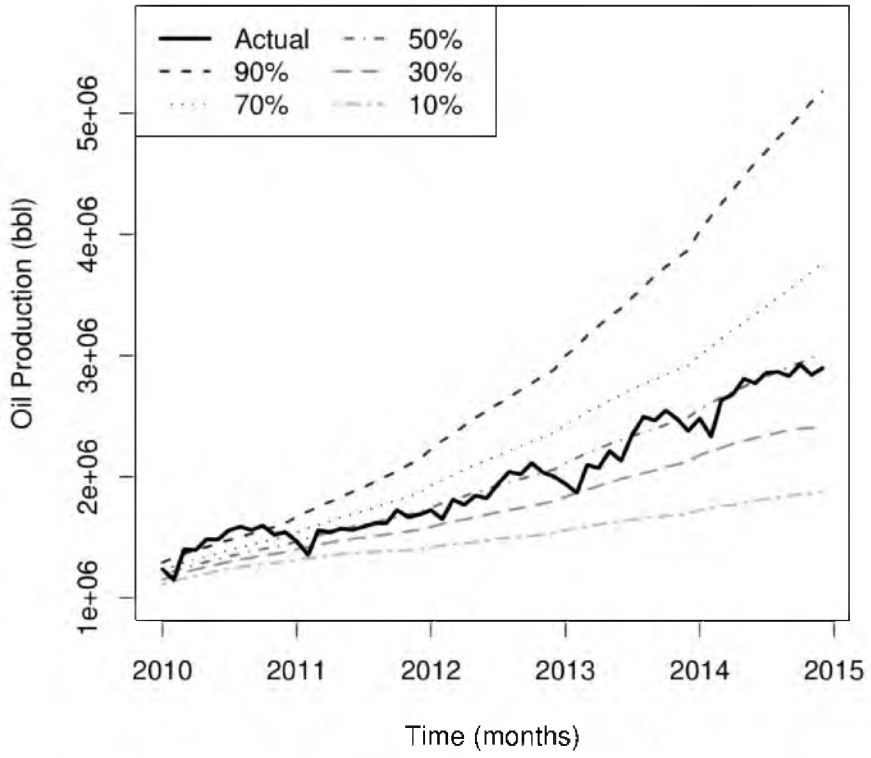

(b)

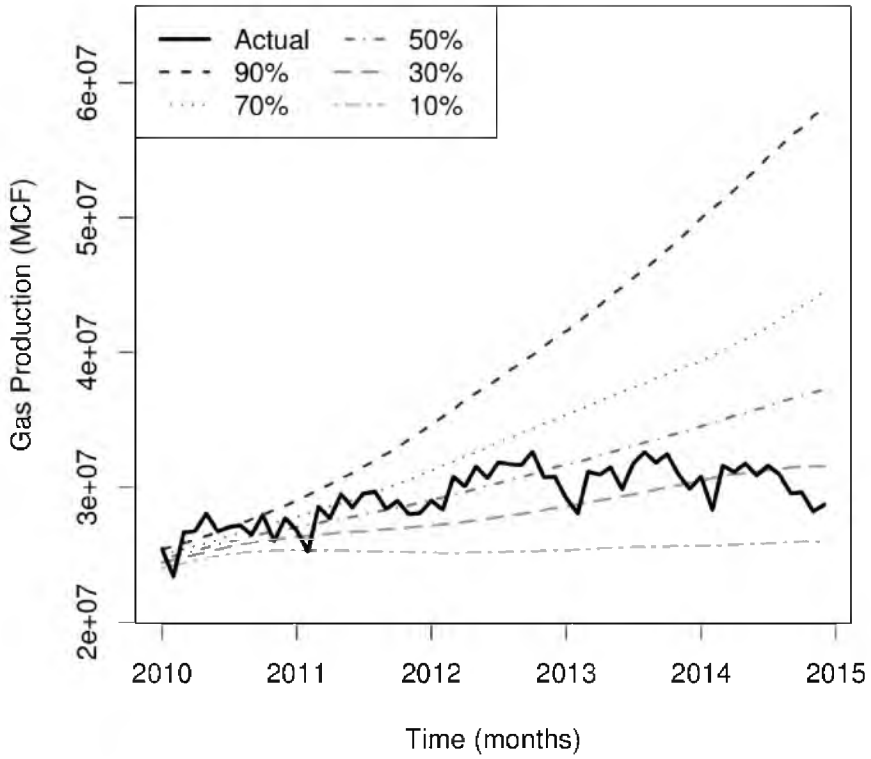

Figure 3.4: Production forecast for the cross-validation case for (a) oil and (b) gas production.

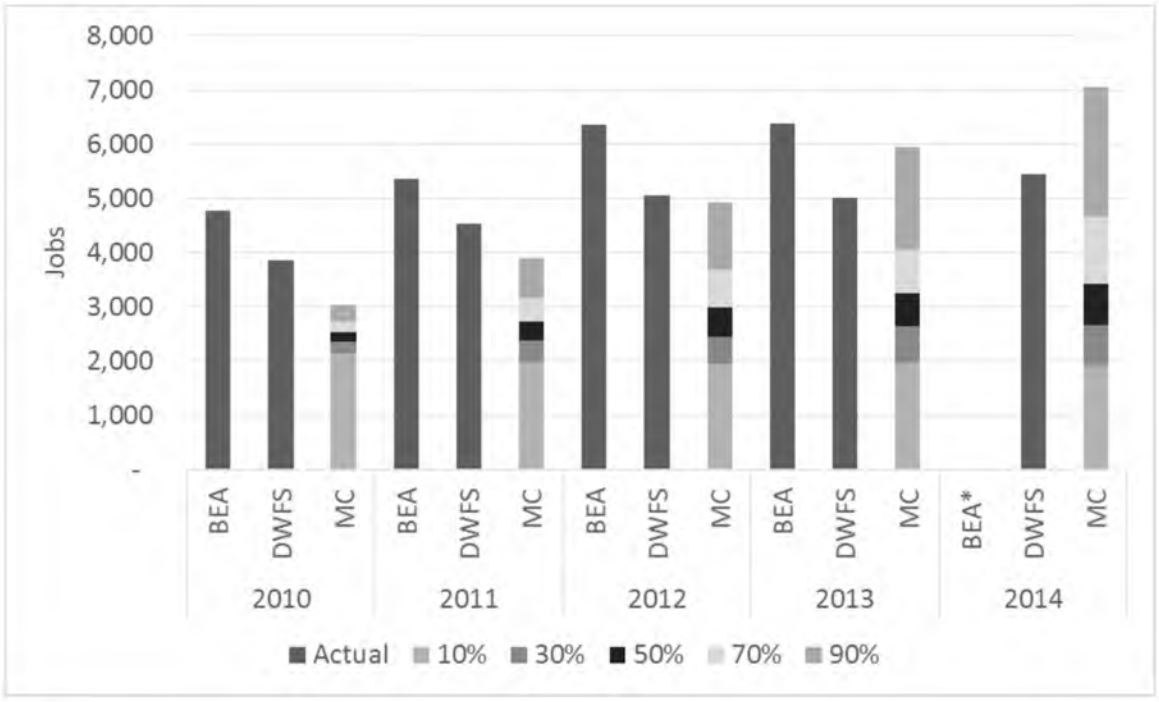

Figure 3.5: MC-simulated job creation for the cross-validation case in the mining industry using the RIMS II multiplier method vs. jobs data from U.S. BEA (2015) and Utah DWFS (2015). Simulation results are shown as stacked bars, with the top of each stacked bar representing the result for that percentile of the MC simulation results. U.S. BEA jobs data are for all employment in the mining industry in the Uinta Basin. Utah DWFS data are limited to employees (i.e., sole proprietors or independent contractors are excluded) in the oil and gas and mining support industries in the Uinta Basin. *Note that no jobs data were available from U.S. BEA for 2014.

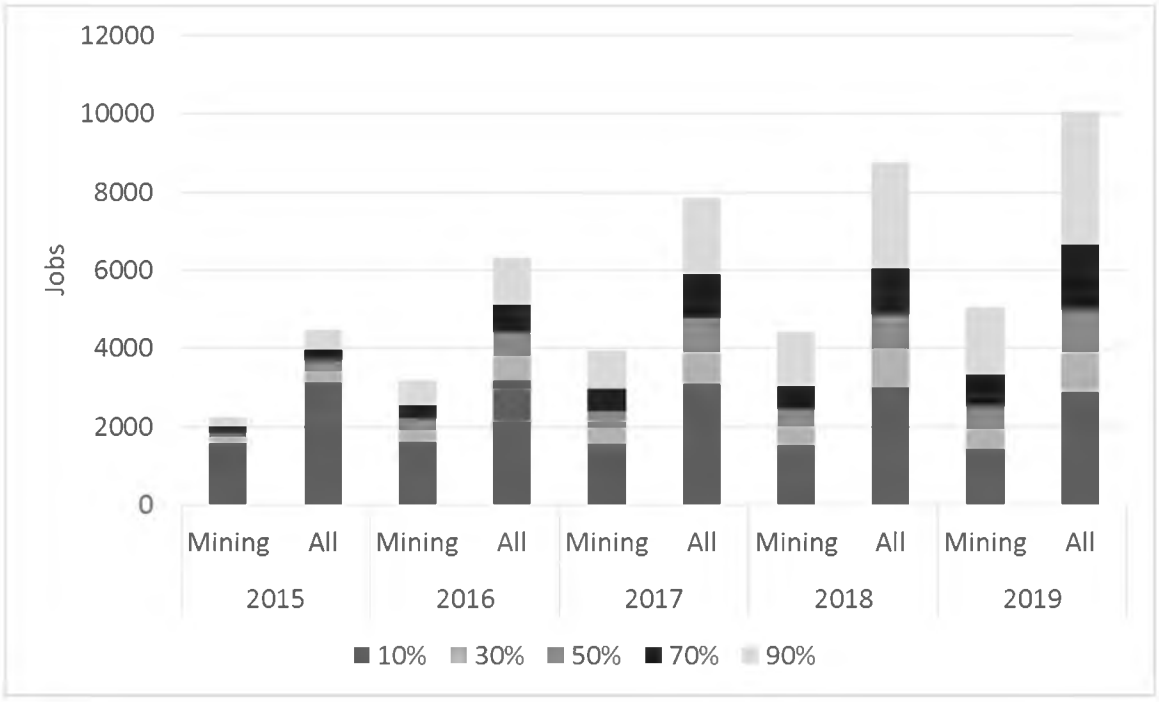

Figure 3.6: MC-simulated job creation for the prediction case in the mining industry (Mining) and in all industries (All) using the RIMS II multiplier method. The top of each stacked bar represents the result for that percentile of the MC simulation results.

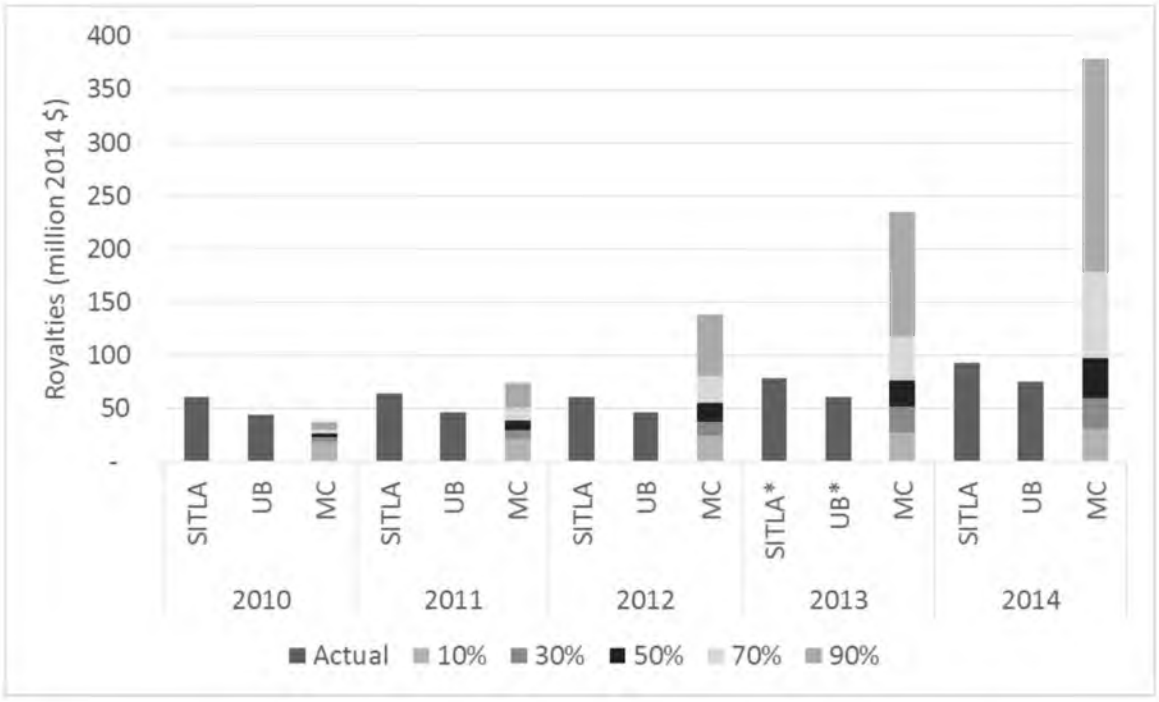

Figure 3.7: Comparison of MC-simulated royalties from oil and gas production on state lands in the Uinta Basin with statewide oil and gas royalty payments to Utah's SITLA (2015) and Uinta Basin (UB) royalty payments to SITLA. The top of each stacked bar represents the result for that percentile of the MC simulation results. SITLA did not report oil and gas revenue in fiscal-year 2013, so the 2013 value is for the entire SITLA minerals program (oil, gas, and mining).

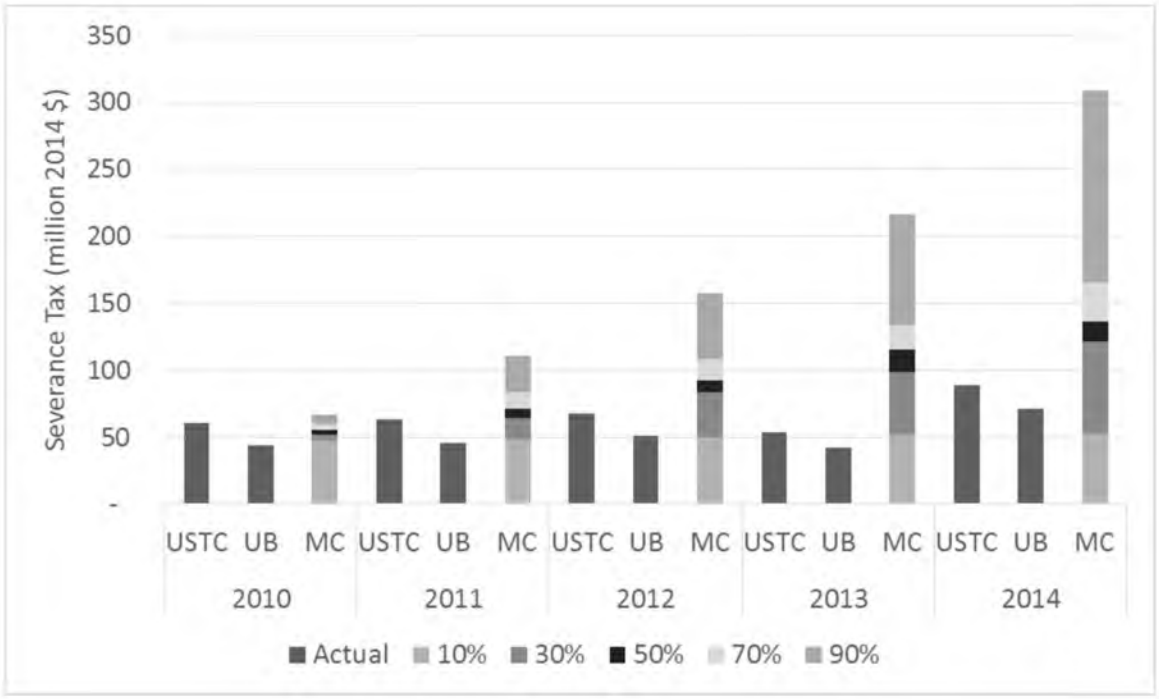

Figure 3.8: Comparison of MC-simulated severance taxes from all oil and gas production in the Uinta Basin with total statewide oil and gas severance taxes (Utah State Tax Commission, 2015b) and Uinta Basin (UB) severance taxes. The top of each stacked bar represents the result for that percentile of the MC simulation results.

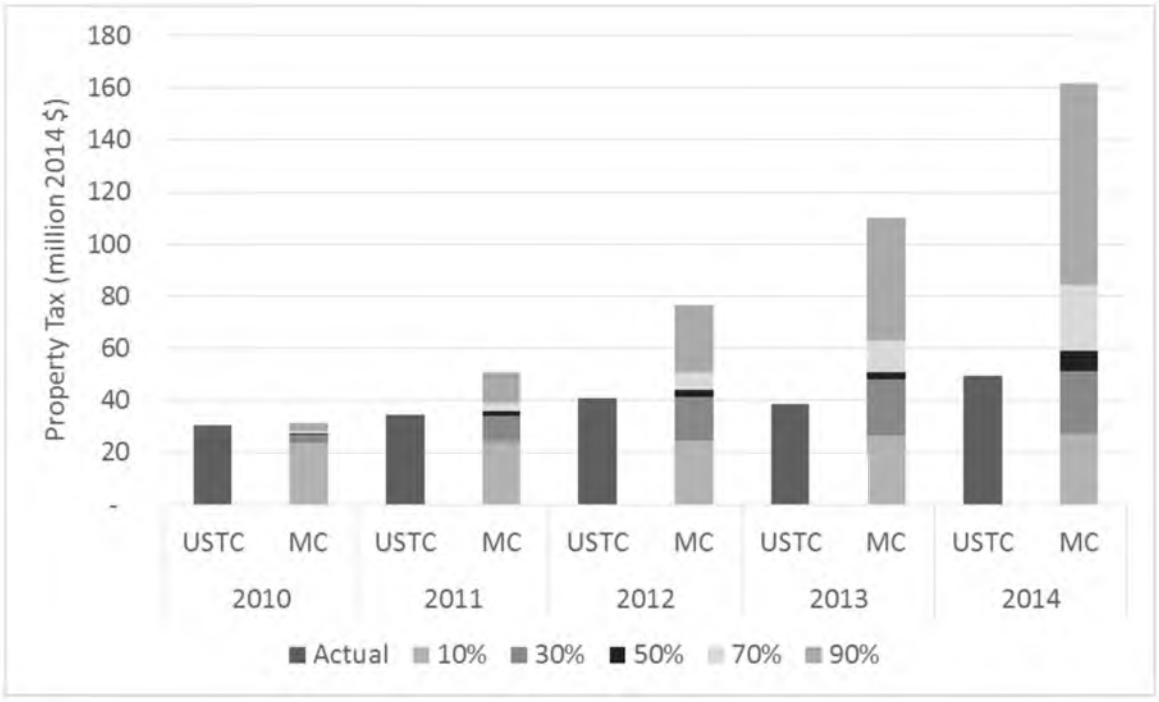

Figure 3.9: Comparison of MC-simulated property taxes for all oil and gas wells in the Uinta Basin with total Uinta Basin oil and gas property taxes from the Utah State Tax Commission (2015a) (USTC). The top of each stacked bar represents the result for that percentile of the MC simulation results.

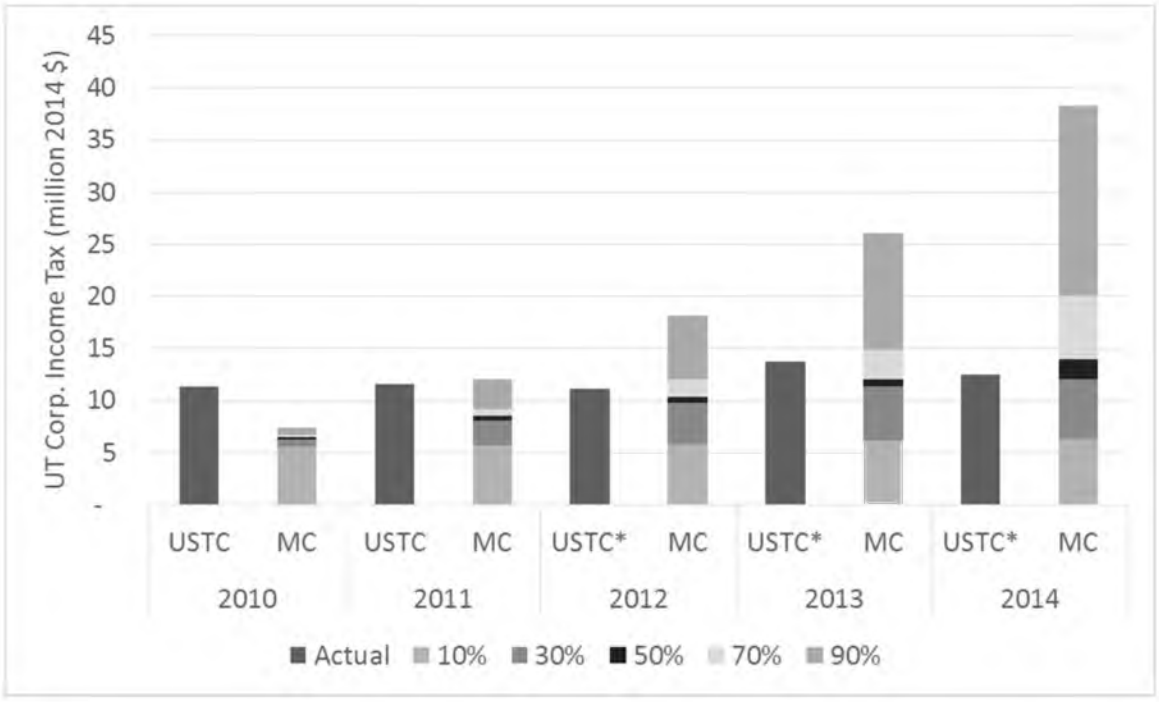

Figure 3.10: MC-simulated corporate income taxes vs. actual corporate income tax payments for the statewide oil and gas industry from the Utah State Tax Commission (2011; 2015b) (USTC). The top of each stacked bar representing the result for that percentile of the MC simulation results.

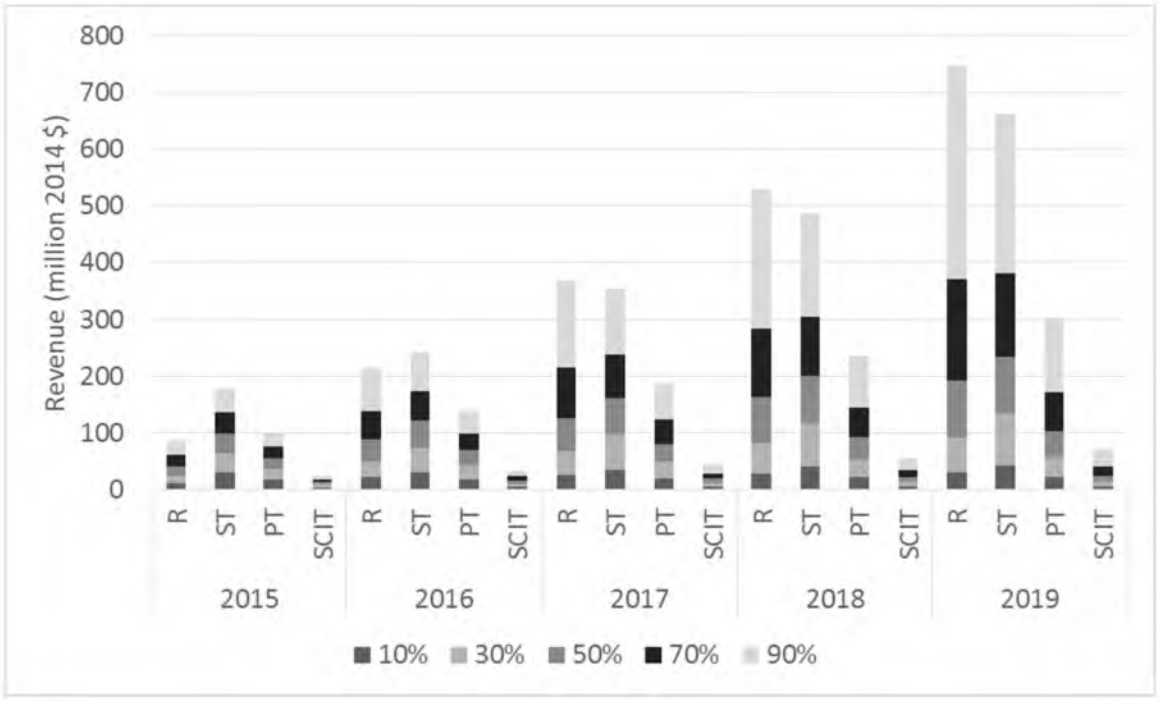

Figure 3.11: MC-simulated revenue for the state of Utah from all sources (R = royalties, ST = severance tax, PT = property tax, SCIT = state corporate income tax) for prediction case. Top of each stacked bar representing the result for that percentile of the MC simulation results.

Table 3.1: Property tax conversion factors (f_{PT}). Property tax (PT) data are from the USTC (2015a). Oil and gas production volumes (P_{oil} and P_{gas}) are from Utah's DOGM (2015). Oil and gas prices (OP and GP) are averages of historical prices from EIA (2015e; 2015g). Oil and gas production volumes, gross revenue (GR), and property taxes are for the Uinta Basin only.

Year	PT (million 2014 $)	OP (2014 $/bbl)	P_{oil} (million bbl)	GP (2014 $/MCF)	P_{gas} (million MCF)	GR (billion 2014 $)	f_{PT}
2000	$5.95	$39.25	7.56	$4.81	97.03	$0.76	0.78%
2001	$7.58	$32.23	8.18	$5.10	107.84	$0.81	0.93%
2002	$7.67	$31.69	7.31	$3.68	116.86	$0.66	1.16%
2003	$7.74	$37.17	7.41	$5.97	123.20	$1.01	0.77%
2004	$10.52	$49.06	9.56	$6.49	147.32	$1.43	0.74%
2005	$14.40	$65.27	11.04	$8.41	184.14	$2.27	0.63%
2006	$21.44	$70.23	11.36	$7.14	226.04	$2.41	0.89%
2007	$21.06	$70.90	13.01	$6.80	243.90	$2.58	0.82%
2008	$27.56	$94.73	15.26	$8.32	300.22	$3.94	0.70%
2009	$29.77	$55.93	15.47	$3.84	312.33	$2.07	1.44%
2010	$30.30	$73.93	17.53	$4.63	319.19	$2.77	1.09%
2011	$34.61	$87.03	18.96	$3.95	338.86	$2.99	1.16%
2012	$40.84	$85.57	22.78	$2.60	369.67	$2.91	1.40%
2013	$38.49	$86.07	27.04	$3.67	370.01	$3.68	1.04%
2014	$49.50	$79.05	32.94	$4.25	363.03	$4.15	1.19%

Table 3.2: Net taxable income conversion factors (f_{NTI}). Net taxable income (*NTI*) data are from the USTC (2015a). Oil and gas production volumes (P_{oil} and P_{gas}) are from Utah's DOGM (2015). Oil and gas prices (*OP* and *GP*) are averages of historical prices from EIA (2015e; 2015g). Oil and gas production volumes, gross revenue (*GR*), and net taxable income are for the entire state of Utah.

Year	*NTI* (million 2014 $)	*OP* (2014 $/bbl)	P_{oil} (million bbl)	*GP* (2014 $/MCF)	P_{gas} (million MCF)	*GR* (billion 2014 $)	f_{NTI}
2009	$73.21	$55.93	22.94	$3.84	449.73	$3.01	2.43%
2010	$227.09	$73.93	24.67	$4.63	440.26	$3.86	5.88%
2011	$231.76	$87.03	26.29	$3.95	462.58	$4.12	5.63%

CHAPTER 4

ECONOMIC ANALYSIS OF IN SITU OIL SHALE PROCESSING

In preparation for Utah Oil Shale – Science, Technology, and Policy Perspectives.

4.1 Introduction

The production of oil from oil shale in the western United States was first commercially attempted in the mid 1910s (EPA Oil Shale Work Group, 1979). In the roughly 100 years since, oil shale has never made the jump from being a "potential" to "proven" source of oil, primarily because no one has demonstrated the economic viability of oil shale relative to other production methods for conventional oil. Consequently one of the key questions to consider in assessing any oil shale production technology or process is "how much will it cost?" Unfortunately, it is difficult to answer this question with any certainty precisely because oil shale is unproven, and as a result, the values of important input parameters and costs are unknown. The reports and studies (STRAAM Engineers, 1979; Bartis et al., 2005; Bezdek, Wendling, and Hirsch, 2006; INTEK Inc., 2009; Wilkey et al., 2013) that have analyzed the costs of developing oil shale do not fully consider the impact of varying their input parameters or costing assumptions. However, as will be discussed in this chapter, much more can be learned about the potential cost range and optimal design of oil shale technologies by rigorously exploring this parameter space.

4.2 Process Description

The in situ production process analyzed here is assumed to be located near Coyote Wash in the Uinta Basin and to have a heating period of seven years. The mass and energy balances for in situ retorting during the heating period are taken from detailed computational fluid dynamics (CFD) simulations performed by Hradisky and Smith (2016). The major processing steps considered in this cost analysis are shown in Figure

4.1 and discussed below. Some of the numbers and values given in the process descriptions are varied as part of the DOE analysis; see Section 4.3.2. These steps only cover the extraction of oil from in situ oil shale. Since oils produced via in situ retorting will most likely require upgrading and will definitely require transportation to market (neither of which is included in this cost analysis), any oil sold by the process shown in Figure 4.1 would sell at a discount compared to benchmark crudes such as West Texas Intermediate.

4.2.1 Drilling

The first step of the process is drilling the wells for heating and producing the oil shale deposit. Two types of wells are drilled, heating wells and producer wells. Heating wells contain the electrical resistance heaters used to heat the formation (see Section 4.2.2). Producer wells collect retorted oil and gas from the formation. The ratio of heating to production wells is assumed to be 12:1 (Wellington et al., 2003). Both well types require drilling (defined as drilling the actual wellbore and placing and cementing the drill casing), and producer wells are assumed to also require completion (defined as perforating and hydraulically fracturing). All wells are drilled horizontally.

In order to estimate well parameters (well lengths, costs, drilling times, etc.), the online database of the Utah Division of Oil, Gas and Mining (DOGM) was searched for horizontal wells drilled in the state of Utah in the last five years. A total of 132 horizontal wells were identified; these wells form the well sample dataset used in this study (Utah DOGM, 2015). Key details about well geometry, drilling, and completion time, and capital costs are discussed below.

4.2.1.1 Well Geometry

Based on the geology of the oil shale deposit at Coyote Wash, the middle of the oil shale deposit is assumed to be located at a vertical depth of 2,500 feet (ft). All wells, regardless of type, are assumed to have the same geometry: a vertical section that runs from the surface to a depth of 1,912 ft, a 90° turn segment which is 924 ft long (made by deflecting each individual 30-ft pipe segment in the turn by 3° from the previous pipe segment), and a lateral segment for either heating or production (depending on well type) that has a variable length. The total length of each well (the sum of the vertical, turn, and lateral segments) is estimated from a log-normal distribution fitted to the total lengths of all wells in the well sample dataset; see Figure 4.2. The length of the lateral (e.g., heating) segment is found by subtracting the lengths of the vertical and turn segments from the total well length. All other aspects of well geometry, such as the number of wells drilled, well spacing, vertical offset, etc., are defined by the in situ retorting simulations described in Hradisky and Smith (2016).

4.2.1.2 Well Drilling and Completion Time

All of the wells required for each in situ retorting scenario must be drilled prior to heating. The two factors that determine how long this takes are: (1) how many drilling rigs are available (i.e., how many wells can be drilled simultaneously), and (2) how long it takes to drill each well. Multiple drilling rigs are required to drill the wells in a timely fashion. The number of rigs available is assumed to be 14, which is half of Utah's annual average rig count between 2008–2013 (Baker Hughes, 2015). The length of time it takes to drill each well was estimated based on the elapsed time between the spud dry date (the

start date of a well's drilling activity) and the date that the target depth was reached (when drilling activity ceases) as reported in the Utah DOGM database for all wells in the sample dataset. Producers and heaters are assumed to take the same amount of time to drill. While this assumption ignores the additional time that must be spent on completion for producer wells, there are time delays during drilling activity in the original dataset (such as waiting for a drilling rig to arrive on site) that would not likely occur with an in situ oil shale drilling project. Based on the available data, the drilling time is best fit using a log-normal distribution (see Figure 4.3), from which drilling times can be varied as part of the DOE analysis.

4.2.1.3 Well Drilling and Completion Capital Costs

Drilling costs typically increase exponentially with total well length and completion costs with the length of the lateral segment. Unfortunately, cost data were too sparsely reported in the well sample dataset (15 wells had drilling costs, 39 had completion costs) to find a good fit for well costs versus length using regression techniques. As a result, the drilling costs are fitted using a normal distribution (Figure 4.4) and completion costs are fitted using a log-normal distribution (Figure 4.5). The costs for each well are then drawn from these distributions in the DOE analysis.

4.2.2 Heating System

Numerous heating systems have been proposed for in situ oil shale production, ranging from downhole-fired heaters to fuel cells to microwave systems (INTEK Inc., 2011). However, the only in situ heating systems that are commercially available at present are electrical resistance heating systems. Therefore, electrical resistance heaters

are used as a basis in this analysis. The heating system consists of a heat-tracing line that converts electricity into heat in the lateral segment of each heating well. The oil shale deposit is then heated through the wall of the drill casing as described in Hradisky and Smith (2016). The capital cost of the heat tracing system (~$50/ft) is based on a case study using mineral-insulated, electric heat-tracing lines in California heavy oil wells (McQueen, Parman, and Williams, 2009).

4.2.3 Electrical Grid

The electrical power demand for each scenario is specified as a function of time by the results of each in situ retorting simulation, all of which are plotted in Figure 4.6 (assuming a lateral well length of 8,500 ft, which is the median lateral well length in the well sample dataset). Electrical power is purchased from Utah's electrical grid, requiring power lines and a substation. The electrical line is assumed to cost $959,700 per mile, equivalent to a 230 kilovolt, 400 megawatt (MW), single-circuit transmission line, and the substation to cost 10% of the total cost of the electrical line (Black & Veatch, 2014). Since the exact length of the shortest route to a suitable grid connection point is unknown, the length of the electrical line is assumed to be 50 miles, which is roughly 50% longer than the straight-line path from Coyote Wash to Vernal, Utah, the largest city in the Uinta Basin. Based on these assumptions, the capital cost for the electrical grid connection is $53 million.

Alternative designs involving the construction of an electrical plant onsite were considered, but given the electrical heating demands of the in situ retorting scenarios, there was no economic justification for building onsite generators. For example, consider

the median energy demand curve in Figure 4.6, which has an initial demand of 6.8 gigawatt-hours per day (GWh/day) (283 MW). Demand drops dramatically to approximately 2.8 GWh/day (117 MW) after the first month and then gradually tapers off to less than 1.0 GWh/day (42 MW) after about 1216 days. Given the median curve's cumulative energy requirements (2,933 GWh), the total electricity cost is $178 million. In comparison, if a 100-MW, natural-gas, combined-cycle power plant were built onsite, the capital cost would be $196 million, assuming Williams six-tenth's scaling (Williams, 1947) and Energy Information Administration (EIA) power plant cost data (U.S. EIA, 2013). The electricity purchase option is the economic winner, even before considering other factors such as (a) the time value of money (upfront capital cost versus ongoing future expense spread out over the seven years of heating/production), (b) the cost of building a pipeline and purchasing fuel to supply the plant before sufficient produced gas is available, and (c) the gap between initial demand and the 283 MW capacity that must still be purchased for the first three years. In reality, the more pressing issue is likely whether or not the grid would have the capacity to supply the energy demand (especially the initial demand). As a point of comparison, Utah's annual average power output is 4.9 GW (U.S. EIA, 2015d). Therefore the median initial demand (at median lateral length) is 5% of the state's power output.

4.2.4 In Situ Retort

The simulated in situ retort is described in detail in Hradisky and Smith (2016). It is in the retort that the oil shale kerogen is pyrolyzed as prescribed by the local temperature field and the kerogen kinetics. In all scenarios, heating occurs for seven

years. The results from each in situ retorting simulation specify, as a function of time, the power requirements for heating and the total mass of products from the kerogen pyrolysis. The maximum possible oil production would occur if 100% of the kerogen were converted to oil and were immediately recovered from the deposit. In reality, kerogen decomposes into oil, gas, and coke, and any produced oil would have to travel through the deposit, delaying production and leaving some oil behind.

These issues are addressed by specifying two mass fractions as part of the DOE analysis: x_r, which represents the fraction of converted hydrocarbons (i.e., pyrolysis products) that are recovered from the formation, and x_g, which represents the fraction of the converted hydrocarbons that is gas (the balance is assumed to be oil). The mass fraction of converted hydrocarbons recovered from the formation, x_r, was modeled as a normal distribution based on the reported product recovery values in Spinti (2016) and in Ryan et al. (2010). The mass fraction of oil converted into gas, x_g, was also modeled as a normal distribution based on values from the same sources.

By specifying these two parameters, the volume of produced oil (v_o) and gas (v_g) can be calculated using Equation 4.1 and 4.2:

$$v_o = \frac{m_k}{\rho_o} \cdot x_r(1 - x_g) \tag{4.1}$$

$$v_g = \frac{m_k}{\rho_g} \cdot x_r \cdot x_g \tag{4.2}$$

where m_k is the mass of converted kerogen (as calculated by the in situ retort simulation) and ρ_o and ρ_g are the densities of the produced oil and gas, respectively. The density of the oil is assumed to be 843 kilograms per cubic meter (kg/m^3), equivalent to an API gravity of 36°. This density is based on the reported properties of shale oil produced via

Shell's In Situ Conversion Process (Beer et al., 2008). The oil and gas heating values, otherwise known as energy density, are taken from property tables for oil and gas produced from 26.7-GPT oil shale (U.S. Department of Energy, 1979). The shale oil heating value is 42.55 megajoules per kilogram (MJ/kg), the gas density is 1.24 kg/m^3, and the gas heating value is 22.78 MJ/kg.

4.2.5 Production, Separation, and Storage System

Any fluids generated from the in situ retort must be produced and then separated and stored at the surface. The design of the production, separation, and storage (PSS) system is based on EIA oil and gas lease equipment and operating costs for primary oil production in the Rocky Mountain region (U.S. EIA, 2010b). EIA's PSS system includes equipment for production by artificial lift with electric motors through a wellhead separator and into a tank battery. Both capital and annual operating costs are presented as a function of well depth. Capital costs are given for a well producing up to 20 barrels of oil per day (BPD) with a water volume fraction of up to 10%. Annual operating costs, on the other hand, assume a production rate of 10 BPD per well. For an 11,000-foot-long well (the median total well length in the well sample dataset) producing at these rates (sizing for 20 BPD for capital costs and charging annual operating costs at 10 BPD), the PSS capital and operating costs are approximately $322,000 and $57,000 per year, respectively, as calculated by linear interpolation using the available well length data points. Since the production rate varies in each scenario, these costs are scaled to meet the maximum production rate of each in situ retort simulation; see Section 4.3.1.1 for a discussion of the cost-scaling methods.

After separation, produced oil and gas are sold at the wellhead as is, while water is sent offsite for disposal. The 'break-even' price for produced oil at the wellhead is one of the model outputs. Note that the produced oil would sell at a discount relative to market prices for other crudes because of upgrading and transportation costs required for bringing the oil to market (e.g., a refinery). Produced gas prices are modeled as a normal distribution based on actual natural gas wellhead prices in the Uinta Basin over the last five years (U.S. EIA, 2015c); see Figure 4.7. They are varied as part of the DOE analysis. Any water that is produced is gravity-separated in the tank battery system and sent offsite for disposal, a cost that is included in the EIA PSS operating costs model.

4.3 Assessment Methodology

This assessment combines discounted cash flow and DOE analyses to determine the economic viability of each scenario. The first component, a discounted cash flow analysis, is used to determine the oil supply price for each scenario. The second component, a DOE analysis, is used to find the ranges of input parameter values for which a future project is economically viable. The actual computation for both components was performed in R (R Core Team, 2015). Each analysis technique is described in detail below.

4.3.1 Discounted Cash Flow Analysis

The cash flow (CF) for any project is defined as the sum of all costs and revenue that accrue in a specified amount of time. For this assessment, the basis is the discounted cash flow accounting method described by Seider et al. (2009). Applying Seider's methodology to the in situ oil shale process described in Section 4.2, the cash flow at any

time step *t* is:

$$CF(t) = S(t) - C_V(t) - C_F(t) - T(t) - R(t) - C_{WC} - C_{TDC} - C_L - C_S - C_{RIP} - C_P - C_{DC} - C_{WR} \quad (4.3)$$

where:

- CF = Annual cash flow
- $S(t)$ = Gross sales revenue
- $C_V(t)$ = Variable operating costs
- C_F = Fixed operating costs
- $T(t)$ = Total taxes
- $R(t)$ = Royalties on oil and gas production
- C_{WC} = Working capital
- C_{TDC} = Total depreciable capital costs (i.e., heating system, PSS, etc.)
- C_L = Capital cost of mineral leases and of land on which production facilities are built
- C_S = Capital cost of startup
- C_{RIP} = Capital cost of royalties for intellectual property
- C_P = Capital cost of permitting
- C_{DC} = Capital cost of heating wells (drilling) and production wells (drilling and completion)
- C_{WR} = Capital cost of well reclamation

Equation 4.3 is generalized so that it covers any time step *t* of any scenario. However, no time step *t* includes all of the terms listed, and some terms are paid for over many time

steps. Terms that are functions of time vary because the oil production rate varies. Each of the scenarios analyzed follows the same relative investment schedule outlined in Table 4.1.

Time steps in the model are tracked on a daily basis. Each scenario begins in the design phase, where mineral rights are leased (C_L), all aspects of the project are permitted (C_P), and 25% of C_{TDC} is spent. The duration of the design phase is assumed to be equal to one-third of the construction phase. In the construction phase, all wells are drilled (C_{DC}) and the remainder of the total depreciable capital costs (C_{TDC}) is invested. The amount of time spent in the construction phase is equal to the amount of time necessary to drill all wells in the scenario or nine months (whichever is greater). Startup occurs in the time step immediately following the completion of construction and concurrently with the beginning of the production phase. Working capital is invested (C_{WC}) and royalties for intellectual property (C_{RIP}) and startup capital (C_S) are spent. The production phase begins after construction is complete. No further capital is invested during this period, but variable expenses and other costs that are functions of time (labor, taxes, royalties, etc.) are paid. The last step of the project, shutdown, occurs in the time step immediately following the end of the production phase, at which time the working capital is reclaimed, production is terminated, and well reclamation costs (C_{WR}) of $30,400 per well (Andersen, Coupal, and White, 2009) are paid.

To account for the time value of money, the cash flow for each year of the project is multiplied by a discount factor *f*, defined as:

$$f_n = \frac{1}{(1 + r_d)^n} \tag{4.4}$$

where r_d is the desired annual discount rate (i.e., interest rate) that the entity financing the project wishes to make each year, n, of a given project. Summing the discounted cash flows for each year of a project gives the net present value (NPV) of the project:

$$NPV = \sum f_n CF_n \tag{4.5}$$

When Equation 4.5 equals zero (i.e., the NPV of the project is zero), the discount rate in Equation 4.4 is defined as the internal (or investor's) rate of return (IRR). IRR is a common financial metric used to compare the value of different projects. Equation 4.5 can also be used to find the oil supply price, which is the oil price needed to produce an NPV of 0 at a given IRR. The IRR was selected as one of the parameters for this analysis. The IRR value ranges, with a mean of 15%, were selected based on recommendations from Seider (Seider et al., 2009) and from reported IRR values for conventional oil projects (Standard & Poor's, 2011).

4.3.1.1 Capital Costs

The capital costs in Equation 4.3 were estimated using a combination of several techniques: vendor estimates, Williams' six-tenths rule (Williams, 1947), statistical analysis of publicly available cost data, and Seider's capital costing method (Seider et al., 2009). Vendor estimates were used for the downhole heating system (McQueen, Parman, and Williams, 2009) and electrical grid connections (Black & Veatch, 2014). Williams' six-tenths rule was used for estimating the scaled costs of the PSS system. According to Williams, economies of scale in process equipment can be modeled using the following equation:

$$C = C_o \left(\frac{Q}{Q_o}\right)^{0.6} \left(\frac{I}{I_o}\right) \quad (4.6)$$

where C is the cost, Q is the material capacity (in this case, the oil production rate), I is an appropriate cost index or inflation index (the Consumer Price Index was used here), and o refers to the base value of the subscripted variable. As discussed in Section 4.2, the capital costs of drilling and completion were obtained from publicly available cost data (Utah DOGM, 2015). Finally, the capital costs for all other terms in Equation 4.3, such as working capital, land, and permitting, were estimated based on the capital costing model of Seider et al. (2009) as shown below in Table 4.2.

4.3.1.2 Operating Costs

The operating costs in each scenario can be differentiated into variable (C_V) and fixed (C_F) costs based on whether or not they are functions of the in situ production operation. The variable costs for the process proposed in Section 4.2 are the costs of operating the PSS system and of buying electricity for the heater system. Electricity is purchased at $0.0607 per kilowatt-hour, which is the average retail price of electricity for industrial users in the state of Utah in 2014 (U.S. EIA, 2015b). PSS operating costs reported in Section 4.2.4 are scaled linearly with the actual daily production for each scenario.

The fixed costs for the process are the costs of labor, maintenance, property taxes and insurance, all of which are estimated as suggested by Seider et al. (2009). Labor costs related to operations are estimated according to assumed hourly wages ($30/hour) and the number of operators required (three per shift, following Seider's recommendations). The process is continuously manned during the production phase. Maintenance is estimated as

5% of C_{TDC} for all of the wages, salaries, and benefits paid to maintenance labor as well as the required materials, services and overhead. Salaried labor costs, including process engineers for technical assistance and control laboratory staff, are assumed to be $82,510 per person per shift per year (U.S. Bureau of Labor Statistics, 2014). Finally, management, including accounting and business services, supervisors, human relations, and the mechanical department, is budgeted as operating overhead based on specific percentages of the total salaries, wages and benefits of the operators, maintenance personnel, lab personnel and engineers. Property taxes and insurance are assumed to be 1% of C_{TPI}. These and other fixed costs are defined in Table 4.3.

4.3.1.3 Corporate Tax, Royalties and Severance Tax

Oil and gas produced through in situ retorting (or any other method) is subject to a number of taxes and royalties. The first (and most straightforward to calculate) is royalty payments, defined as a percentage of the gross sales of the produced oil or gas. For most types of oil and gas production, the percentage collected is 12.5%. However, starting with the passage of the Energy Policy Act of 2005, royalty rates for oil produced from oil shale have been in political limbo. In its initial response to the Energy Policy act of 2005, the U.S. Bureau of Land Management (BLM) proposed a starting rate of 5% for 5 years, followed by an increase of 1% per year up to 12.5%. Subsequent revisions to that proposal/decision have left royalty rates unclear. The BLM's most recent programmatic environmental impact statement for oil shale identified a variety of different methods for setting royalty rates, such as determining them by public comment for each lease during the lease sale, using a sliding scale based on market prices for oil and gas, or establishing

a minimum rate of 12.5% with an option for the Secretary of the Interior to increase the rate in the future (U.S. BLM, 2013). For this analysis, a 12.5% royalty rate is used for both oil and gas.

The state of Utah collects severance taxes on oil and gas using a split rate system based on the market price of each product at the wellhead. The first $13 per barrel (/bbl) for oil and $1.50/MCF for gas are taxed at a rate of 3%; any additional value above these thresholds is taxed at a rate of 5%. An additional 0.2% of the total value (TV) is taxed as a conservation fee (r_{cf}). This set of tax rules is implemented using Equation 4.7:

$$ST = TV\{r_{cf} + [0.03(1 - f_{st}) + 0.05f_{st}]\} \quad (4.7)$$

where ST is the severance tax due to the state on a dollar-per-barrel basis and f_{ST} is the fraction of TV above the threshold value. The results of Equation 4.7 are then multiplied by the volume of oil or gas produced to find the total severance tax due for each product. Finally, corporate incomes taxes are calculated assuming the top rates of 5% and 35% at the state and federal levels, respectively, of taxable income (TI). TI is defined as:

$$TI = P(S - C_V - d) - C_F - D - R - ST \quad (4.8)$$

where d is depletion, D is depreciation, and all other variables are as defined previously. Cost depletion is used to determine d assuming that the cost depletion factor, p_t, is equal to the capital cost of land divided by the total planned oil production. The depletion charge in any given year is then the number of barrels of oil extracted that year multiplied by the depletion factor p_t. A ten-year Modified Accelerated Cost Recovery System method is used for calculating depreciation, with the first depreciation charge occurring at startup. Since state corporate income taxes (T_S) are deductible from federal corporate income taxes (T_F), the total corporate tax liability is given by the following equations:

$$T_S = t_s \cdot TI \tag{4.9}$$

$$T_F = t_f \cdot (TI - T_S) \tag{4.10}$$

where t_S and t_F are the respective state and federal corporate tax rates. Given that property taxes are accounted for as a fixed expense, the total tax liability used in Equation 4.3 is the sum of ST, T_S, and T_F.

4.3.1.4 Model Outputs

Model outputs include the oil supply price, an itemized breakdown of capital and operating costs, and the estimated external energy ratio (EER). EER is the ratio of the energy obtained from the produced oil and gas to the energy required for heating, as defined in Equation 4.11:

$$EER = \frac{v_o \rho_o ED_o + v_g \rho_g ED_g}{E_{in}} \tag{4.11}$$

where E_{in} is the energy input required for retorting, and ED_o and ED_g are the energy densities of oil and gas, respectively, as specified in Section 4.2.4, and the other parameters are as identified in Equations 4.1 and 4.2.

4.3.2 Design of Experiments Analysis

In the DOE analysis technique, the values of the input parameters are varied systematically to determine the contribution of each parameter to the overall system response. In this DOE analysis, the output response is the oil supply price. There are two types of input parameters. Those parameters marked as "well geometry" were varied for the in situ retort analysis discussed in Hradisky and Smith (2016) and are summarized here in Table 4.4. The parameters marked as "economic" were added in this chapter.

Economic parameters are modeled as either normal or log-normal distributions and are summarized in Table 4.5.

Latin hypercube sampling (LHS) was used to select 2000 unique combinations of the "economic" input parameters given in Table 4.5. LHS is a statistical method for selecting sets of parameter values that ensures that there is no overlap in any of the randomly selected parameter values. A small fraction (49) of these points were excluded for returning nonphysical values of at least one parameter (e.g., negative wellhead gas prices, negative gas fractions, etc.). In order to reduce the computational expense of finding an optimal set of LHS points, the randomly selected probability values for drilling costs were also applied to completion costs. For example, if the 40th percentile was selected for drilling costs, then the 40th percentile was also selected for completion costs. Using the discounted cash flow methodology discussed in Section 4.3.1, each of these input parameters combinations were then used to calculate the oil supply price for all 242 designs in Hradisky and Smith (2016) (spanning the ranges of the "well geometry" input parameters). The result was 472,142 unique input parameter combinations (or scenarios) in the DOE analysis.

Next, linear regression was performed to fit the oil supply price results as the sum of all the input parameters using Equation 4.12:

$$(OSP) = a \cdot H_{space} + b \cdot V_{space} + c \cdot V_{angle} + d \cdot V_{location} + e \cdot r + f \cdot n_{row} + g \cdot n_{well} + h \cdot t_{Drill} + i \cdot C_{DC} + j \cdot L + k \cdot x_r + l \cdot x_g + m \cdot gp + n \cdot IRR \quad (4.12)$$

where *OSP* is the oil supply price, the lower case variables *a* through *n* are all fitted coefficients, and all other terms are the input parameters listed in Tables 4.4 and 4.5.

Multiplying the fitted coefficients by the average value of each term then reveals the contribution (on average) of each term to the oil supply price.

4.4 Results and Discussion

4.4.1 Oil Supply Price Results

Raw results from the analysis of the 472,142 scenarios are presented in Figures 4.8 and 4.9. Figure 4.8 shows oil supply price versus each of the 14 input parameters. Figure 4.9 replicates Figure 4.8 but only shows the results from scenarios that have oil supply prices $\leq$ EIA's 2015 Annual Energy Outlook average wellhead oil price for the Rocky Mountain region between 2015 and 2040 under the high-oil-price forecasting assumption. This "economically viable" oil price is approximately $174/bbl (U.S. EIA, 2015b). This limit was picked because historically EIA has tended to underpredict oil prices by as much as half of the actual price.

Two types of plots are shown in Figures 4.8 and 4.9. The first type is hex-binning, which counts the number of points located in a particular region of the plot and colors regions with higher numbers of points more darkly. This plot type is used whenever the input parameter is varied (more or less) continuously. The second type, a violin plot, is used for the input parameters that have discrete values, well radius and number of well rows. Only five values of r and ten values of n_{row} were considered. The violin plot shows the probability that a value y (oil supply price) will occur for each discrete x value of the input parameter. Thicker regions indicate greater numbers of results. While all of the plots show edges to the hexbin region, these edges are unlikely to be true limits. The DOE analysis conducted here only sampled a small portion of all the possible

combinations of well geometry and economic input parameters in Tables 4.4 and 4.5 (0.0045% of all the unique combinations of 13 parameters if each parameter was sampled at the 10^{th}, 20^{th}, 30^{th}, … 90^{th} percentiles). However, the actual distribution (i.e., shape) of the results is representative of the full parameter space.

The oil supply price results in Figure 4.8 and 4.9 display some general trends. Horizontal well spacing (Hs_{pace}) between 20 ft to 40 ft is highly likely to lead to oil supply prices in the \$100–\$1000/bbl region; increasing horizontal spacing above 40 ft tends to substantially increase the maximum oil supply price results. Vertical spacing (V_{space}) of about 60 ft results in an order of magnitude increase in the oil supply price results, perhaps indicating that well geometries with that spacing are missing an important oil shale layer. From the violin plots for the number of rows (n_{row}), it is clear that at least two well rows are required to achieve low oil supply prices. The plot for the number of wells (n_{well}) shows that having either too few or too many wells leads to higher prices. In terms of the economic parameter set, shorter drilling times, lower drilling and completion costs, longer wells, higher recovery fractions, lower gas fractions, and lower IRR values all lead to lower oil supply prices. Gas prices appear to have negligible impact on oil supply prices.

Many of the economic parameter trends are obscured by the impact of the in situ designs in Figure 4.8 but are more noticeable in Figure 4.9. As discussed in Hradisky and Smith (2016), the well geometry parameters play a large role in determining the in situ retort's EER. The EER, which collectively captures the impact of the well geometry parameters and the values of x_r and x_g, was calculated for each of the scenarios using Equation 4.11. The results are shown in Figure 4.10a for the full dataset and in Figure

4.10b for the economically viable dataset. Since most of the in situ designs have low EER values, there is a high density of oil supply price results around $10,000/bbl visible in Figure 4.10a. A second cluster of results is visible in the region between EER values of 4–10, which results in oil supply prices between $100–$200/bbl. These two clusters are visible in all of the economic parameter plots in Figure 4.8. The economically viable set in Figure 4.9 effectively "zooms" in on the cluster in the EER range of 4–10.

The plot of the economically viable set in Figure 4.10b shows that, given the selected LHS sample set, an EER value of at least 2.5 is required to achieve oil supply prices ≤ $174/bbl. Imposing this EER limit excludes 128 of the original 242 well geometry designs from consideration. Interestingly, the in situ designs with the highest EER do not necessarily have the lowest oil supply prices. The best in situ design from the perspective of EER values (EER = 12.5) produces approximately 40% less oil after 500 days than the in situ design with the lowest oil supply prices (EER = 10.1).

Another interesting way of looking at the data is to calculate the median value of each input parameter at different oil supply price thresholds and to observe how it changes. Table 4.6 shows these median values for the full-results dataset and for results less than three price thresholds: $174/bbl (the average EIA high oil forecast price), $100/bbl, and $75/bbl. The largest change in the input parameters occurs when moving from the full-results dataset to the economically viable dataset, which removes from nearly half of the well geometry designs from consideration (although almost every economic parameter set is still included at this stage). At the $100/bbl and $75/bbl thresholds, the well geometry parameter set narrows further with the most substantial changes in the elimination of unfavorable economic parameter sets.

All of these trends are reflected quantitatively in the regression analysis results shown in Table 4.7. The regression analysis was performed with the full dataset. The relative impact of each input term, calculated by normalizing all the impact values by the largest impact term, is shown in Figure 4.11. As in the graphical analysis above, well geometry input parameters have the largest impact. Increasing well spacing (in either the horizontal or vertical direction) leads to the largest increases in the oil supply price, while increasing well radius or the number of rows leads to the largest reductions in oil supply price.

All of these results can be explained by considering the physics of heat transfer in the oil shale deposit. Since the oil shale deposit is being heated conductively, the rate of heat transfer to any point in the deposit is proportional to the inverse square of the distance between the heater and that point. Therefore, increasing the well spacing dramatically increases the amount of time that must elapse before the heating zones of adjacent wells begin to overlap, thus reducing the heating efficiency of the retort system. Increasing the well radius leads to larger amounts of surface area acting as a heat source. Since the retorting simulations specify a constant-temperature boundary condition, the total heat flux from a well will increase linearly with well radius. Higher numbers of well rows leads to more overlapping heating zones, both of which improve efficiency.

Interestingly, increasing the number of wells (n_{well}) increases the oil supply cost. On the one hand, each additional well increases capital and operating costs, but each well also gives more production and at least one additional overlapping heating zone (depending on the number of rows of wells, n_{row}). Part of this result may be explained by the use of only first-order interactions in Equation 4.12, which excludes any possible

interactions between input terms such as n_{well} and n_{row}. The first-order model has 15 terms, all statistically significant except for drilling time, and an R^2 of 0.58. If the model considered all second-order interactions (every possible combination of two input parameters multiplying each other, e.g. $a \cdot n_{well}n_{row} + b \cdot n_{row}C_{Drill} + \cdots + xyz \cdot gpIRR$), then the model would have 120 terms, 90 of which are statistically significant (i.e. p-value ≤ 0.05), and an $R^2 = 0.74$. Nevertheless, Equation 4.14 is more likely to be the better model because it is less prone to overfitting and it explains the majority of the variation in the oil supply price results.

4.4.2 Detailed Breakdown of Costs

A detailed economic breakdown of both the capital costs and per-barrel costs for the economically viable well sets are shown in Figures 4.12 and 4.13, respectively. In these boxplots, the middle line represents the median value, the top and bottom of the box represent the 75th and 25th percentiles of the results, and the whiskers on the top and bottom represent the maximum and minimum values. Also note that the y-axis in Figure 4.12 is shown on a log-scale. The capital cost breakdown in Figure 4.12 clearly shows that the single biggest cost driver is well drilling and completion (C_{DC}), accounting for 42% of C_{TCI} on average for the economically viable scenarios. For comparison, the next largest cost driver, the allocated costs for utilities (i.e., the electrical line, or C_{alloc}), is 16% of C_{TCI} on average. It should also be noted that given the capital costing methodology outlined in Table 4.2, the only independently calculated capital costs are for the heating system, PSS, electrical grid connection (C_{alloc}), and well drilling and completion. All other capital cost categories (C_{ss}, C_{cont}, C_L, C_S, and C_{WC}) are defined as

percentages of other terms.

The per-barrel cost breakdown in Figure 4.13 shows that taxes are the largest per-barrel cost. The amount of money paid in taxes is proportional to the amount of profit taken, as specified in each scenario by the IRR selection. Increasing the IRR results in higher per-barrel profits, which in turn results in higher taxes and royalty payments. After profits, taxes, and royalties, the next largest expense is the cost of capital (C_{TCI}). Electricity purchases, which are (on average) 91% of the variable operating costs (C_V), are the fourth-biggest expense. However, as noted in Section 4.2.3, the cost of building and running a dedicated power plant would be even higher. Fixed operating costs are negligible as both the labor and maintenance required for an in situ operation are minimal.

4.5 Conclusions

In situ oil shale could be economically viable if oil prices recover. Of the scenarios tested in this work, 36% have oil supply prices less than $174/bbl (average oil price between 2015 and 2040 under EIA's high oil price forecast). However, if oil prices only recover to $90/bbl (average oil price between 2015–2040 under EIA's reference forecast), then only 5% of the scenarios would be viable. The primary driver of oil supply prices is the EER, which depends on well geometry parameters, particularly horizontal and vertical well spacing, well radius, and the number of well rows. However, even with ideal EER values, the profitability of oil shale projects is hindered from a financial perspective by (1) the long time delay between the start of the project and the start of production, and (2) the capital expense of drilling and completing wells, both of which

make low oil supply prices difficult to achieve.

4.6 References

Andersen, M., R. Coupal, and B. White. 2009. "Reclamation Costs and Regulation of Oil and Gas Development with Application to Wyoming." In *Western Economics Forum*. Laramie, WY: Western Agricultural Economics Association. http://ageconsearch.umn.edu/bitstream/92846/2/0801005.pdf.

Baker Hughes. 2015. "North America Rotary Rig Count Archive - U.S. Monthly Average by State through 2013." *North America Rotary Rig Count Archive*. http://phx.corporate-ir.net/phoenix.zhtml?c=79687&p=irol-reportsother.

Bartis, J.T., T. LaTourrette, L. Dixon, D.J. Peterson, and G. Cecchine. 2005. "Oil Shale Development in the United States - Prospects and Policy Issues." Santa Monica, CA.

Beer, G.L., E. Zhang, S. Wellington, R. Ryan, and H. Vinegar. 2008. "Shell's In Situ Conversion Process - Factors Affecting the Properties of Produced Shale Oil." In *26th Oil Shale Symposium*. Golden, CO: Colorado School of Mines. http://www.ceri-mines.org/documents/28thsymposium/presentations08/PRES_3-2_Beer_Gary.pdf.

Bezdek, R.H., R.M. Wendling, and R.L. Hirsch. 2006. "Economic Impacts of U.S. Liquid Fuel Mitigation Options." Pittsburgh, PA.

Black & Veatch. 2014. "Capital Costs for Transmission and Substations." Salt Lake City, UT. https://www.wecc.biz/Reliability/2014_TEPPC_Transmission_CapCost_Report_B+V.pdf.

EPA Oil Shale Work Group. 1979. "EPA Program Status Report: Oil Shale - 1979 Update." Washington, DC. https://books.google.com/books?id=ET9SAAAAMAAJ&source=gbs_navlinks_s.

ICSE. 2013. "A Market Assessment of Oil Sands and Oil Shale Resources." Salt Lake City, UT. http://www.icse.utah.edu/assets/for_download/pdfs/projects/2013OilShaleMarketAssessment.pdf.

INTEK Inc. 2009. "National Strategic Unconventional Resource Model - A Decision Support System." Washington, DC.

———. 2011. "Profiles of Companies Engaged in Domestic Oil Shale and Tar Sands Resource and Technology Development." *Secure Fuels from Domestic Resources*.

Washington, DC. http://energy.gov/sites/prod/files/2013/04/f0/SecureFuelsReport2011.pdf.

McQueen, G., D. Parman, and H. Williams. 2009. "Enhanced Oil Recovery of Shallow Wells with Heavy Oil: A Case Study in Electro Thermal Heating of California Oil Wells." *2009 Record of Conference Papers - Industry Applications Society 56th Annual Petroleum and Chemical Industry Conference, PCIC 2009*. doi:10.1109/PCICON.2009.5297168.

R Core Team. 2015. "R: A Language and Environment for Statistical Computing." Vienna, Austria. http://www.r-project.org/.

Ryan, R.C., T.D. Fowler, G.L. Beer, and V. Nair. 2010. "Shell's In Situ Conversion Process−From Laboratory to Field Pilots." In *Oil Shale: A Solution to the Liquid Fuel Dilemma*, edited by O. Ogunsola, A. Hartstein, and O. Ogunsola, 161–83. American Chemical Society. doi:10.1021/bk-2010-1032.ch009.

Seider, W.D., J.D. Seader, D.R. Lewin, and S. Widagdo. 2009. *Product & Process Design Priniciples: Synthesis, Analysis and Design*. 3rd ed. New York, NY: John Wilkey & Sons.

Standard & Poor's. 2011. "Is Natural Gas Drilling Economic at Current Prices?" *CreditWeek*, December. http://www.standardandpoors.com/spf/swf/oilandgas/data/document.pdf.

STRAAM Engineers. 1979. "Capital and Operating Cost Estimating System Handbook: Mining, Retorting, and Upgrading of Oil Shale in Colorado, Utah, and Wyoming." Irvine, CA.

U.S. BLM. 2013. "Secretary Salazar Finalizes Plan Promoting Responsible Oil Shale and Tar Sands Research, Demonstration and Development." http://www.blm.gov/wo/st/en/info/newsroom/2013/march/nr_03_22_2013.html.

U.S. Bureau of Labor Statistics. 2014. "Utah - May 2014 Occupational Employment and Wage Estimates." Washington, DC. http://www.bls.gov/oes/current/oes_ut.htm#17-0000.

U.S. Department of Energy. 1979. "Oil Shale Data Book." Washington, DC: U.S. Department of Commerce National Technical Information Service. https://www.ntis.gov/Search/Home/titleDetail/?abbr=PB80125636.

U.S. EIA. 2010. "Oil and Gas Lease Equipment and Operating Costs 1994 Through 2009." Washington, DC. http://www.eia.gov/pub/oil_gas/natural_gas/data_publications/cost_indices_equipment_production/current/coststudy.html.

———. 2013. “Updated Capital Cost Estimates for Utility Scale Electricity Generating Plants.” http://www.eia.gov/forecasts/capitalcost/pdf/updated_capcost.pdf.

———. 2015a. “Annual Energy Outlook 2015.” Washington, DC. http://www.eia.gov/forecasts/aeo/pdf/0383(2015).pdf.

———. 2015b. “Average Retail Price of Electricity to Ultimate Customers.” *Electric Power Annual*. http://www.eia.gov/electricity/data.cfm#sales.

———. 2015c. “U.S. Natural Gas Prices.” *Monthly Report of Natural Gas Purchases and Deliveries to Consumers*. http://www.eia.gov/dnav/ng/ng_pri_sum_dcu_nus_m.htm.

———. 2015d. “Utah Electricity Profile 2013.” *State Electricity Profiles*. http://www.eia.gov/electricity/state/utah/.

Utah DOGM. 2015. “Data Research Center.” *Division of Oil, Gas & Mining - Oil and Gas Program*. http://oilgas.ogm.utah.gov/Data_Center/DataCenter.cfm.

Wellington, S., I. Berchenko, E.P. Rouffignac, T. Fowler, R. Ryan, G. Shahin, G. Stegemeier, H. Vinegar, and E. Zhang. 2003. In situ thermal processing of an oil shale formation using a controlled heating rate. US20030142964 A1, issued 2003. https://www.google.com/patents/US20030142964.

Williams, R. 1947. “Six-Tenths Factor Aids in Approximating Costs.” *Chemical Engineering* 54 (12): 124–25.

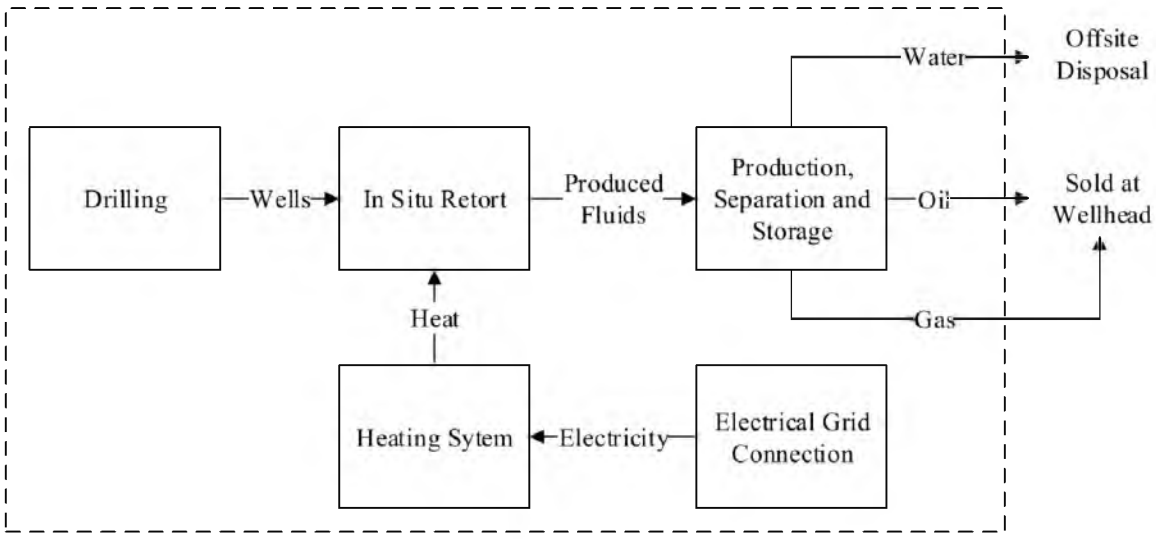

Figure 4.1: Process flow diagram for in situ oil shale production. Blocks represent major process steps and pieces of equipment; arrows represent the flow of process inputs/outputs between them.

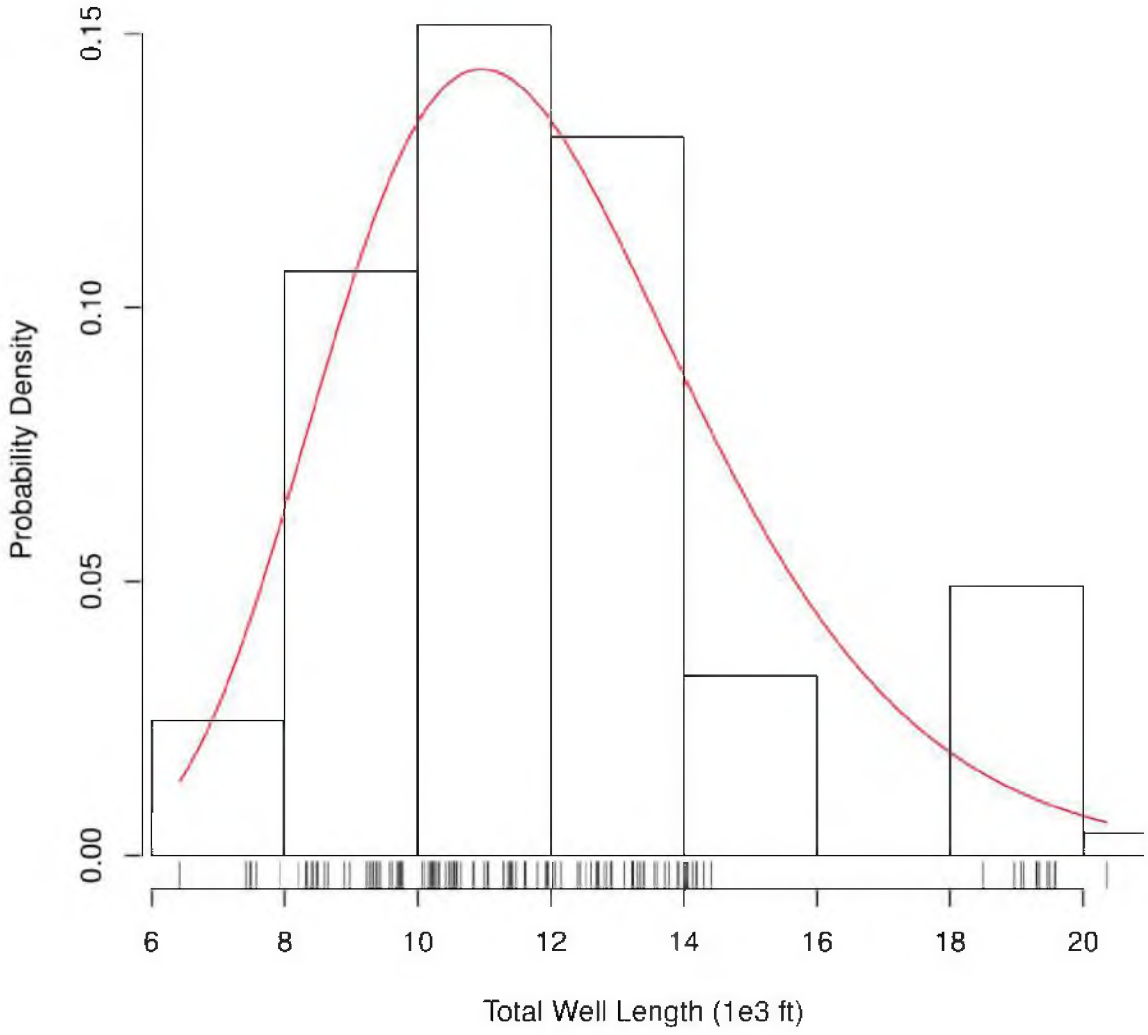

Figure 4.2: Log-normal distribution fit of total well lengths from well sample dataset (Utah DOGM 2015). Histogram and tick marks on x-axis show the original data points while the red line indicates the best log-normal probability distribution function (PDF) fit. Fit parameters: log-mean = 9.363, log-standard deviation = 0.246.

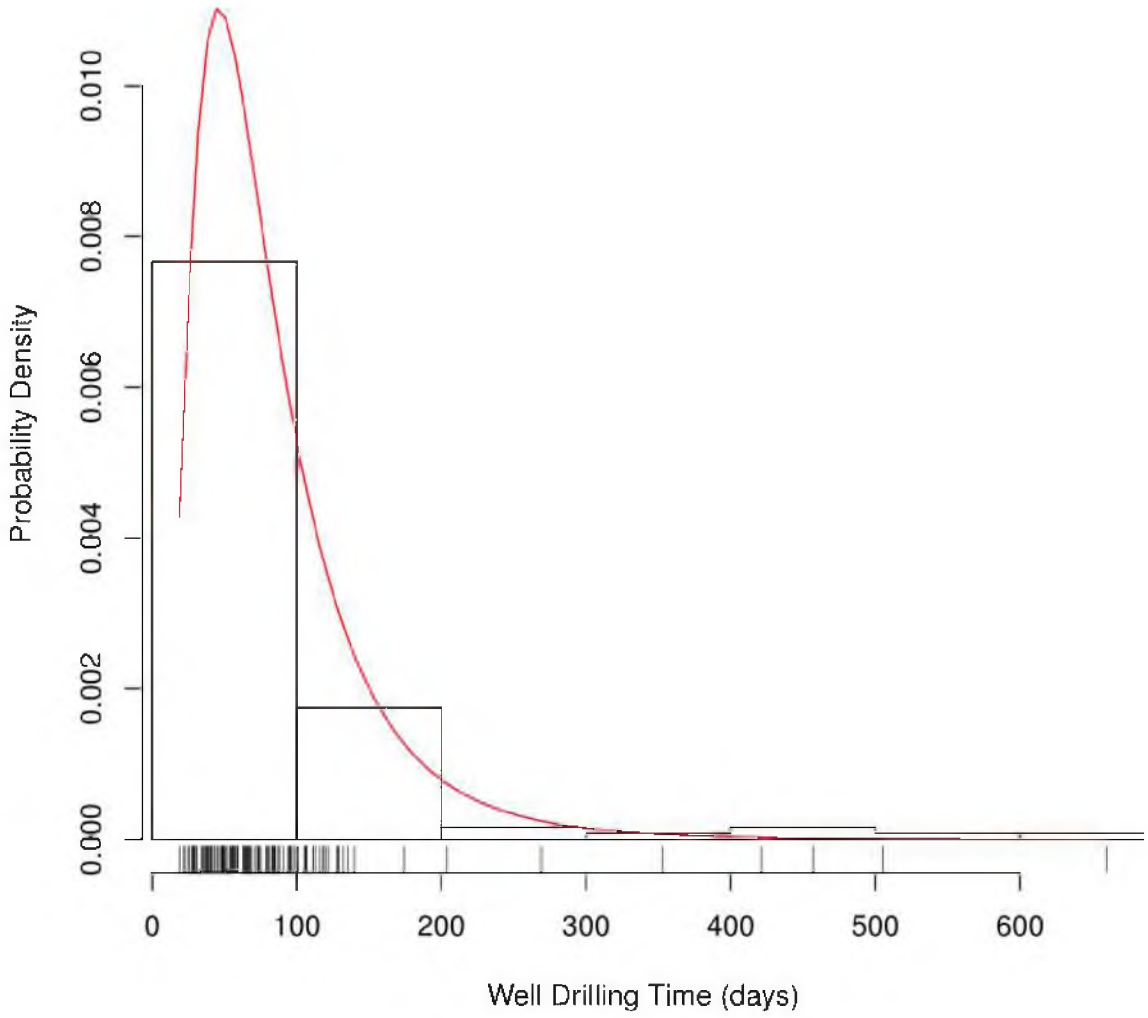

Figure 4.3: Log-normal distribution fit of well drilling time from well sample dataset (Utah DOGM 2015). Fit parameters: log-mean = 4.238, log-standard deviation = 0.641.

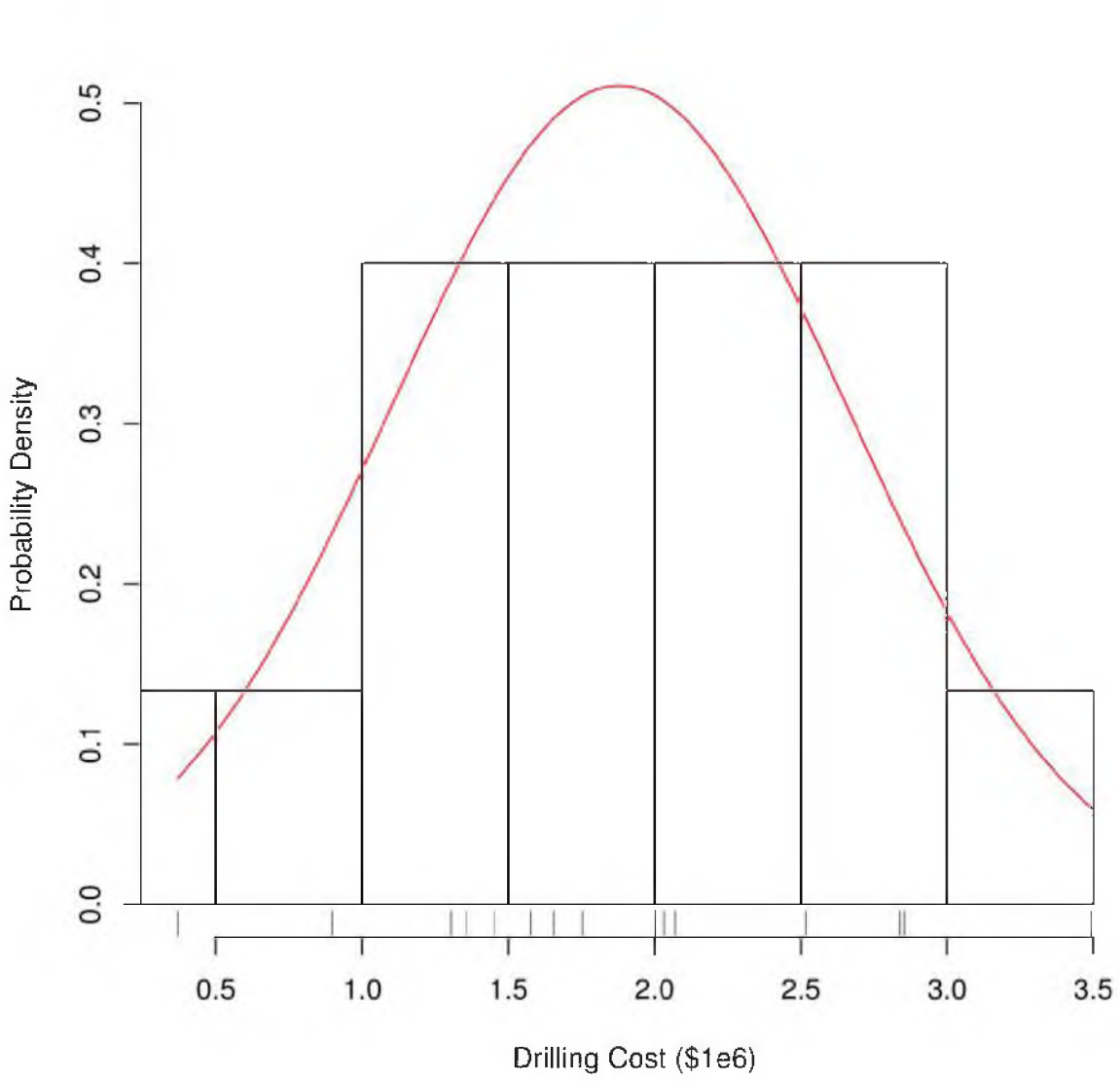

Figure 4.4: Normal distribution fit of drilling costs from well sample dataset (Utah DOGM 2015). Fit parameters: mean = 1.88e6, standard deviation = 0.78e6.

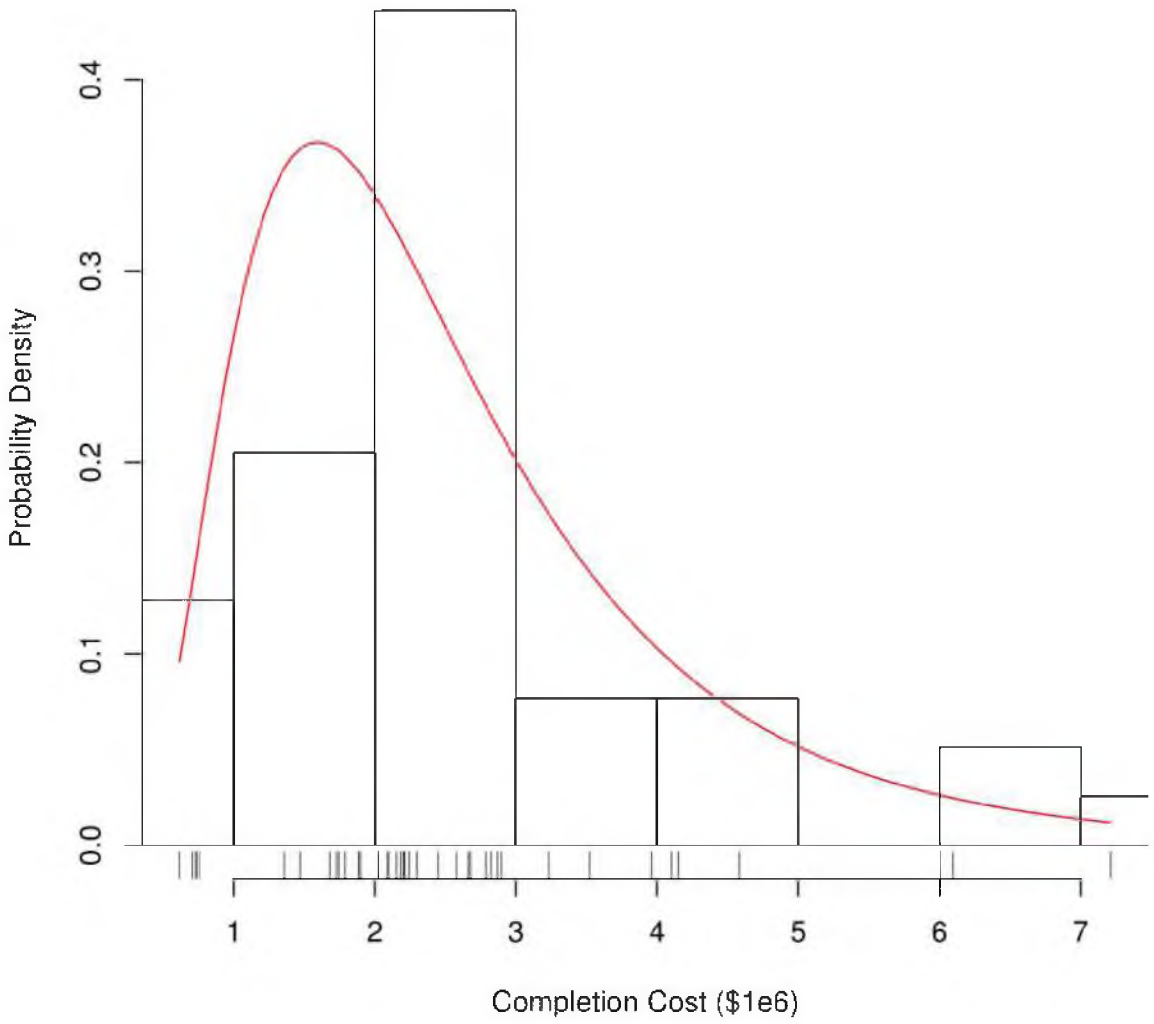

Figure 4.5: Log-normal distribution fit of completion costs from well sample dataset (Utah DOGM 2015). Fit parameters: log-mean = 14.614, log-standard deviation = 0.577.

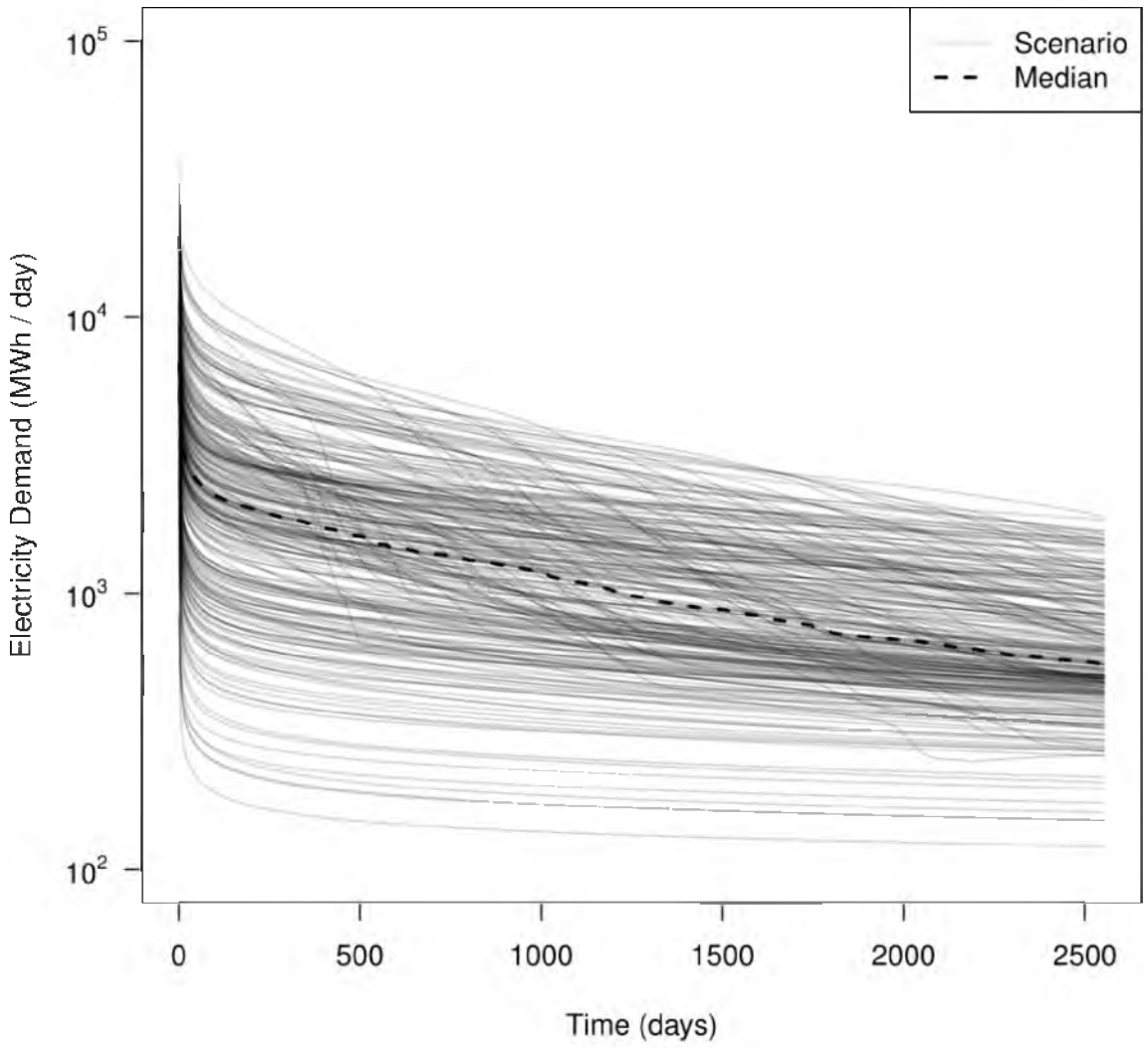

Figure 4.6: Daily electrical energy demand curves for all 242 in situ retort scenarios. The y-axis is on a log-scale. The median of all curves is shown as a dotted line.

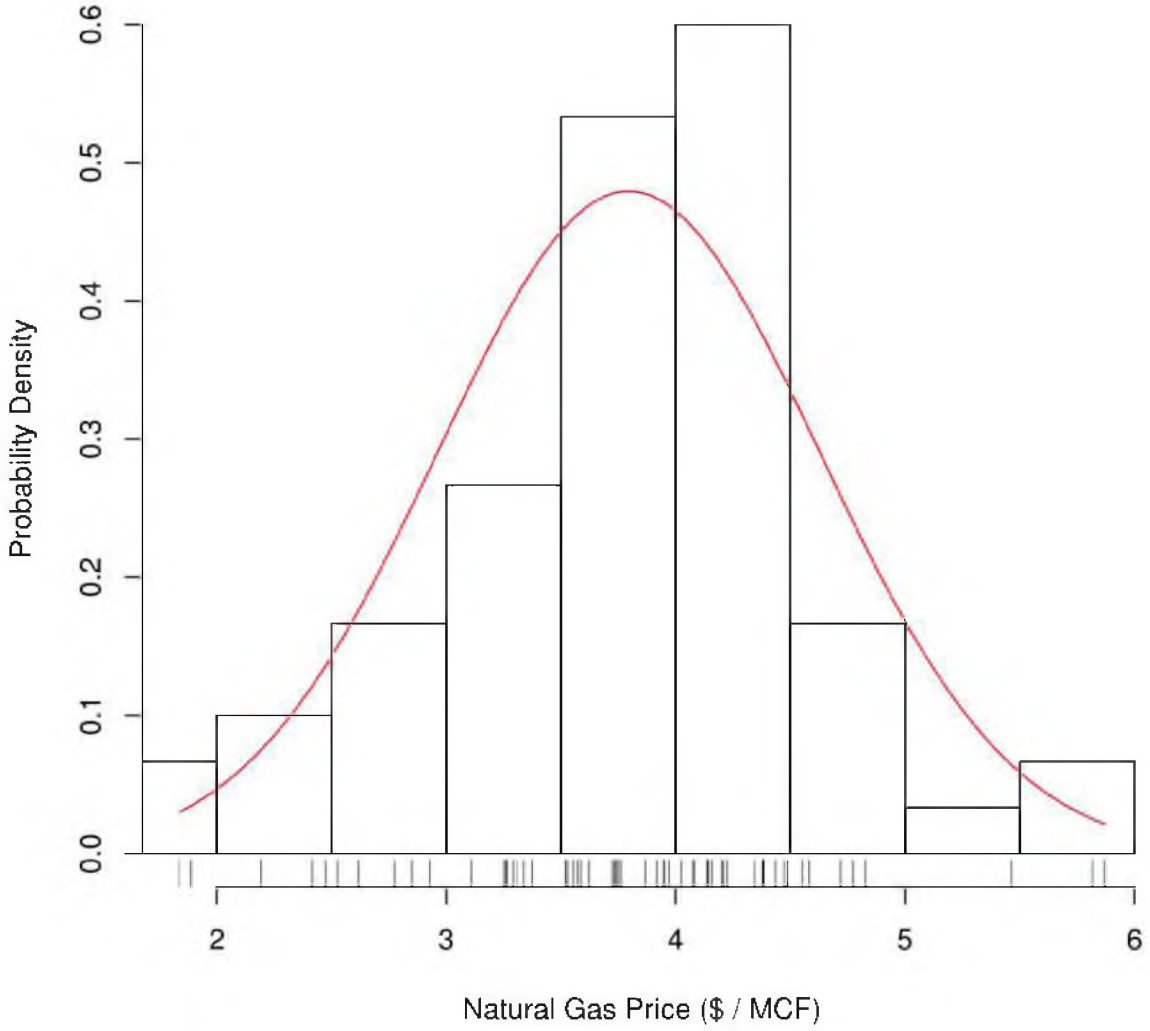

Figure 4.7: Normal distribution fit of monthly natural gas wellhead prices in dollars per thousand standard cubic feet ($/MCF) over the January 2010 to December 2014 time period (U.S. EIA 2015b). Fit parameters: mean = 3.80, standard deviation = 0.83.

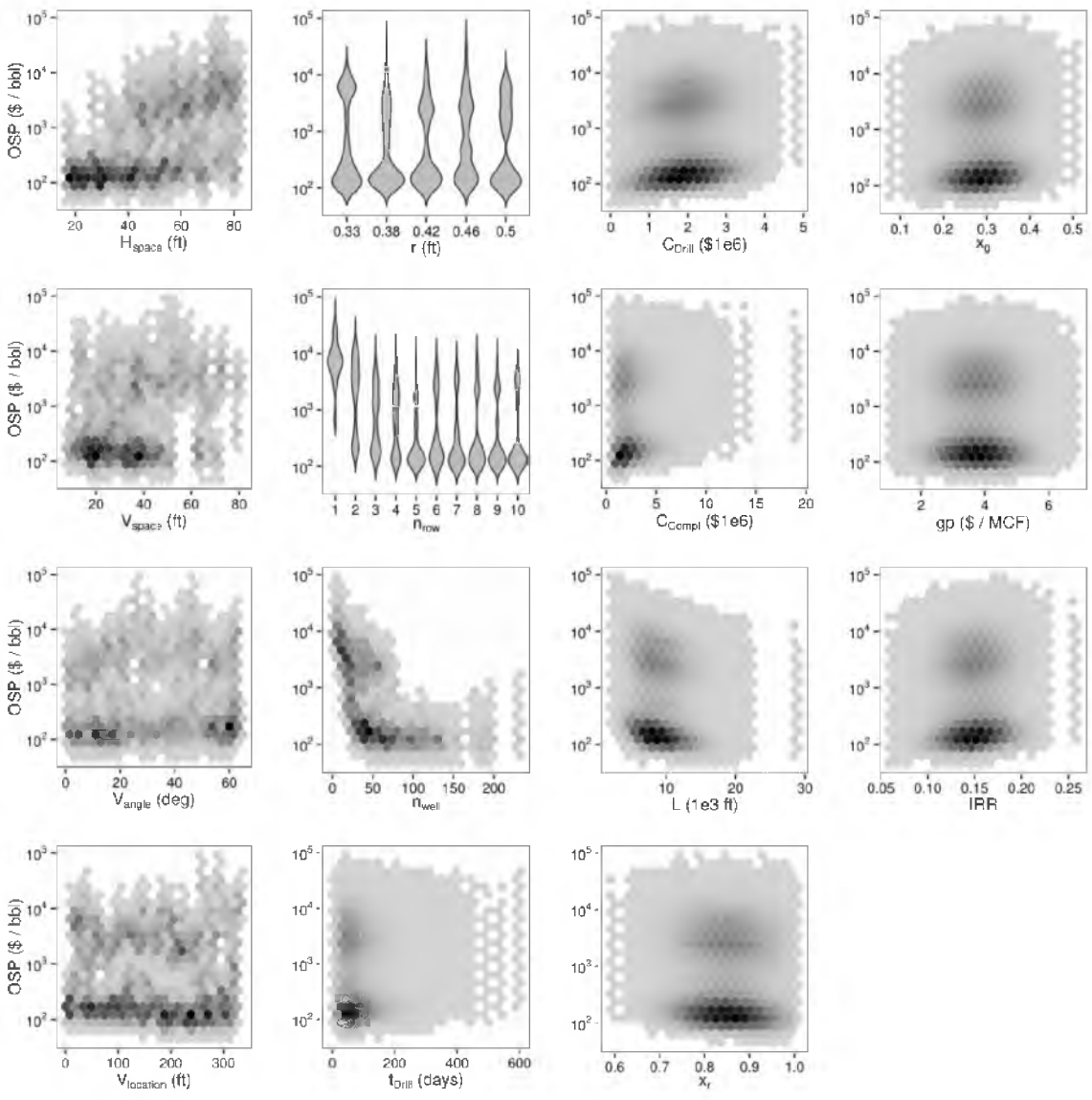

Figure 4.8: Hexbin xy-scatterplots and violin plots of oil supply price versus the input parameters in Tables 4.4 and 4.5. The y-axis for all plots is on a log-scale.

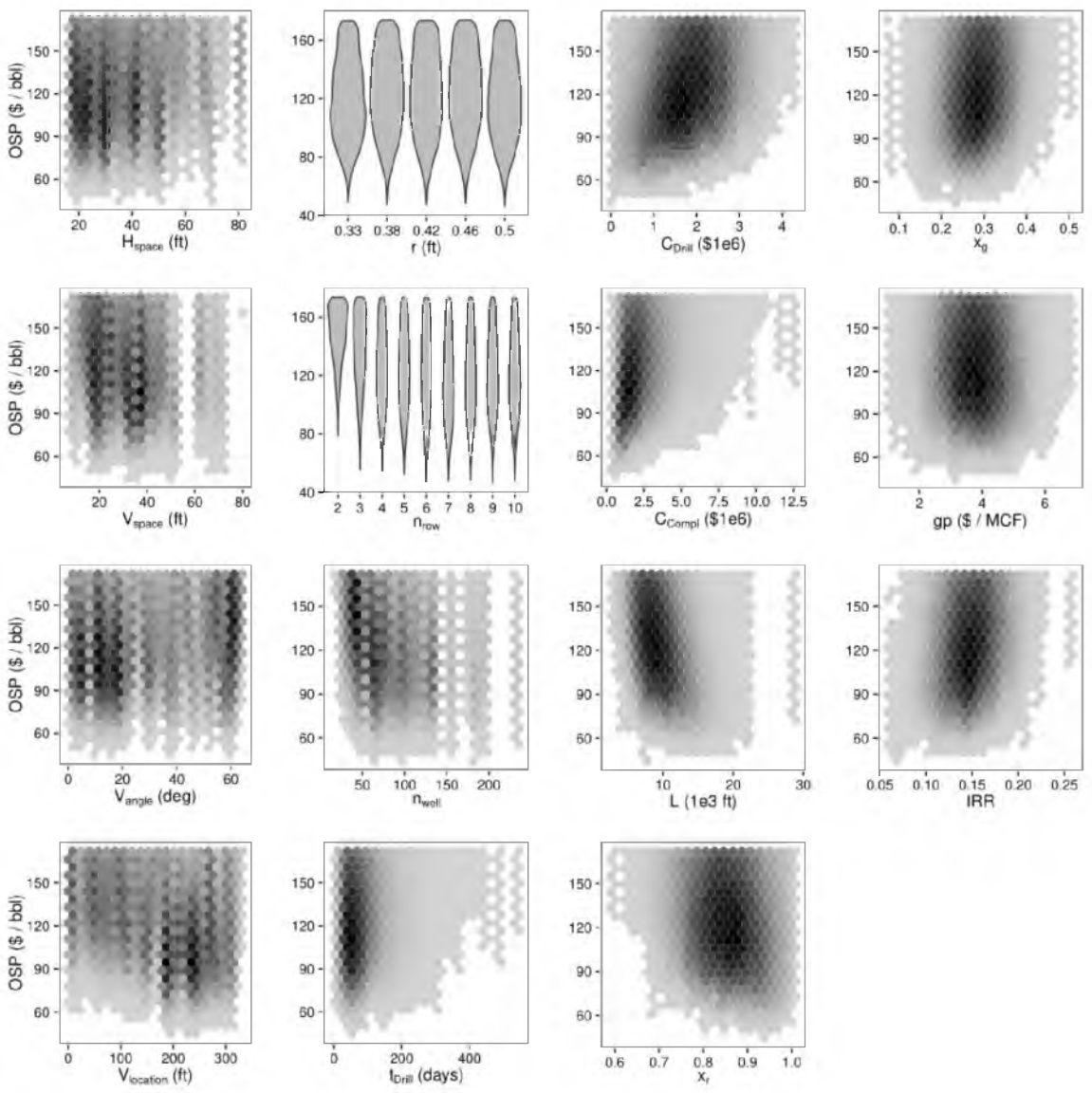

Figure 4.9: Hexbin xy-scatterplots and violin plots of oil supply price versus the input parameters in Tables 4.4 and 4.5 for scenarios with oil supply prices ≤ $174/bbl. The y-axis is on a linear scale.

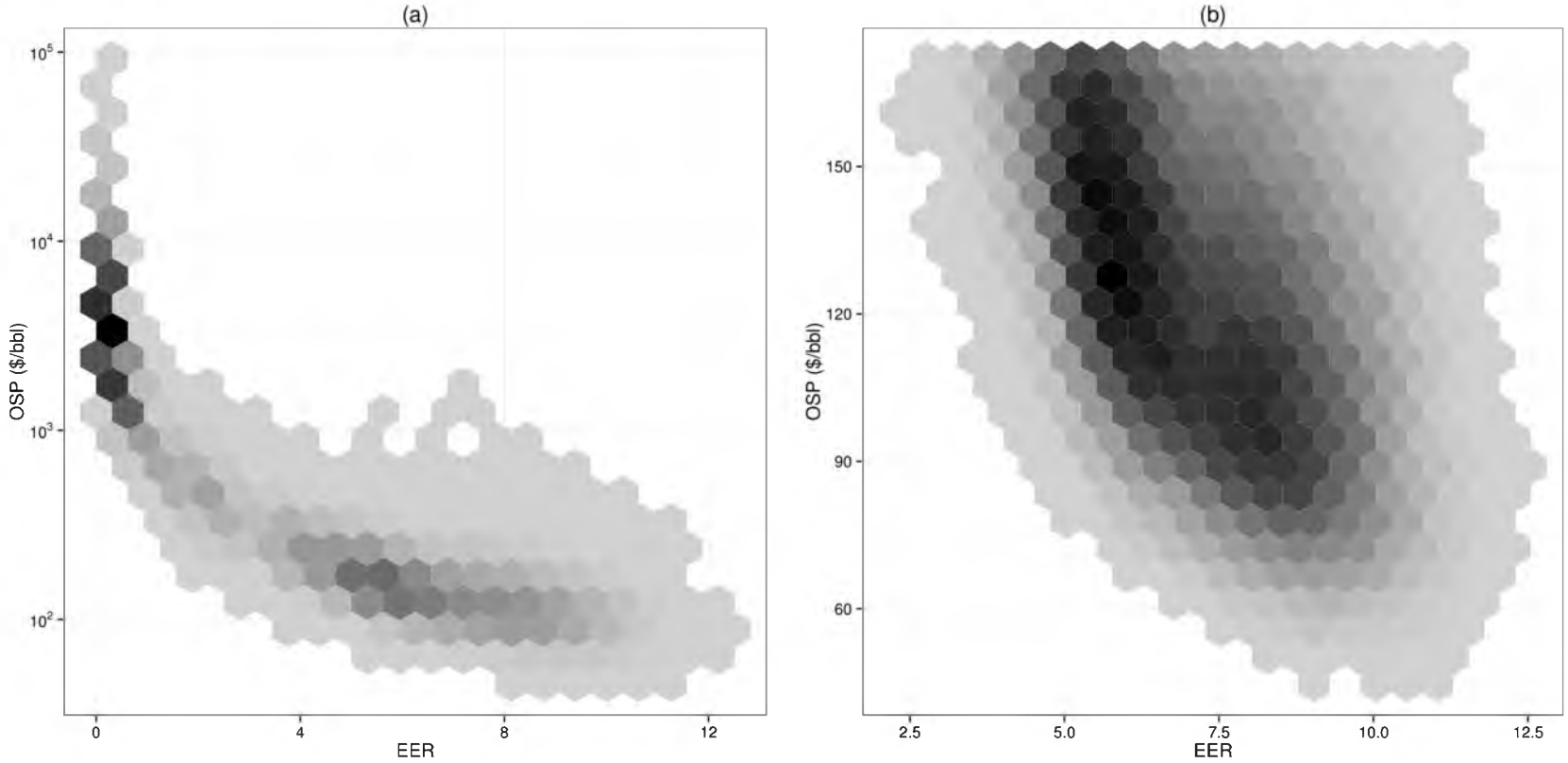

Figure 4.10: Hexbin xy-scatterplots of oil supply price versus EER for (a) all scenarios (note that the y-axis is on a log-scale) and (b) for scenarios with oil supply prices $\leq$ \$174/bbl.

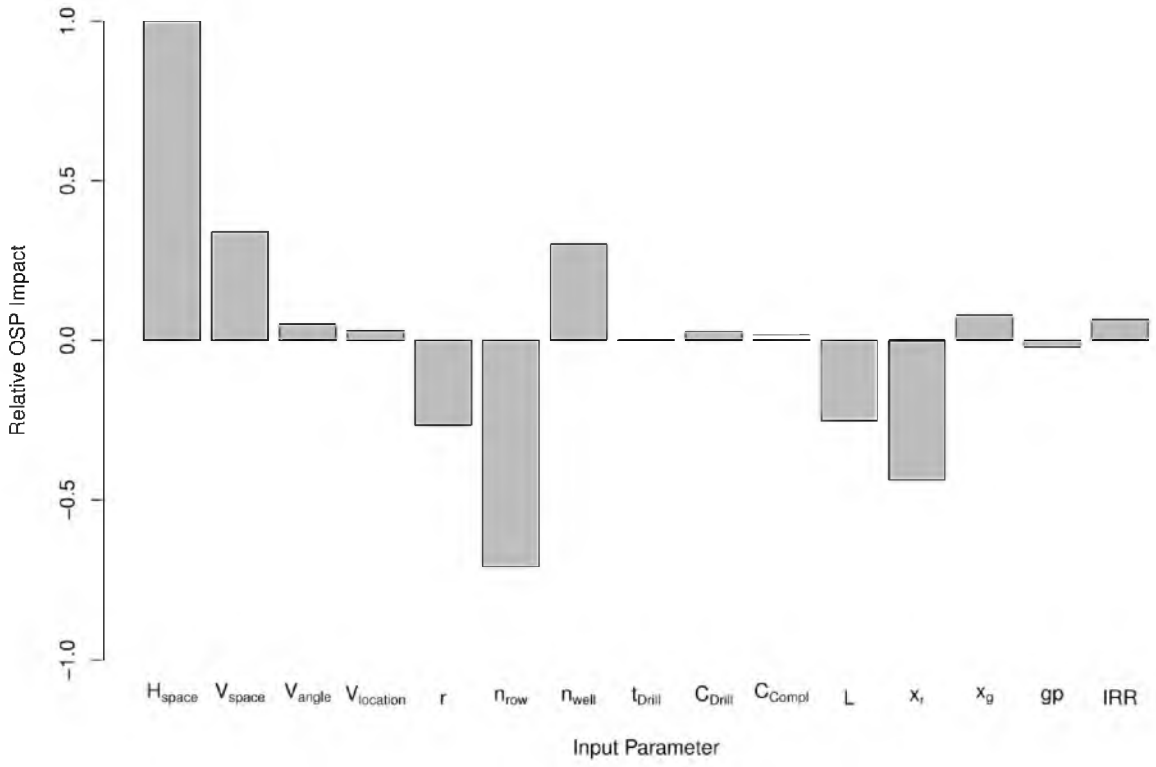

Figure 4.11: Relative oil supply price impact of each input parameter. Increases in parameters with positive impact values result in higher oil supply prices, while increases in parameters with negative impact values result in lower oil supply prices.

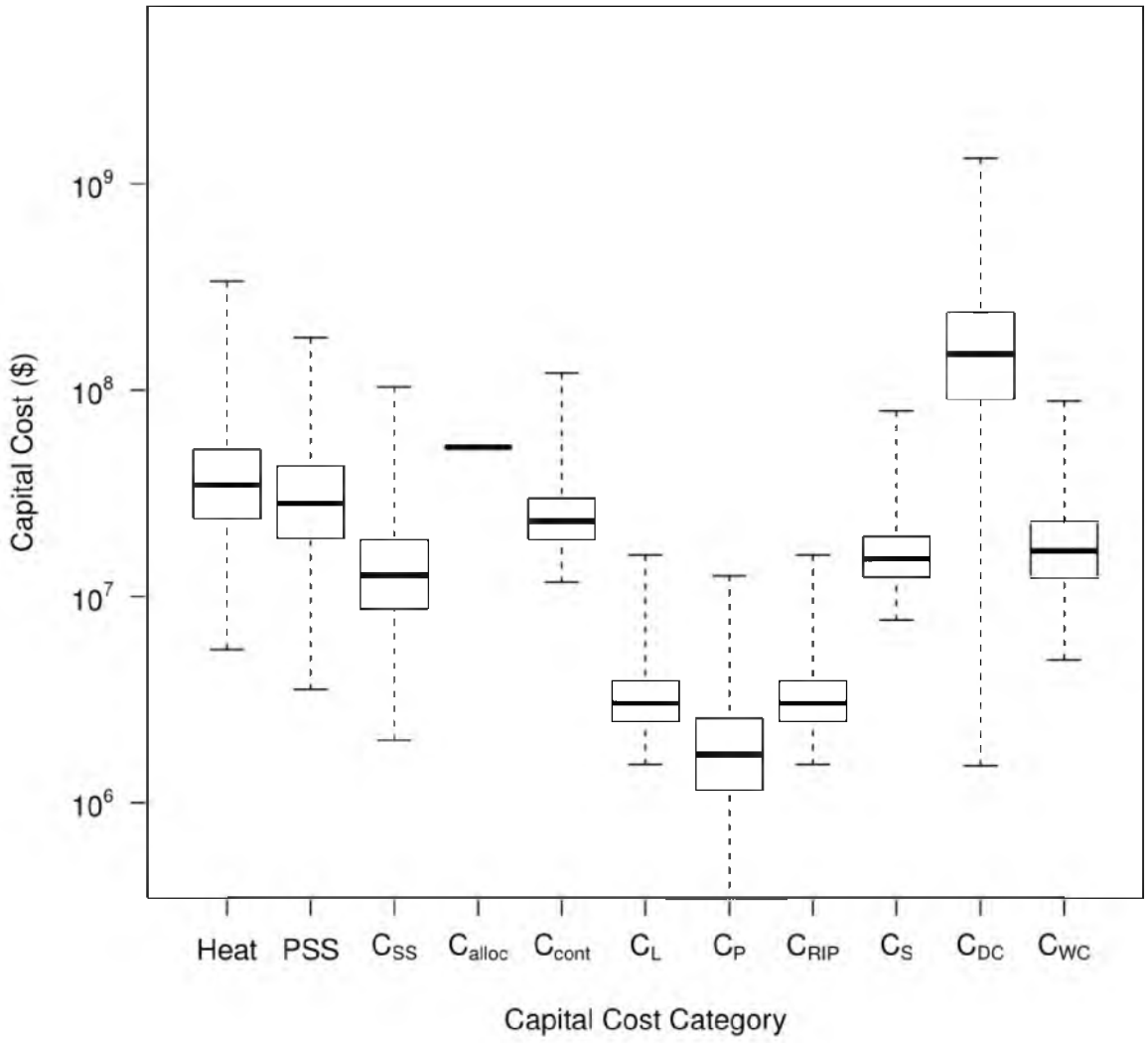

Figure 4.12: Capital cost breakdown for wells with oil supply price ≤ $174/bbl. Heat is the heating system, PSS is the production, separation, and storage system, and all other terms are as defined in Table 4.2.

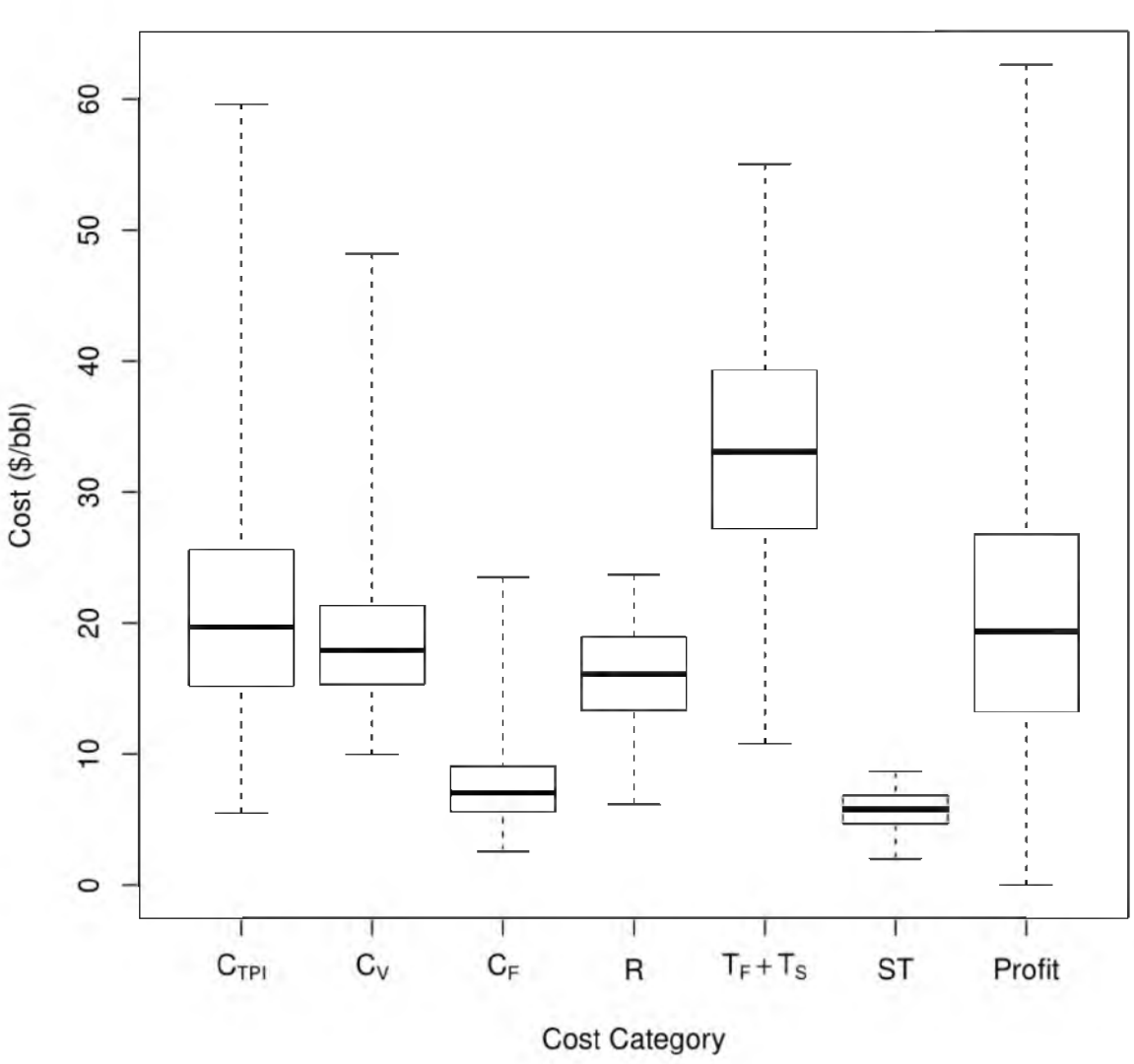

Figure 4.13: Costs on a dollar-per-barrel basis for wells with oil supply price ≤ $174/bbl. Profit is the net earnings on each barrel of oil necessary to produce each scenario's specified IRR. All other terms are as defined in Section 4.3.1.

Table 4.1: Capital investment schedule

Phase	Investment							
	C_{TDC}	C_L	C_P	C_{DC}	C_{WC}	C_{RIP}	C_S	C_{WR}
Design	X	X	X	–	–	–	–	–
Construction	X	–	–	X	–	–	–	–
Startup	–	–	–	–	X	X	X	–
Production	–	–	–	–	–	–	–	–
Shutdown	–	–	–	–	X	–	–	X

Table 4.2: Capital costing method, modified from Seider et al. (2009).

Category	Symbol and Definition
Total Bare Module Investment (TBM)	C_{TBM} = sum of costs for heating and PSS systems
Cost of site preparation and service facilities	C_{SS} = 20% of C_{TBM}
Allocated costs for utility plants	C_{alloc} = cost of electrical grid connection
Total Direct Permanent Investment (DPI)	$C_{DPI} = C_{TBM} + C_{site} + C_{serv} + C_{alloc}$
Cost for contingencies & contractor fees	C_{cont} = 15% of C_{DPI}
Total Depreciable Capital (TDC)	$C_{TDC} = C_{DPI} + C_{cont}$
Cost of mineral rights and land leases	C_L = 2% of C_{TDC}
Cost of permitting	C_P = \$0.10 / bbl of oil produced
Cost of royalties for intellectual property	C_{RIP} = 2% of C_{TDC}
Cost of plant startup	C_S = 10% of C_{TDC}
Cost of drilling and completing wells (DC)	C_{DC} = Estimated as part of DOE analysis
Total Permanent Investment (TPI)	$C_{TPI} = C_{TDC} + C_L + C_P + C_{RIP} + C_S + C_{DC}$
Working Capital (WC)	C_{WC} = 5% of C_{TPI}
Total Capital Investment (TCI)	$C_{TCI} = C_{TPI} + C_{WC}$

Table 4.3: Fixed costs included in scenario analyses; modified from Seider et al. (2009) and U.S. BLS (2014).

Cost	Method of Calculation
Labor for Operations	
Wages and Benefits (LW)	LW = \$30/operator-hour
Salary and Benefits (LS)	LS = 15% of LW
Operating Supplies and Services	6% of LW
Technical Assistance	\$82,510/(operator/shift)/year
Control Laboratory	\$82,510/(operator/shift)/year
Maintenance (M)	5% of C_{TDC}
Wages and Benefits (MW)	43.48% of M
Salary and Benefits (MS)	10.87% of M
Materials and Services	43.48% of M
Maintenance Overhead	2.17% of M
Operating Overhead	
General Plant Overhead	7.1% of (LW + LS + MW + MS)
Mechanical Department Services	2.4% of (LW + LS + MW + MS)
Employee Relations Department	5.9% of (LW + LS + MW + MS)
Business Services	7.4% of (LW + LS + MW + MS)
Property Tax	1.0% of C_{TPI}
Insurance	0.4% of C_{TPI}
General Expenses	
Administrative Expense	\$200,000/(20 employees)/year
Management Incentive Compensation	1.25% of net profit

Table 4.4: Well geometry input parameters and value ranges for DOE analysis.

Input Parameter	Type	Range
Horizontal well spacing (H_{space}, ft)	Well Geometry	16.70–81.89
Vertical well spacing (V_{space}, ft)	Well Geometry	8.37–80.74
Offset angle (V_{angle}, degrees)	Well Geometry	0.11–63.39
Location of 1st row of wells in formation ($V_{location}$, ft)	Well Geometry	0.30–328.02
Well radius (r, inch)	Well Geometry	4–6
Number of well rows (n_{row})	Well Geometry	110
Number of wells (n_{well})*	Well Geometry	5232

* Note: The number of wells is calculated from the parameters for the number of rows and the well spacing.

Table 4.5: Economic input parameters, distribution types, fit parameters, and percentiles for DOE analysis. In table headings, SD = standard deviation, P10 = 10th percentile, and P90 = 90th percentile. Mean and SD values for log-normal distributions are the log-mean and log-standard deviation.

Input Parameter	Distribution	Mean	SD	P10	P90
Drilling time (t_{Drill}, days)	Log-normal	4.24	0.641	30	158
Drilling capital cost (C_{Drill}, \$1e6/well)	Normal	1.88	0.781	\$0.89	\$2.9
Completion capital cost (C_{Compl}, \$1e6/well)	Log-normal	14.6	0.577	\$1.1	\$4.7
Total well length (L, ft)	Log-normal	9.36	0.246	8,497	15,962
Recovery mass fraction (x_r)	Normal	0.85	0.071	0.76	0.94
Gas mass fraction (x_g)	Normal	0.29	0.057	0.22	0.36
Wellhead natural gas price (gp, \$/MCF)	Normal	3.80	0.832	\$2.73	\$4.86
IRR	Normal	0.15	0.025	11.8%	18.2%

Table 4.6: Median values of input parameters and of EER (model output) at different oil supply price cutoff thresholds.

Item	Full Range	≤ $174/bbl	≤ $100/bbl	≤ $75/bbl
Horizontal well spacing (H_{space}, ft)	49.0	34.7	30.5	30.1
Vertical well spacing (V_{space}, ft)	33.7	31.2	32.9	32.6
Offset angle (V_{angle}, degrees)	31.1	26.7	18.9	18.9
Location of 1st row of wells in formation ($V_{location}$, ft)	168.6	187.8	229.1	234.3
Well radius (r, inch)	5	5	5	5
Number of well rows (n_{row})	5	7	7	7
Number of wells (n_{well})	43	73	88	88
Drilling time (t_{Drill}, days)	69	67	62	58
Drilling capital cost (C_{Drill}, $1e6/well)	$1.89	$1.75	$1.41	$1.02
Completion capital cost (C_{Compl}, $1e6/well)	$2.23	$2.02	$1.57	$1.18
Total well length (L, ft)	11,617	12,325	13,690	15,268
Recovery mass fraction (x_r)	84.8%	85.5%	87.0%	89.5%
Gas mass fraction (x_g)	29.0%	28.4%	27.3%	26.3%
Wellhead natural gas price (gp, $/MCF)	$3.79	$3.80	$3.84	$3.85
IRR	15.0%	14.7%	14.1%	13.8%
EER	3.92	7.18	8.41	9.06
Number of well geometry parameter sets	242	134	112	76
Number of economic parameter sets	1,951	1,915	1,164	383
Percent of all LHS cases	100%	35.5%	8.4%	1.4%

Table 4.7: Regression results and impact analysis.

Input Parameter	Fitted Coefficient	Median Value	Impact Factor
Horizontal well spacing (H_{space}, ft)	154.31	48.95	7,554
Vertical well spacing (V_{space}, ft)	76.39	33.67	2,572
Offset angle (V_{angle}, degrees)	12.36	31.13	385
Location of 1st row of wells in formation ($V_{location}$, ft)	1.35	168.57	227
Well radius (r, inch)	-401.47	5	-2,007
Number of well rows (n_{row})	-1,071	5	-5,353
Number of wells (n_{well})	52.92	43	2,276
Drilling and completion time (t_{Drill}, days)	0.08	69	5
Drilling cost (C_{Drill}, $1e6/well)	1.11E-04	1.89E+06	209
Completion cost (C_{Compl}, $1e6/well)	5.65E-05	2.23E+06	126
Well lateral/heating length (L, ft)	-0.16	11617	-1,903
Recovery mass fraction (x_r)	-3,888	0.85	-3,298
Gas mass fraction (x_g)	2,029	0.29	589
Wellhead gas price (gp, $/MCF)	-40.54	3.79	-154
IRR	3,248	0.15	487

CHAPTER 5

ECONOMIC ANALYSIS OF EX SITU OIL SHALE PROCESSING

In preparation for SPE Economics & Management. Economic analysis of ex situ oil shale processing. J.E. Wilkey, T.A. Ring, J.C. Spinti

5.1 Introduction

The production of oil from oil shale in the western United States was first commercially attempted in the mid 1910s (EPA Oil Shale Work Group, 1979). In the roughly 100 years since, oil shale in the United States has never made the jump from being a "potential" to "proven" source of oil, primarily because no one has demonstrated the economic viability of oil shale relative to other production methods for conventional oil. Consequently, one of the key questions to consider in assessing any oil shale production technology or process is "how much will it cost?" Unfortunately, it is difficult to answer this question with any certainty precisely because U.S. oil shale is unproven, and as a result, the values of important input parameters and costs are unknown.

Oil shale processing techniques are typically differentiated by whether they occur in place (in situ) or above ground (ex situ). Both processing techniques have their own input parameter uncertainties which can impact economic viability. Wilkey, Spinti, and Ring (2016) analyzed a set of 14 different input parameters for in situ oil shale to determine the impact of each parameter on oil supply prices for that processing method. In this study, we apply the same approach to ex situ oil shale to improve upon the oil supply price estimates from previous studies (Bartis et al., 2005; Bezdek, Wendling, and Hirsch, 2006; Wilkey et al., 2013; INTEK Inc., 2009; STRAAM Engineers, 1979; Aguilera, 2014) by thoroughly analyzing the impact of varying input parameters and costing assumptions. We identify six parameters that have large uncertainties and/or first-order impacts on the oil supply price for an ex situ oil shale scenario in Utah's Uinta Basin. We then rigorously explore the parameter space to determine likely values for oil supply price and to identify which parameters have the largest impact on cost. The

methodology outlined in this paper is useful for estimating costs of other oil shale projects in the future.

5.2 Methodology

5.2.1 Overview

In this work, we use a discounted cash flow (DCF) analysis to calculate the oil supply price (OSP), which is the oil price necessary for an ex situ oil shale process to be profitable at a specified level as a function of a set of input parameters. A full factorial design of experiments (DOE) analysis is used to probe the input parameter space and to produce a range of OSPs resulting from these inputs. The system boundaries and process steps included in our analysis are shown in Figure 5.1. Every block in the diagram represents a processing step for which capital costs are estimated, and arrows represent flows of materials and energy between steps. A brief description of the ex situ process model is given next, followed by a discussion of the DCF and DOE analysis methods.

5.2.2 Process Description

In this study we consider just the costs of extracting oil from oil shale via underground mining and surface retorting using the Paraho Direct process. This ex situ oil shale scenario was analyzed by researchers at the University of Utah's Institute for Clean and Secure Energy (Wilkey et al., 2013), and that analysis is the basis for the work discussed here. The process, capital costs, and operating requirements are summarized below in Table 5.1.

In the ICSE (2013) scenario, oil shale is mined from a location in the northeast corner of Utah's Uinta Basin at a depth of 500 – 1,000 feet (ft), which contains a 60–130

ft thick zone of oil shale that averages 25 gallons per ton (GPT). The oil shale is mined underground via a room and pillar method where some of the ore is left behind to support the mine ceiling. Ore is mined at a rate sufficient to meet the operating scale of the retort, crushed, and then sent to the surface for retorting. The Paraho Direct retorting process is classified as a vertical, co-gravity, direct-heated retort system (STRAAM Engineers, 1979) and is reasonably similar to process designs for the current generation of oil shale surface retorts. Raw crushed oil shale is fed in through the top of the retort and moves downward by gravity through (a) mist formation, (b) retorting, (c) combustion, and finally (d) cooling zones. Temperature and heat transfer in each zone is managed using counter-current air and recycle gas, which are injected through a set of air distributors. Oil mist and produced gas are collected from the top of the retort. Oil is condensed and sold as-is to market, while any produced gases are recycled through the retort and other onsite utilities for use as a fuel gas. It should be noted that the produced oil would likely sell at a discount compared to other benchmark crudes because of inferior product properties (low API gravity, high sulfur and nitrogen content, etc.).

In addition to the mine and retort, a number of other support facilities must be built in the ICSE (2013) scenario. A water pipeline is constructed from the site to the nearby White River (5 miles from site), and a water reservoir (sized to hold 90 days of process water) is constructed on site. Additional onsite utilities include a cooling water plant and a steam plant. Lastly, a 230 kilovolt (kV) electrical power line is built from the nearest town (Bonanza, UT, 6.5 miles from site) and an electrical substation is constructed onsite to connect the facility to the electrical grid.

5.2.3 DCF Analysis

The cash flow for any project is defined as the sum of all costs and revenue that accrue in a specified amount of time. For this study, the annual cash flow in any year *t* is given by:

$$CF(t) = P(t) \cdot \big(S(t) - C_V(t)\big) - C_F - T(t) - R(t) - C_{TDC} - C_L - C_S - C_{RIP} - C_P \pm C_{WC} \quad (5.1)$$

where:

- $CF(t)$ = Annual cash flow
- $P(t)$ = Production capacity (fraction of year during which plant is in operation)
- $S(t)$ = Gross sales revenue
- $C_V(t)$ = Variable operating costs
- C_F = Fixed operating costs
- $T(t)$ = Taxes (corporate income, severance, and property taxes)
- $R(t)$ = Royalties on oil and gas production
- C_{TDC} = Total depreciable capital costs (mine, retort, utilities, etc.)
- C_L = Capital cost of mineral leases and of land on which production facilities are built
- C_S = Capital cost of startup
- C_{RIP} = Capital cost of royalties for intellectual property
- C_P = Capital cost of permitting
- C_{WC} = Working capital

Equation (5.1) is generalized so that it covers any year of any scenario generated as part of the DOE analysis. However, no single year includes all of the terms listed and some costs are spread over several years. Terms that are functions of time vary because the oil production rate varies throughout the project. The project schedule used for all scenarios is outlined in Table 5.2. The first year of the project is spent on design and permitting work (25% of C_{TDC} spent), followed by three years of construction work (C_L is spent in the beginning of year 2, remaining 75% of C_{TDC} is spent evenly throughout the three years of construction). After construction is complete, the remaining capital cost terms are spent (C_S, C_{RIP}, and C_{WC}), and production ramps up over the course of two years until the facility is in operation 330 days (90%) per year. Full-scale production continues for 20 years through year 26, at the conclusion of which the process is shut down and all of the working capital is recovered.

To account for the time value of money, the cash flow for each year of the project is multiplied by a discount factor *f*, defined as:

$$f(t) = \frac{1}{(1 + r_d)^t} \tag{5.2}$$

where r_d is the desired annual discount rate (i.e., interest rate) that the entity financing the project wishes to make each year *t* of a given project. Summing the discounted cash flows for each year of a project gives the net present value (NPV) of the project:

$$NPV = \sum f(t) \cdot CF(t) \tag{5.3}$$

When Eq. (5.3) equals zero (i.e., the NPV of the project is zero), the discount rate in Eq. (5.2) is defined as the internal (or investor's) rate of return (IRR). IRR is a common financial metric used to compare the value of different projects. Equation (5.3) can also

be used to find the OSP, which is the oil price needed to produce an NPV of 0 at a given IRR.

5.2.3.1 Capital Costs

The capital costs in Equation (5.1) are estimated using a combination of three techniques: cost estimation studies, Williams' six-tenths rule (Williams, 1947), and Seider's capital costing method (Seider et al., 2009). Methods from other cost estimation studies are used for calculating the cost of the water pipeline (Boyle Engineering Corporation, 2002), water reservoir (RSMeans, 2002), and electrical grid connection (Black & Veatch, 2014). Williams' six-tenths rule is used for estimating the scaled costs of the mine and retort reported by ICSE (2013). According to Williams, economies of scale in process equipment can be modeled using the equation

$$C = C_o \left(\frac{Q}{Q_o}\right)^{0.6} \left(\frac{I}{I_o}\right) \tag{5.4}$$

where C is the cost, Q is the material capacity (in this case, the oil production rate), I is an appropriate cost index or inflation index such as the Consumer Price Index (CPI) used here (U.S. Bureau of Labor Statistics, 2015), and o refers to the base value of the subscripted variable. The capital costs for all other terms in Eq. (5.1) (cooling water and steam utility plants, site preparation, startup, working capital, etc.) are estimated based on the capital costing model of Seider et al. (2009) as shown below in Table 5.3.

5.2.3.2 Operating Costs

The operating costs in each scenario can be differentiated into variable (C_V) and fixed (C_F). Variable costs scale with the production capacity factor P and include the costs for operating the mine, utilities (water, steam, and electricity), and conducting research. Fixed costs are constant expenses and do not vary with the production capacity factor P; they include the costs of labor, maintenance, and insurance. Costs from all sources are adjusted for inflation using the CPI (U.S. Bureau of Labor Statistics, 2015) and are presented in Table 5.4 in 2014 dollars. Final operating costs in each scenario are calculated based on the volume of oil or shale required to meet the production capacity specified as part of the DOE analysis.

5.2.3.3 Taxes and Royalties

Oil and gas produced through ex situ retorting (or any other method) is subject to a number of taxes and royalties. The first (and most straightforward to calculate) is royalty payments (R), which are given by:

$$R = r \cdot OP \cdot V_{oil} \tag{5.5}$$

where r is the royalty rate, OP is the oil price (in dollars per barrel or $/bbl), and V_{oil} is the volume of oil sold. Royalty rates on conventional oil production are 12.5% of gross sales, however the U.S. Bureau of Land Management (BLM) has not issued a final decision on oil shale royalty rates. In its initial response to the Energy Policy act of 2005, the U.S. BLM proposed a starting rate of 5% for 5 years, followed by an increase of 1% per year up to 12.5%. However, in its most recent programmatic environmental impact statement for oil shale, the U.S. BLM identified a variety of different methods for setting

royalty rates, such as determining them by public comment for each lease during the lease sale, using a sliding scale based on market prices for oil and gas, or establishing a minimum rate of 12.5% with an option for the Secretary of the Interior to increase the rate in the future (U.S. BLM, 2013). For this analysis, royalty rates for oil production are allowed to vary from 5% to 20% and are selected for each scenario as part of the DOE analysis.

The state of Utah collects severance taxes on oil using a split rate system based on the market price of oil at the wellhead. The first $13/bbl are taxed at a rate of 3% and any additional value above that threshold is taxed at a rate of 5%. An additional 0.2% of the market value is taxed as a conservation fee (r_{cf}). This set of tax rules is implemented using Eq. (5.6):

$$ST = OP \cdot \{r_{cf} + [0.03 \cdot (1 - f_{st}) + 0.05 \cdot f_{st}]\} \tag{5.6}$$

where ST is the severance tax due to the state on a $/bbl basis and f_{ST} is the fraction of OP above the threshold value. The results of Eq. (5.6) are then multiplied by the volume of oil produced to find the total severance tax due.

Corporate income taxes are calculated assuming the top rates of 5% and 35% at the state and federal levels, respectively, of taxable income (TI). TI is defined as:

$$TI = P(S - C_V - d) - C_F - D - R - ST \tag{5.7}$$

where d is depletion, D is depreciation, and all other variables are as defined previously. Cost depletion is used to determine d, assuming that the cost depletion factor is equal to the capital cost of land (C_L) divided by the total planned oil production. The depletion charge in any given year is then the number of barrels of oil extracted that year multiplied by the depletion factor. A ten-year Modified Accelerated Cost Recovery System method

is used to calculate depreciation, with the first depreciation charge occurring at startup. Since state corporate income taxes (*TS*) are deductible from federal corporate income taxes (*TF*), the total corporate tax liability is given by:

$$T_S = t_S \cdot TI \tag{5.8}$$

$$T_F = t_F \cdot (TI - T_S) \tag{5.9}$$

where t_S and t_F are the respective state and federal corporate tax rates.

Finally, property taxes are assumed to be 1% of C_{TPI}, and the total tax liability used in Eq. (5.1) is the sum of severance taxes, corporate income taxes (state and federal), and property taxes.

5.2.4 Design of Experiments Analysis

In the DOE analysis technique, the values of a set of input parameters are varied systematically to determine the contribution of each parameter to the overall system response. In this DOE analysis, the output response is the oil supply price (OSP). The input parameters varied in this analysis are:

1. Oil shale grade (Fischer Assay GPT of shale)
2. Production scale (barrels per day or BPD of oil produced)
3. Mine and retort capital expense (capex)
4. Mine and retort operating expense (opex)
5. Royalty rates charged on oil production
6. Internal rate of return (IRR)

Note that the mine and retort capex/opex are expressed as a fraction relative to their base values given in Table 5.1 and Table 5.4. This set of input parameters was selected

because (a) ICSE (2013) has shown that they have the largest impact on the OSP, and (b) the potential range of reasonable values for each term is fairly large.

We use two types of DOE sampling methods. In the first, we assume a uniform distribution and calculate the 0^{th} (minimum) through 100^{th} (maximum) percentile values at every 10^{th} percentile (i.e. 0^{th}, 10^{th}, 20^{th}, etc.) for each input parameter. Next, every unique combination of every parameter is generated (a full-factorial DOE analysis). Given the sample spacing and the number of parameters, this results in 11^6 (approximately 1.77 million) sets of parameter values or "scenarios" for which the OSP is found using the DCF analysis. The OSP results from the uniform distribution are then used to fit an empirical OSP function:

$$eOSP = a \cdot G + b \cdot OPD + c \cdot f_{cap} + d \cdot f_{op} + e \cdot r + f \cdot IRR \qquad (5.10)$$

where *eOSP* is the empirical estimate of the OSP at a grade *G*, *OPD* is the production scale, f_{cap} and f_{op} are the mine and retort capex and opex fractions, respectively, *r* is the royalty rate, and *IRR* is the internal rate of return. All coefficients are found through linear regression. The contribution of each parameter (on average) to the OSP is then found by inserting the mean value of each parameter into Eq. (5.10).

In the second analysis, each input parameter is assumed to have a normal rather than a uniform distribution. Each normal distribution is defined by a mean and a standard deviation (SD), and each parameter is sampled at every 9^{th} percentile between the 5^{th} and 95^{th} percentile (i.e., the 5^{th}, 14^{th}, … 95^{th} percentile); for a normal distribution, the 0^{th} and 100^{th} percentiles would result in values of $\pm\infty$). As with the uniform distribution, every unique combination of every parameter is generated. This process results in a sample space of the same size (11^6) as the uniform distribution DOE analysis, but the sample

points are spaced more closely around the mean value of each parameter. This second approach allows us to estimate the "most likely" range of OSP results for an ex situ oil shale project.

The minimum, maximum, mean, and SD assumed for each parameter are given in Table 5.5. Oil shale grade values were selected based on ranges reported by Vanden Berg (2008). Production scale and capex/opex fractions were picked to cover the same range of retorting capital and operating costs as STRAAM (1979). Royalty rates reflect the range of rates proposed by BLM. IRR values are picked based on IRR values reported for recent conventional oil projects (Standard & Poor's, 2011) and recommended values from Seider et al. (2009).

5.3 Results and Discussion

5.3.1 Uniform Distribution

The OSP results for the uniform distribution are shown in Figure 5.2 using an x-y bin scatterplot. In this type of plot, the number of results in each x-y grid square is shown using shading, with darker colors indicating locations with higher result counts. In the uniform distribution DOE analysis, OSP results range from \$16/bbl – \$1,319/bbl. Oil shale grade, scale, capex fraction, and IRR all have large impacts on the OSP results, while royalty rates have a relatively minor impact and the opex fraction is even less impactful.

The results of fitting Eq. (5.10) to the uniform OSP results are given in Table 5.6. Overall, the fit to Eq. (5.10) is excellent ($R^2 = 0.92$). Applying the mean value of each parameter to the fit and normalizing the result produces the bar plot shown in Figure 5.3;

the raw values behind this calculation are shown in the last two columns of Table 5.6. Negative values indicate that increases in that parameter lead to lower OSPs, and positive values indicate that increases in that parameter result in higher OSPs. Oil shale grade has the largest impact on reducing the OSP, followed by production scale. Unsurprisingly, IRR has the largest impact on increasing the OSP, followed by f_{cap}. The royalty rate and f_{op} both increase OSP, but their impact is an order of magnitude smaller than either IRR or f_{cap}.

5.3.2 Normal Distribution

The OSP results for the normal distribution DOE are shown in Figure 5.4. All of the trends noted previously for the uniform distribution are still visible; G and OPD have the largest impact on reducing OSP while IRR and f_{cap} have the largest impact on increasing OSP. However, the scale is very different, as OSP results assuming normal distributions for the parameters range from \$22/bbl to \$687/bbl. The OSP decrease on the high end is most likely due to the shift in IRR and f_{cap} values compared to the uniform distribution. For example, it is no longer possible to have a combined 150% f_{cap} and 40% IRR in the normal distribution parameter space. Overall, the OSP results follow a log-normal distribution (see Figure 5.5). The most likely (median) OSP for an ex situ oil shale project under the assumptions in this study is \$94/bbl (10^{th} percentile OSP = \$56/bbl, 90^{th} percentile OSP = \$178/bbl). However, it should be noted again that given the product's properties, any produced oil would sell at a discount compared to other benchmark crude oils.

Figure 5.6 replicates Figure 5.4 but only shows those results from the lower 90^{th}

percentile of the normal distribution OSP results. At this scale there is a clearer picture of the functional relationship between each parameter and OSP. Being in the tails (5^{th} percentile or 95^{th} percentile) of any of the important parameters (G, OPD, f_{cap}, or IRR) significantly pushes the distribution of OSP results up or down. For example, being in the lower 5^{th} percentile of G pushes the median OSP up from \$97/bbl to \$178/bbl; being in the lower 5^{th} percentile of OPD increases the median OSP to \$170/bbl. Interestingly, while there appears to be an equally large concentration of OSP results in the 5^{th} and 95^{th} percentiles of G and OPD, the concentration of results in the 5^{th} percentile of f_{cap} and IRR is much higher than the 95^{th} percentile for those terms. Low values for f_{cap} and IRR are highly likely to result in low OSP values, regardless of what values are selected for other terms.

Figure 5.7 and Figure 5.8 show the range of capital costs and per-barrel costs for the lower 90^{th} percentile of normal distribution OSP results. In these boxplots, the middle line represents the median value, the top and bottom of the box represent the 75^{th} and 25^{th} percentiles of the results, and the whiskers on the top and bottom represent the maximum and minimum values. Also note that the y-axis in Figure 5.7 is shown on a log-scale. The capital cost breakdown in Figure 5.7 clearly shows that the largest costs are for the mine and retort, which account for 60% of the total capital investment (on average). The per-barrel costs in Figure 5.8 show that many of the costs are comparable, with most varying between \$10 to \$20 per barrel. The amount of profit taken is the largest and widest ranging cost category and is a direct result of the IRR specification in each scenario. Profits are directly tied to taxes and royalties, which collectively are even larger than profits (median royalties, corporate income taxes, severance taxes, and property taxes are

$30/bbl for results shown in Figure 5.8). Fixed costs are significant because of the cost of maintenance. Given the assumption that 5% of C_{TDC} is spent on maintenance annually (reasonable for a solids-handling process), maintenance costs are $102 million per year on average.

5.4 Conclusions

Ex situ oil shale could be economically viable if oil prices recover. Assuming that prices return to $90/bbl (average U.S. EIA forecasted oil price for the Rocky Mountain region between 2015-2040 (U.S. EIA, 2015a)), 45% of the scenarios in the normal distribution DOE analysis could be economically viable. Given the product's properties (low API gravity, high sulfur and nitrogen content, etc.) any produced oil would sell at a discount. However even if the discount was 25% compared to EIA's forecasted price (i.e. $67/bbl), 21% of the scenarios would still be viable.

5.5 References

Andersen, M., R. Coupal, and B. White. 2009. "Reclamation Costs and Regulation of Oil and Gas Development with Application to Wyoming." In Western Economics Forum. Laramie, WY: Western Agricultural Economics Association. http://ageconsearch.umn.edu/bitstream/92846/2/0801005.pdf.

Baker Hughes. 2015. "North America Rotary Rig Count Archive - U.S. Monthly Average by State through 2013." North America Rotary Rig Count Archive. http://phx.corporate-ir.net/phoenix.zhtml?c=79687&p=irol-reportsother.

Bartis, J.T., T. LaTourrette, L. Dixon, D.J. Peterson, and G. Cecchine. 2005. "Oil Shale Development in the United States - Prospects and Policy Issues." Santa Monica, CA.

Beer, G.L., E. Zhang, S. Wellington, R. Ryan, and H. Vinegar. 2008. "Shell's In Situ Conversion Process - Factors Affecting the Properties of Produced Shale Oil." In 26th Oil Shale Symposium. Golden, CO: Colorado School of Mines. http://www.ceri-mines.org/documents/28thsymposium/presentations08/PRES_3-2_Beer_Gary.pdf.

Bezdek, R.H., R.M. Wendling, and R.L. Hirsch. 2006. "Economic Impacts of U.S. Liquid Fuel Mitigation Options." Pittsburgh, PA.

Black & Veatch. 2014. "Capital Costs for Transmission and Substations." Salt Lake City, UT. https://www.wecc.biz/Reliability/2014_TEPPC_Transmission_CapCost_Report_B+V.pdf.

EPA Oil Shale Work Group. 1979. "EPA Program Status Report: Oil Shale - 1979 Update." Washington, DC. https://books.google.com/books?id=ET9SAAAAMAAJ&source=gbs_navlinks_s.

ICSE. 2013. "A Market Assessment of Oil Sands and Oil Shale Resources." Salt Lake City, UT. http://www.icse.utah.edu/assets/for_download/pdfs/projects/2013OilShaleMarketAssessment.pdf.

INTEK Inc. 2009. "National Strategic Unconventional Resource Model - A Decision Support System." Washington, DC.

———. 2011. "Profiles of Companies Engaged in Domestic Oil Shale and Tar Sands Resource and Technology Development." Secure Fuels from Domestic Resources. Washington, DC. http://energy.gov/sites/prod/files/2013/04/f0/SecureFuelsReport2011.pdf.

McQueen, G., D. Parman, and H. Williams. 2009. "Enhanced Oil Recovery of Shallow Wells with Heavy Oil: A Case Study in Electro Thermal Heating of California Oil Wells." 2009 Record of Conference Papers - Industry Applications Society 56th Annual Petroleum and Chemical Industry Conference, PCIC 2009. doi:10.1109/PCICON.2009.5297168.

R Core Team. 2015. "R: A Language and Environment for Statistical Computing." Vienna, Austria. http://www.r-project.org/.

Ryan, R.C., T.D. Fowler, G.L. Beer, and V. Nair. 2010. "Shell's In Situ Conversion Process−From Laboratory to Field Pilots." In Oil Shale: A Solution to the Liquid Fuel Dilemma, edited by O. Ogunsola, A. Hartstein, and O. Ogunsola, 161–83. American Chemical Society. doi:10.1021/bk-2010-1032.ch009.

Seider, W.D., J.D. Seader, D.R. Lewin, and S. Widagdo. 2009. Product & Process Design Priniciples: Synthesis, Analysis and Design. 3rd ed. New York, NY: John Wilkey & Sons.

Standard & Poor's. 2011. "Is Natural Gas Drilling Economic at Current Prices?" CreditWeek, December.

http://www.standardandpoors.com/spf/swf/oilandgas/data/document.pdf.

STRAAM Engineers. 1979. "Capital and Operating Cost Estimating System Handbook: Mining, Retorting, and Upgrading of Oil Shale in Colorado, Utah, and Wyoming." Irvine, CA.

U.S. BLM. 2013. "Secretary Salazar Finalizes Plan Promoting Responsible Oil Shale and Tar Sands Research, Demonstration and Development." http://www.blm.gov/wo/st/en/info/newsroom/2013/march/nr_03_22_2013.html.

U.S. Bureau of Labor Statistics. 2014. "Utah - May 2014 Occupational Employment and Wage Estimates." Washington, DC. http://www.bls.gov/oes/current/oes_ut.htm#17-0000.

U.S. Department of Energy. 1979. "Oil Shale Data Book." Washington, DC: U.S. Department of Commerce National Technical Information Service. https://www.ntis.gov/Search/Home/titleDetail/?abbr=PB80125636.

U.S. EIA. 2010. "Oil and Gas Lease Equipment and Operating Costs 1994 Through 2009." Washington, DC. http://www.eia.gov/pub/oil_gas/natural_gas/data_publications/cost_indices_equipment_production/current/coststudy.html.

———. 2013. "Updated Capital Cost Estimates for Utility Scale Electricity Generating Plants." http://www.eia.gov/forecasts/capitalcost/pdf/updated_capcost.pdf.

———. 2015a. "Annual Energy Outlook 2015." Washington, DC. http://www.eia.gov/forecasts/aeo/pdf/0383(2015).pdf.

———. 2015b. "Average Retail Price of Electricity to Ultimate Customers." Electric Power Annual. http://www.eia.gov/electricity/data.cfm#sales.

———. 2015c. "U.S. Natural Gas Prices." Monthly Report of Natural Gas Purchases and Deliveries to Consumers. http://www.eia.gov/dnav/ng/ng_pri_sum_dcu_nus_m.htm.

———. 2015d. "Utah Electricity Profile 2013." State Electricity Profiles. http://www.eia.gov/electricity/state/utah/.

Utah DOGM. 2015. "Data Research Center." Division of Oil, Gas & Mining - Oil and Gas Program. http://oilgas.ogm.utah.gov/Data_Center/DataCenter.cfm.

Vanden Berg, M.D. 2008. "Basin-Wide Evaluation of the Uppermost Green River Formation's Oil-Shale Resource, Uinta Basin, Utah and Colorado." Salt Lake City, UT. Utah Geological Survey Special Study 128. http://files.geology.utah.gov/online/ss/ss-128/ss-128txt.pdf.

Wellington, S., I. Berchenko, E.P. Rouffignac, T. Fowler, R. Ryan, G. Shahin, G. Stegemeier, H. Vinegar, and E. Zhang. 2003. In situ thermal processing of an oil shale formation using a controlled heating rate. US20030142964 A1, issued 2003. https://www.google.com/patents/US20030142964.

Williams, R. 1947. "Six-Tenths Factor Aids in Approximating Costs." Chemical Engineering 54 (12): 124–25.

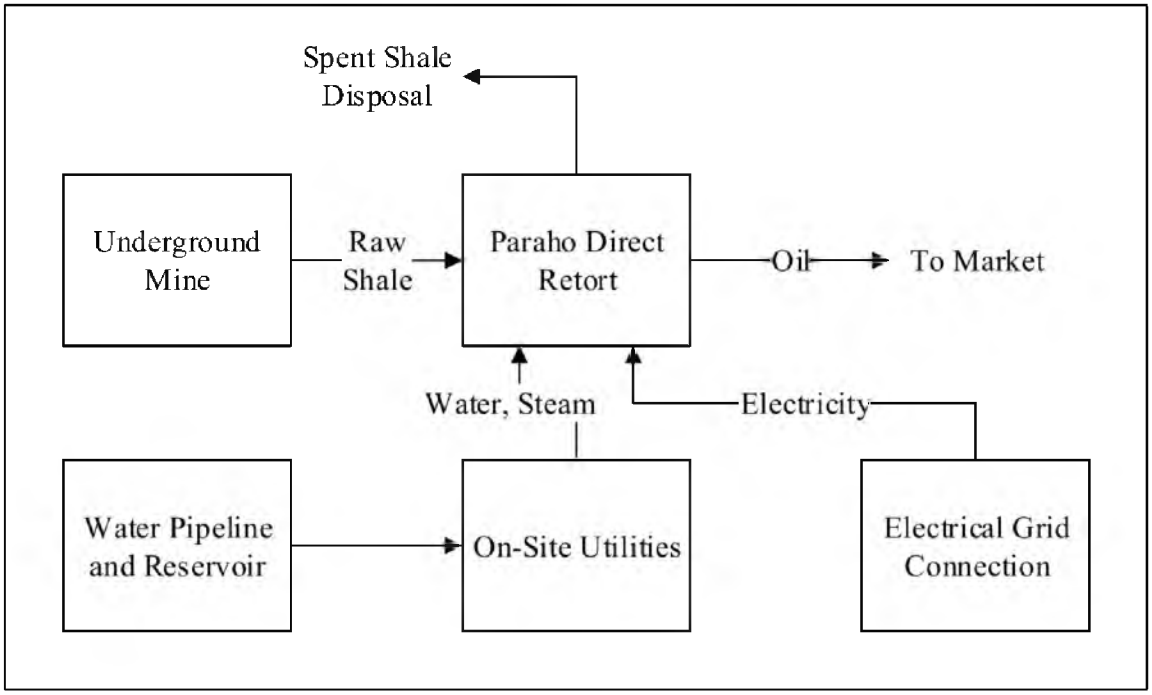

Figure 5.1: Process flow diagram for ex situ oil shale.

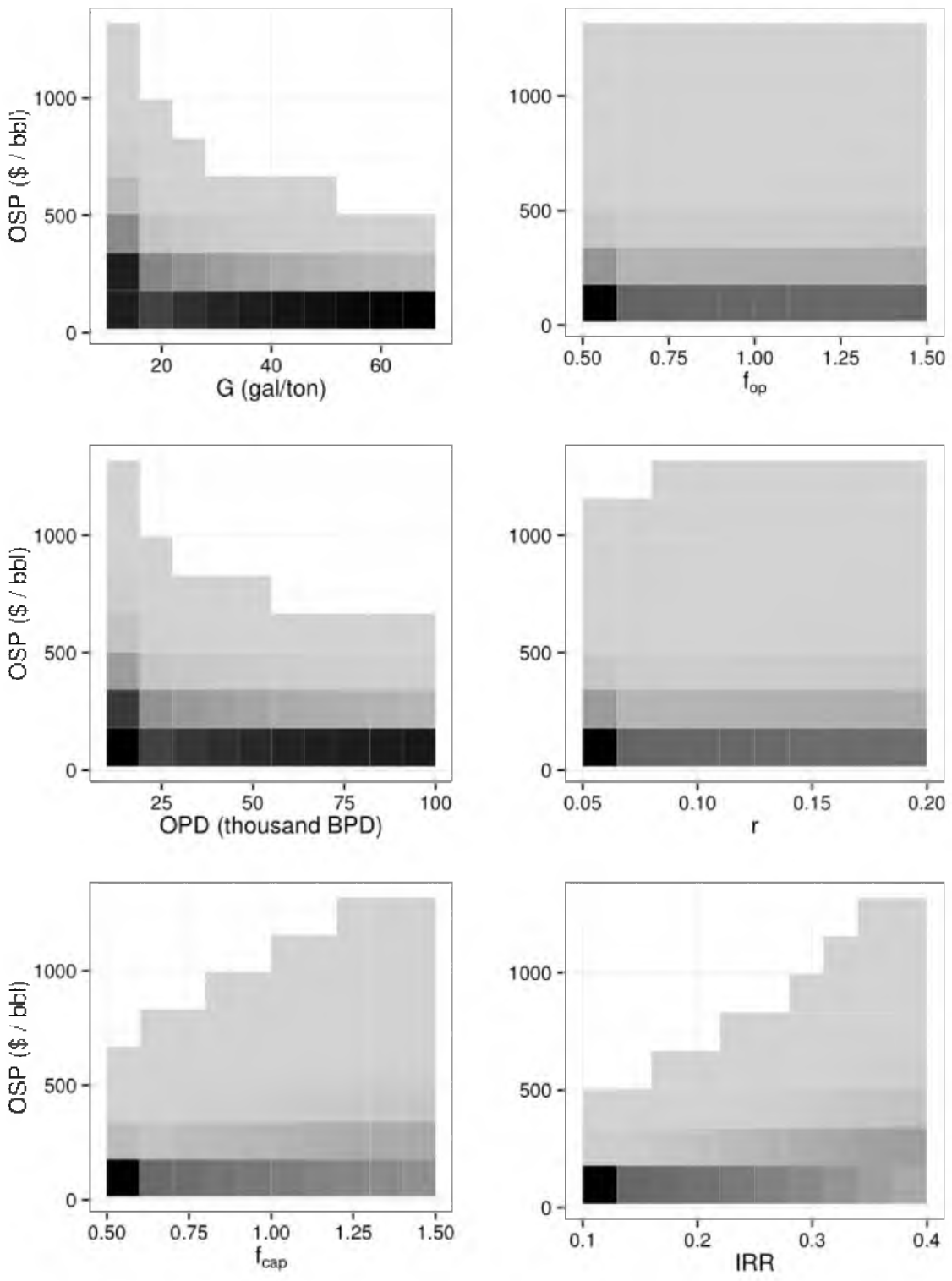

Figure 5.2: OSP results assuming uniform distribution of input parameters within the range given in Table 5.5.

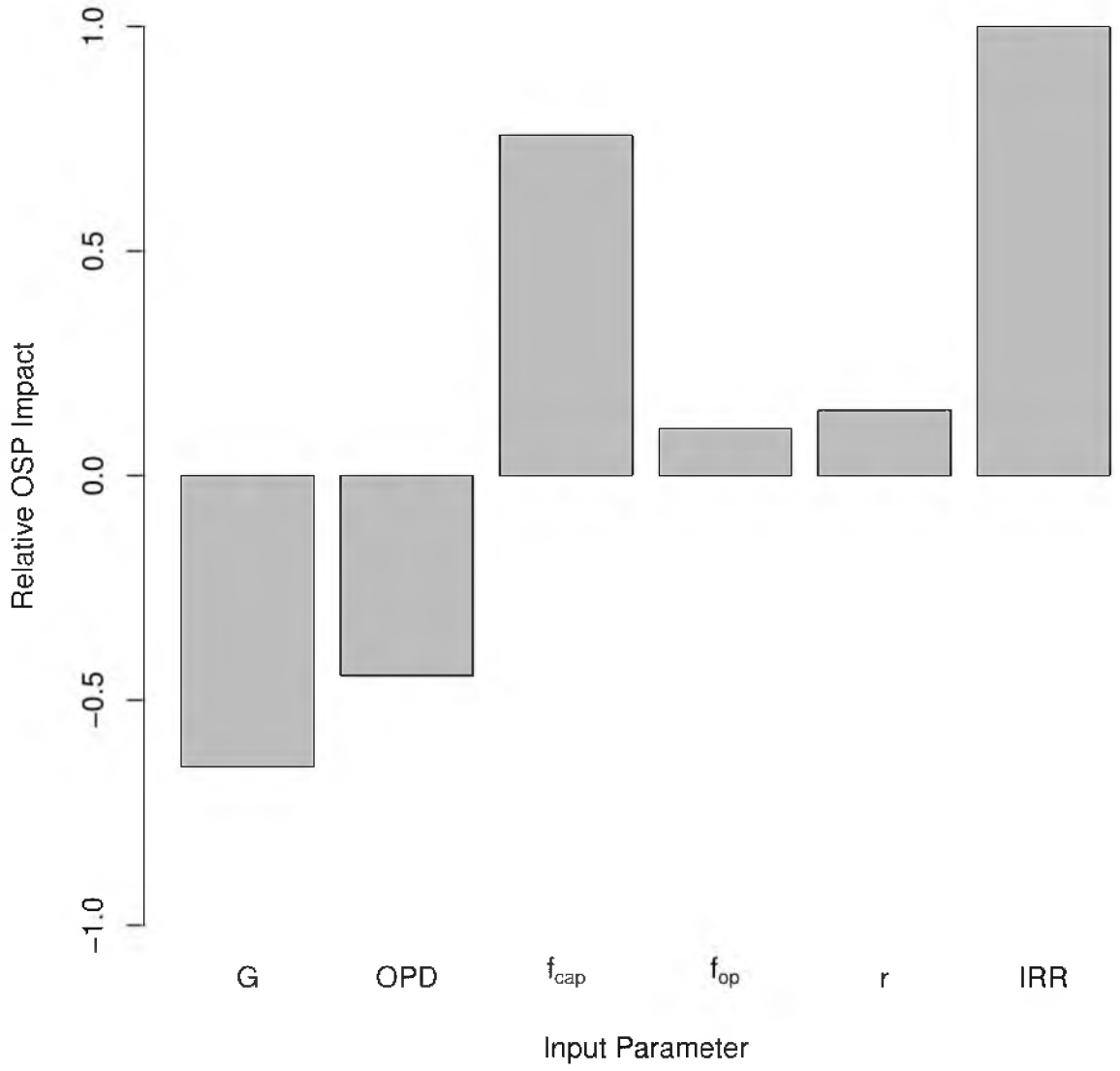

Figure 5.3: Relative OSP impact of each input parameter, assuming a uniform distribution of values.

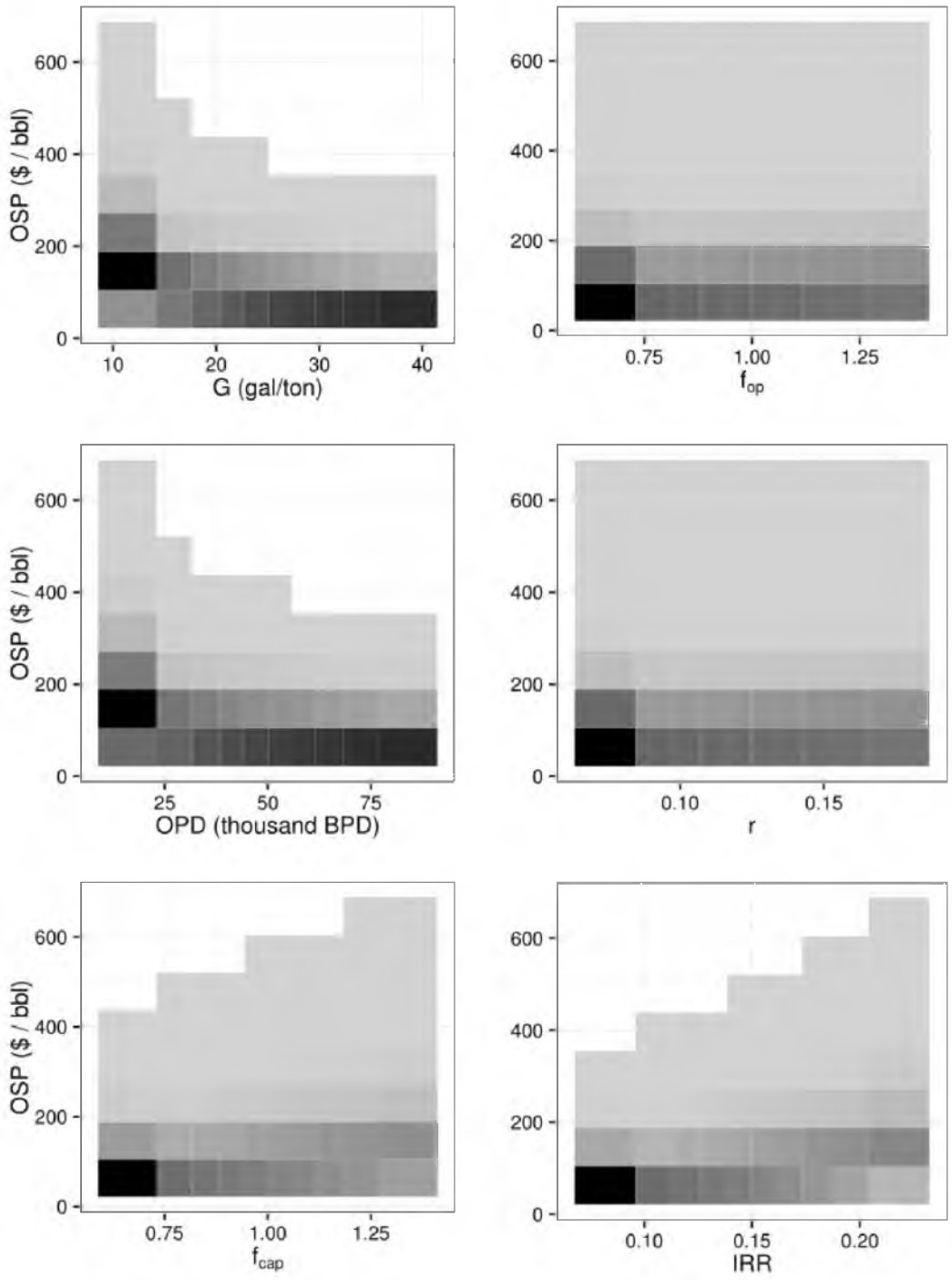

Figure 5.4: OSP results assuming normal distributions of input parameters described by mean and SD values in Table 5.5. Note that the grid-squares are not evenly spaced on the x-axis. The breakpoints between grid-squares on the x-axis have been set to reflect the spacing of the normal distribution parameter points (i.e., more points near the mean, wider spacing near the tails).

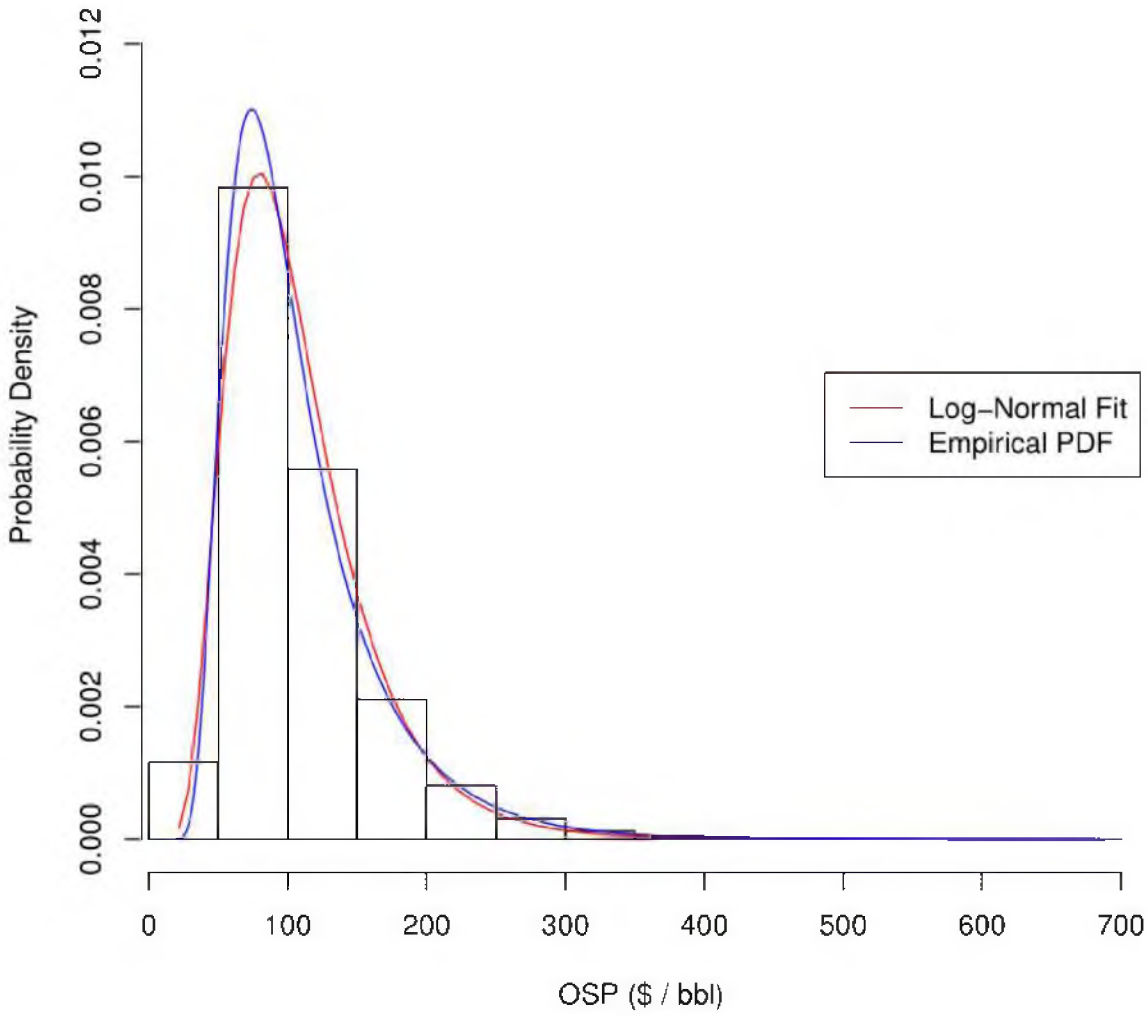

Figure 5.5: Log-normal distribution fit of normal distribution OSP results. The histogram and empirical probability density function (PDF) indicate the distribution of the OSP results. The red line is the best fit (log-mean = 4.578, log-SD = 0.4511) of a log-normal distribution function to the OSP results.

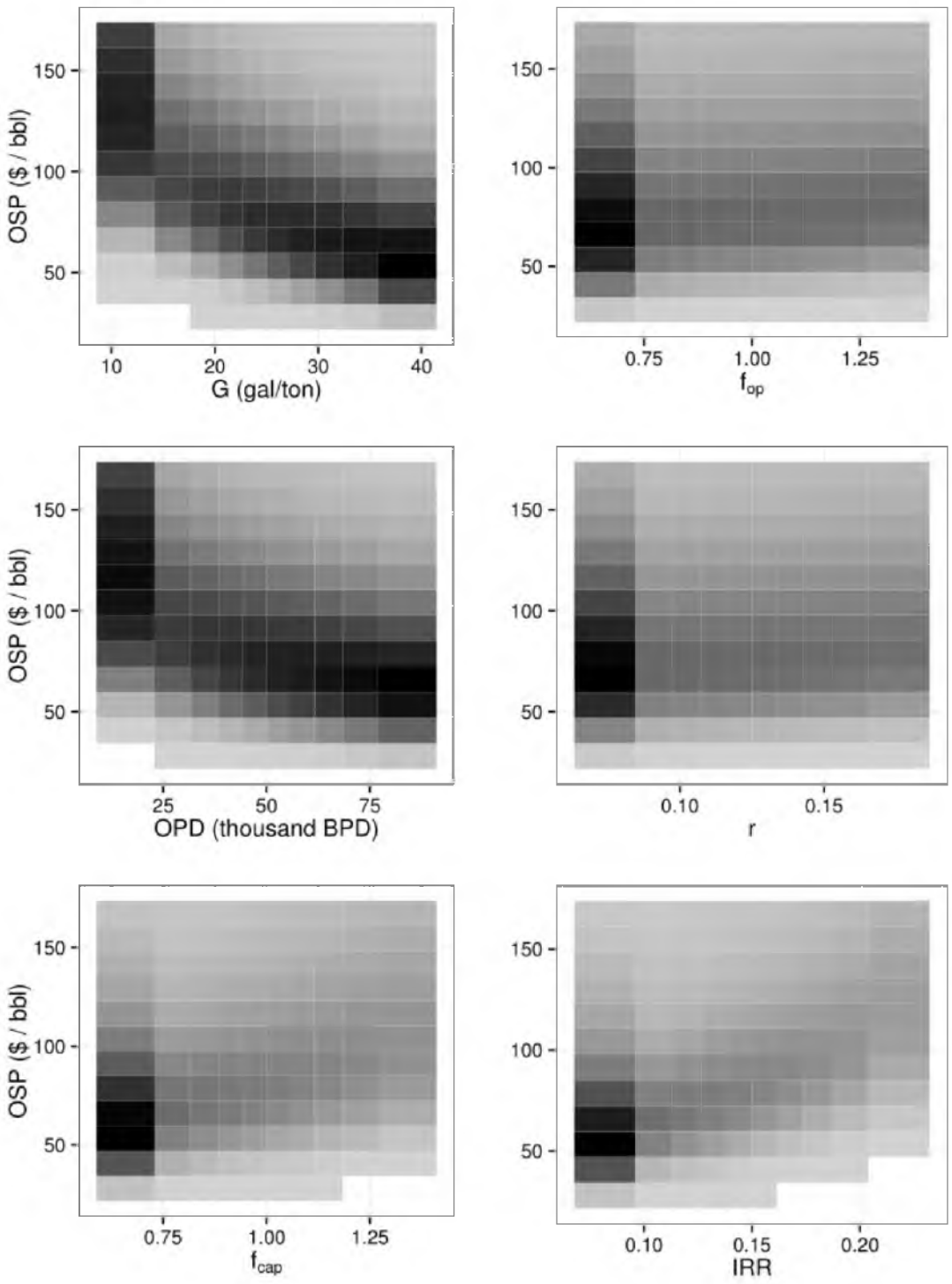

Figure 5.6: Normal distribution OSP results for scenarios in the lower 90th percentile (i.e., OSP $\leq$ \$173/bbl). As with Figure 5.4, note that the breakpoints between grid-squares are not evenly spaced, and have instead been selected to reflect the spacing of parameter points in the normal distribution.

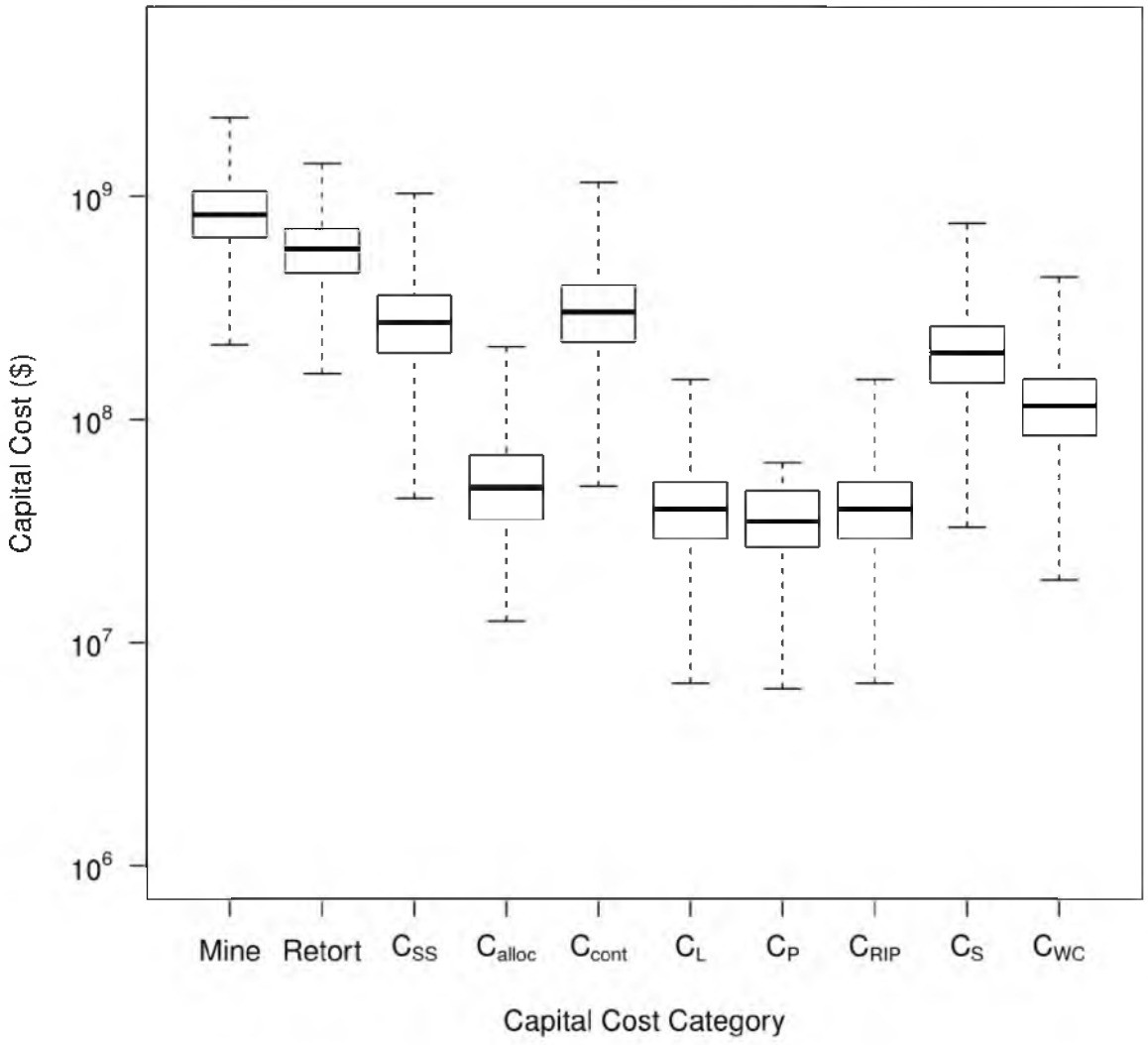

Figure 5.7: Capital cost breakdown for lower 90th percentile of normal distribution OSP results. Note that the y-axis is on a log-scale.

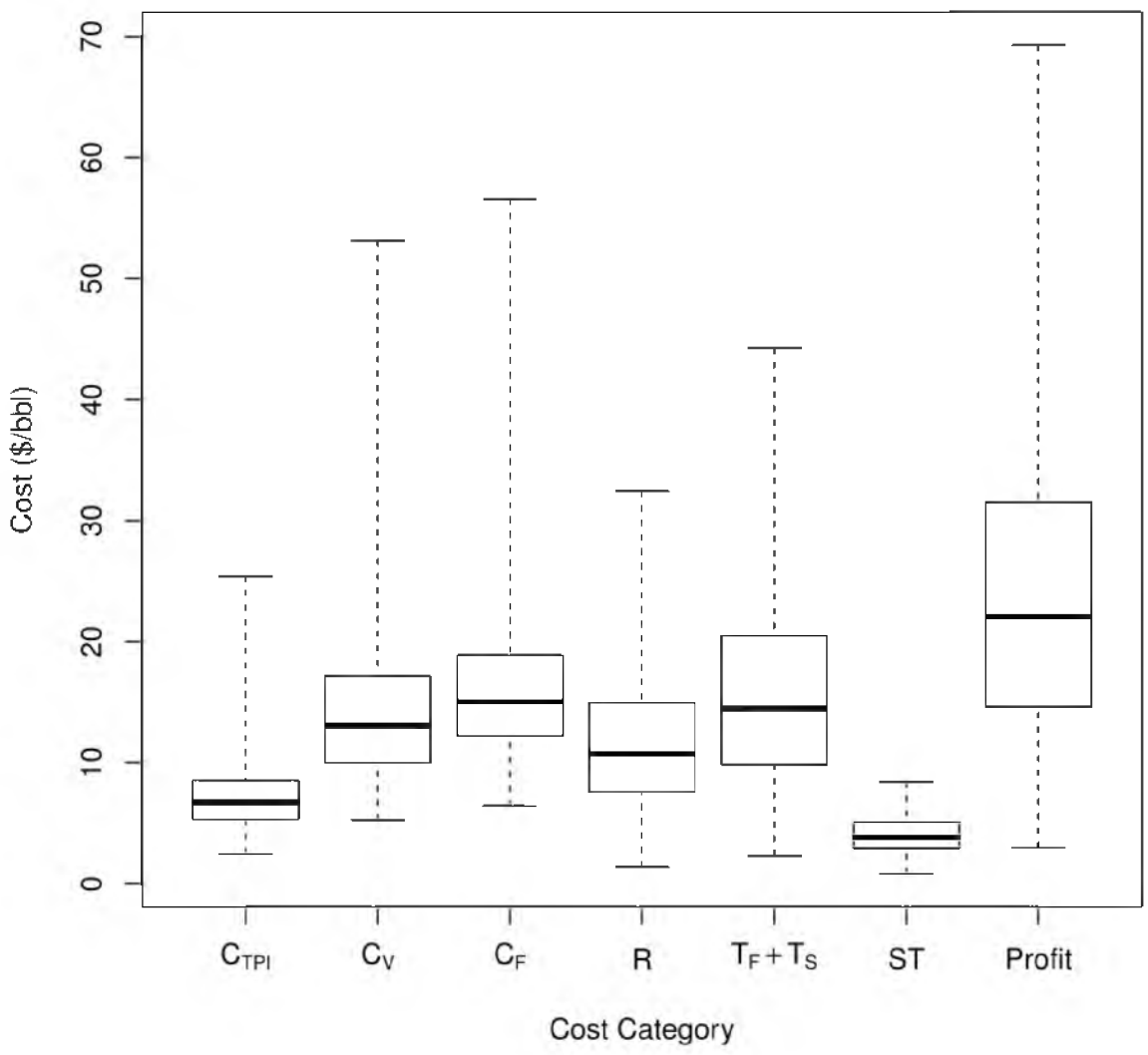

Figure 5.8: Cost per barrel breakdown for lower 90th percentile of normal distribution OSP results.

Table 5.1: Summary of the process details, capital costs, and operating requirements for Paraho Direct retorting process used as a basis in this study (Wilkey et al., 2013).

Category	Item	Value	Units
Material Balance	Mined Shale	95,450	ton/day
	Retored Shale	85,900	ton/day
	Crushing Recovery	90	wt% Mined Shale
	Oil Recovery	92	% of Fischer Assay
	Water Content		
	Raw Shale	2.6	wt%
	Spent Shale	6.9	wt%
Temperature	Retort	1,200	°F
	Spent Shale	295	°F
Product Properties	Distillation Fractions		
	Gas	24.1	wt%
	Naptha	10.5	wt%
	Gas Oil	46.2	wt%
	Bottoms Oil	19.2	wt%
	API Gravity	20	°API
	Sulfur	0.7	wt%
	Nitrogen	1.9	wt%
	Pour Point	70	°F
	Solids	1-2	wt%
Capital Costs	Mine	$773	million 2012 $
	Retort	$534	million 2012 $
Operating Req.	Electricity	161	MW
	Steam (450 psig)	666	klb/hr
	Water	4,319	bbl/hr
	Cooling	69.4	kgal/hr
	Boiler Feed	332	kgal/hr
	Makeup	181	kgal/hr

Note: ton/day = short tons per day, wt% = weight percent, MW = megawatt, klb/hr = thousand pounds per hour, kgal/hr = thousand gallons per hour, bbl/hr = barrels per hour.

Table 5.2: Project schedule.

Action	Year	P	C_{TDC}	C_L	C_S	C_{RIP}	C_P	C_{WC}
Design	1	0	25%				100%	
Construction	2-4	0	75%	100%				
Startup	5	45%			100%	100%		-100%
Startup	6	68%						
Production	7-26	90%						
Shutdown	26	0						100%

Table 5.3: Capital costing method from Seider et al. (2009).

Category	Symbol and Definition
Total Bare Module Investment (TBM)	C_{TBM} = sum of costs for mine and retort
Cost of site preparation and service facilities	C_{SS} = 20% of C_{TBM}
Allocated costs for utility plants	C_{alloc} = sum of costs for water pipeline, reservoir, cooling water, steam, and electrical grid connection
Total Direct Permanent Investment (DPI)	$C_{DPI} = C_{TBM} + C_{site} + C_{serv} + C_{alloc}$
Cost for contingencies & contractor fees	C_{cont} = 15% of C_{DPI}
Total Depreciable Capital (TDC)	$C_{TDC} = C_{DPI} + C_{cont}$
Cost of mineral rights and land leases	C_L = 2% of C_{TDC}
Cost of permitting	C_P = \$0.10 / bbl of oil produced
Cost of royalties for intellectual property	C_{RIP} = 2% of C_{TDC}
Cost of plant startup	C_S = 10% of C_{TDC}
Total Permanent Investment (TPI)	$C_{TPI} = C_{TDC} + C_L + C_P + C_{RIP} + C_S$
Working Capital (WC)	C_{WC} = 5% of C_{TPI}
Total Capital Investment (TCI)	$C_{TCI} = C_{TPI} + C_{WC}$

Table 5.4: Operating costs summary. In mining labor equation, *RM* is the rock mined in units of ton/day of oil shale. Sources are: (1) ICSE (2013), (2) U.S. EIA (2015c), (3) Seider et al. (2009), (4) Heidrick and Godin (2006), (5) InfoMine (2010), and (6) U.S. Bureau of Labor Statistics (2014).

Item	Cost	Source
Variable Expenses		
Mine Operating Cost	1,932/ton shale mined	1
Electricity	$0.0607/kilowatt hour	2
Steam	$13.61/ton	3
Water		
Makeup	$0.158/kgal	1
Cooling	$0.0773/kgal	3
Boiler Feed Water	$1.86/kgal	3
Research	$0.765/bbl oil produced	4
Fixed Expenses		
Employees		
Mine	$1.5791 \cdot RM^{0.5391}$	5
Retort	54 operators/shift	3
Labor for Operations		
Wages and Benefits (LW)	LW = $30/operator-hour	3
Salary and Benefits (LS)	LS = 15% of LW	3
Operating Supplies and Services	6% of LW	3
Technical Assistance	$82,510/(operator/shift)/year	6
Control Laboratory	$82,510/(operator/shift)/year	6
Maintenance (M)	5% of C_{TDC}	3
Wages and Benefits (MW)	43.48% of M	3
Salary and Benefits (MS)	10.87% of M	3

Table 5.4: Continued

Item	Cost	Source
Materials and Services	43.48% of M	3
Maintenance Overhead	2.17% of M	3
Operating Overhead		
General Plant Overhead	7.1% of (LW + LS + MW + MS)	3
Mechanical Department Services	2.4% of (LW + LS + MW + MS)	3
Employee Relations Department	5.9% of (LW + LS + MW + MS)	3
Business Services	7.4% of (LW + LS + MW + MS)	3
Insurance	0.4% of C_{TPI}	3
General Expenses		
Administrative Expense	$200,000/(20 employees)/year	1
Management Incentive Compensation	1.25% of net profit	3

Table 5.5: DOE parameters and value ranges.

Parameter	**Min**	**Max**	**Mean**	**SD**
G (gal/ton Fischer Assay)	10	70	25	10
OPD (BPD)	10,000	100,000	50,000	25,000
f_{cap} (% base capex)	50%	150%	100%	25%
f_{op} (% base opex)	50%	150%	100%	25%
r (% oil sales)	5%	20%	12.5%	3.75%
IRR (%)	10%	40%	15%	5%

Table 5.6: Regression results and impact analysis using uniform distribution OSP results.

Parameter	**Fitted Coefficient**	**Mean Value**	**Impact Factor**
G	-2.598	40	-103.9
OPD	-1.301E-03	55,000	-71.58
f_{cap}	121.6	100%	121.6
f_{op}	16.71	100%	16.71
r	186.6	12.5%	23.32
IRR	642.2	25%	160.5

CHAPTER 6

CONCLUSIONS

This research work has presented forecasts (with uncertainty estimates) of the potential economic and environmental impacts of COG development and identified the oil supply prices at which oil shale processing could be economically viable.

For COG, both the economic and environmental impact estimates rely on a shared method of modeling drilling activity as a function of energy prices and projecting production from new and existing wells using decline curve analysis. In cross-validation tests, these methods have proven highly accurate at matching the actual test data. The largest source of uncertainty in the drilling and production forecasting process stems from the uncertainty and volatility in energy prices. Over the 2015 – 2019 period, median model projections show a 30% decrease in the number of wells drilled in the Uinta Basin. However, oil production rates are expected to double due to projected increases in per-well production rates, while gas production rates are expected to remain flat. Given the projected downturn in the drilling activity and assuming that proposed emission regulations are implemented, the median VOC emissions rate will drop by 45% compared to the previous five year period (2010 – 2014). This result clearly shows that it is possible for overall oil and gas production to increase while reducing overall emissions by raising emissions standards for new wells. In terms of economic impacts, the drop in drilling activity is expected to reduce employment as a result of spending by the oil and

gas industry by 23% compared to the 2010 – 2014 period. Royalty and tax revenue collected by the state of Utah is also expected to drop by 20% due to the drop in energy prices.

For oil shale, both ex situ and in situ processing methods could be economically viable if oil prices recover to levels predicted by U.S. EIA forecasts. Of the two processing options, ex situ oil shale faces fewer economic hurdles. The most likely (median) oil supply price for an ex situ oil shale project under the assumptions in this work would be $94/bbl. By comparison, the median oil supply price for in situ oil shale scenarios is $272/bbl. The key issue facing both processing methods is the large upfront capital cost (on the order of billions of dollars) for drilling wells or building a mine and retorting complex. In situ scenarios are financially hindered compared to ex situ scenarios because most require multiple years of heating before reaching their maximum production rate. The actual time to peak production, the volume of oil produced, and the energy input vary greatly, depending on the specific in situ retort design.

This research work makes a number of original contributions. The COG model presented in Chapter 2 and Chapter 3 provides an accurate and cross-validated method for forecasting (with uncertainty estimates) drilling activity and oil and gas production rates (based on an automated well-by-well decline curve analysis algorithm). The energy price forecasting method is also unique, combining U.S. EIA forecasts (the standard reference for future U.S. energy prices) with the historically observed relative error in those forecasts. The COG model developed here has been adopted by Utah's Division of Air Quality for estimating VOC emissions from the COG industry in the Uinta Basin.

The oil supply price assessment for ex situ and in situ oil shale processing

methods provides a rigorous exploration of the input parameters that have first-order impacts on the supply price. In particular, Chapter 4 couples novel CFD simulations of the heat transfer in a large volume of oil shale source rock (with detailed resolution of the rock layers and the physical properties of each layer) with a detailed DCF analysis (under a myriad of different input assumptions). Finally, the oil supply price assessment gives a transparent and independent estimate of all of the costs for both processing methods.